Faculty of Pharmacy and Biomedical Sciences

Louvain Drug Research Institute
Biomedical Magnetic Resonance Group

Institut de Recherche Expérimentale et Clinique
Pole of Pharmacology and Therapeutics

Tumor microenvironment involvement in the metabolic reprogramming induced by the PDK inhibitor dichloroacetate

Céline Schoonjans

Thesis presented in fulfillment of the requirements for the degree of
"Docteur en Sciences Biomédicales et Pharmaceutiques"

Supervisor: Bernard Gallez
Co-supervisor: Olivier Feron

Academic year 2020-2021

Acknowledgments

Tout d'abord, je voudrais exprimer toute ma gratitude envers mon promoteur, le Professeur Bernard Gallez, pour m'avoir donné l'opportunité de réaliser ma thèse au sein du groupe REMA. Je lui suis particulièrement reconnaissante pour sa confiance et ses conseils tout au long de cette thèse. Je le remercie également pour son implication dans la rédaction des différents rapports que j'ai eu à rédiger.

Je tiens également à remercier mon co-promoteur, le Professeur Oliver Feron, qui a m'a permis, au lancement de ma thèse, de travailler au sein de son équipe et d'y acquérir une expertise qui m'a été utile tout au long de ces 4 années de recherche. Je le remercie aussi pour ses conseils et ses corrections qui m'ont permis de m'améliorer continuellement.

Ce travail n'aurait pas été possible sans le soutien du Télévie et de l'Université Catholique de Louvain, qui m'ont permis, grâce à une allocation de recherches, de me consacrer sereinement à l'élaboration de ma thèse.

Je remercie également les membres de ce Jury de thèse qui m'ont aidé à améliorer la qualité de ce travail grâce à leur contribution. Les Professeurs Laure Blindels, Bénédicte Jordan, Jean-Pascal Machiels et Pierre Sonveaux m'ont toujours donné des commentaires constructifs lors des réunions du comité de thèse. Je suis aussi très reconnaissant envers le jury externe, le Professeure Agnès Noël et le Docteur Anna Rita Cantelmo, d'avoir accepté d'être membre de ce comité de thèse, pour le temps qu'elles ont passé à réviser le manuscrit et pour leurs précieuses suggestions.

Je tiens à exprimer ma plus profonde gratitude à mes collègues du laboratoire REMA, sans qui ce travail n'aurait pas été possible. Un remerciement particulier à Nicolas, pour tous ses conseils RMN et pour le temps qu'il a consacré afin de m'expliquer les mystères de la résonance magnétique. Merci aussi à mes anciens et nouveaux

collègues de bureau, pour toutes nos discussions passionnantes qu'elles soient scientifiques ou non, Céline, Chantale, Donatienne et Jérôme. Je remercie mon ancienne collègue Stefania, pour ses précieux conseils expérimentaux, mais aussi pour tous les bons moments partagés en dehors du laboratoire. Je remercie aussi Lionel, qui a toujours été disponible pour répondre à mes nombreuses questions et pour me partager son expérience. Je remercie Pierre pour tous ses bons conseils et pour son humour inégalable. Je tiens à remercier Florian pour toute son implication dans l'organisation du laboratoire et pour ses remarques constructives. Finalement je remercie toutes les personnes avec qui j'ai eu le plaisir d'interagir au laboratoire REMA, Caner, Chloé, Natacha, Barbara, Yousera, Pauline, Ermelinne, Charlotte, Estelle, Heidi et Marie-Aline.

Je ne remercierais jamais assez Cyril Corbet pour toute son implication dans ma thèse, surtout lors du lancement de celle-ci. Je le remercie de m'avoir partagé son expertise, d'avoir mis à disposition ses modèles expérimentaux et d'avoir toujours été disponible pour me conseiller et pour apporter un regard critique et constructif sur mes résultats.

Je tiens aussi à remercier les différents membres du laboratoire FATH et de l'IREC avec qui j'ai eu l'occasion de travailler ou qui m'ont apporté leur aide et leur enthousiasme : Charline Degavre, Céline Guilbauld, Davide Brusa, Laurenne Petit et Luca Zampieri.

Je suis extrêmement reconnaissante envers mes parents sans qui je ne serais jamais arrivé jusqu'ici. Je remercie aussi tous mes amis, ma famille et anciens colocataires qui ont suivi avec attention l'avancement de ma thèse au quotidien et qui ont toujours été présents pour que nous puissions passer ensemble des moments de qualité. Enfin, je remercie Romain qui m'a accompagné, a toujours cru en moi et a toujours trouvé les mots pour m'encourager tout au long du doctorat.

Foreword

Reprogramming energy metabolism is a key hallmark of cancer cells and an enticing target for anti-tumor therapy. Research on cancer metabolism has moved from pathway attention to network consideration. Indeed, tumor metabolism continuously adapts to new constraints in the tumor microenvironment reflecting the interaction between several signaling pathways. It is now recognized that this microenvironment plays a crucial role in tumor development and adaptation. Success of anti-cancer treatments that target tumor metabolism is not only dependent on cancer cells response but also on the interaction of the drug with the surrounding tumor microenvironment. Therefore, the aim of this thesis is to explore the impact of the tumor microenvironment on the effect of a prototypical metabolic modulator, namely dichloroacetate (DCA).

In the introduction, the different sources of energy that can be used by cancer cells are described in order to get an overview of the major bioenergetic and biosynthetic pathways involved in cellular metabolism. Then, we will describe how the hypoxic, acidic and nutrient-deprived microenvironment can account for metabolic plasticity. After that, we will review the literature on the effects of DCA as a metabolic modulator for its use in anti-cancer therapy. Besides cancer cells, treatments targeting the metabolism of endothelial cells (ECs) recently emerged as a new mode of anti-angiogenic therapy. It has been observed that DCA decreases tumor angiogenesis but a direct effect of DCA on ECs has never been demonstrated. We will expose the role of angiogenesis in cancer and the rationale behind the use of metabolic

modulators such as DCA to target ECs. Finally, magnetic resonance spectrometry techniques used to monitor cancer cell metabolism will be described.

The Results part contains two research papers written during the thesis. The first article describes the impact of extracellular acidosis on the anti-proliferative action of DCA and on the metabolic plasticity induced by DCA. The second article describes the effect of DCA on the metabolism of ECs, their viability, proliferation and migration.

The last part of the thesis summarizes and discusses the above results and presents perspectives opened by our work.

At the end of the manuscript, a methodology section describes ^{13}C NMR fluxomic experiments and acid-adapted cancer cells models. Thereby offering an overview of the methodology we used, in order to ease data interpretation and discussion.

TABLE OF CONTENTS

LIST OF ABBREVIATIONS **1**

INTRODUCTION **5**

1. Bioenergetics of cancer cells **5**

1.1. Aerobic glycolysis and TCA cycle dependency 6

- Origin of the Warburg Effect 8
- Consequences of the Warburg Effect 14

1.2. Amino acid metabolism 16

- Glutamine metabolism 17
- Serine metabolism 20
- Role of other amino acids 22

1.3. Fatty acid synthesis and oxidation 26

2. Microenvironment drives tumor metabolic plasticity **29**

2.1. Hypoxia enhances metabolic plasticity 31

2.2. Metabolic reprogramming induced by extracellular acidosis 33

2.3. How cancer cells escape to nutrient deprivation 37

3. Dichloroacetate to target tumor metabolism **40**

3.1. Inhibition of PDK by dichloroacetate 41

- Biodistribution and metabolism of DCA 41
- Mechanism of action of DCA on PDK 42

3.2. Anti-cancer action of DCA 46

- Proliferation inhibition and apoptosis induction 47
- Extracellular acidosis reduction and metastasis inhibition 50
- Angiogenesis inhibition 50
- Lipid metabolism dysregulation 51
- Enhancement of anti-tumor immunoreactivity 52

3.3. DCA in combined therapies 52

3.4. DCA in cancer clinical trials 54

3.5. Derivatives of DCA 56

4. Metabolism in tumor angiogenesis 57
4.1. Glycolytic switch to angiogenic switch 57
4.2. Metabolic reprogramming of tumor endothelial cells 60
4.3. Anti-angiogenic therapies: past and future 63

5. Magnetic resonance spectroscopy to measure cancer cell metabolism and oxygen consumption 64
5.1. ^{13}C NMR spectroscopy to follow glucose and glutamine metabolism 64
- NMR basics 64
- ^{13}C NMR to measure cellular metabolism 68

5.2. Quantification of cellular oxygen consumption by EPR spectroscopy 71

AIMS OF THE THESIS 75

1. Rationale and general aim 75

2. Specific aims 76
2.1. Unraveling the impact of acidosis-induced metabolic reprogramming in tumor cells exposed to DCA 76
2.2. Exploring the effects of PDK inhibition by DCA on endothelial cells .. 77

RESULTS 79

1. INFLUENCE OF ACIDOSIS-INDUCED METABOLIC REPROGRAMMING ON DCA RESPONSE 79

2. IMPACT OF DCA ON ENDOTHELIAL CELLS 91

DISCUSSION AND PERSPECTIVES 113

1. Discussion of the principal findings about DCA 113
1.1. Tumor microenvironment modulates the sensitivity of cancer cells to DCA 113
- Why less glycolytic acid-adapted cancer cells are more sensitive to the glycolytic modulator DCA? 114
- How does extracellular acidosis modulate DCA uptake? 115
- How adaptation to extracellular acidosis increases DCA sensitivity? 118

1.2. DCA can directly act on non-cancerous cells in the tumor microenvironment 120
1.3. DCA and BPTES induces metabolic adaptations in glutamine pathway 122

2. Limitations and Perspectives 123
2.1. Biological tools to study extracellular acidosis 123
2.2. Interplay between acidic and hypoxic environments in DCA response 125
2.3. Potential biomarkers of sensitivity to DCA 126
2.4. Is DCA the better way to inhibit PDK in cancer? 129
2.5. DCA and angiogenesis 131
2.6. What consequences of DCA action on other non-cancerous cells in the microenvironment 133

3. General conclusion 137

Methodology section 139

1. ^{13}C RMN fluxomics methodology 139

2. Acid-adapted-cancer cells model 142

BIBLIOGRAPHY 145

LIST OF ABBREVIATIONS

^{12}C	carbon 12
^{13}C	carbon 13
15N-PDT	4-oxo-2,2,6,6-tetramethylpiperidine-dl6-1-oxyl
3PG	3-phosphoglycerate
ACACB	acetyl-CoA carboxylase beta
ACC	acetyl-CoA carboxylase
Acetyl-CoA	acetyl-coenzyme A
ACSS	acyl-CoA synthetase short chain family member
ADP	adenosine diphosphate
alpha-KG	alpha-ketoglutarate
Asn	asparagine
ATP	adenosine triphosphate
B_0	external magnetic field
BAD	Bcl-2 agonist of cell death
BAX	BCL2-associated X protein
BCAAs	branched-chain amino acids
bFGF	basic fibroblast growth factor
Ca^{2+}	cation calcium
CAFs	cancer-associated fibroblasts
CO_2	carbon dioxide
DCA	dichloroacetate
DNA	deoxyribonucleic acid
EAAS	essential amino acids
ECs	endothelial cells
EGF	epidermal growth factor
EPR	electron paramagnetic resonance
ERK5	extra regulated Kinase 5
ETC	electron transfer chain
F1,6P	fructose-1,6-phosphate
F6P	fructose-6-phosphate
$FADH_2$	flavin adenine dinucleotide
FAO	fatty acid oxidation
FAS	fatty acid synthesis

FID	free induction decay
Foxo3	Forkhead Box O3
G6P	glucose-6-phosphate
G6PDH	glucose-6-phosphate dehydrogenase
Gln	glutamine
Glu	glutamate
GLUT	glucose transporter
GSTZ1	glutathione transferase zeta 1
H^+	proton
H_2O_2	hydrogen peroxide
HCO_3^-	bicarbonate
HIF-1α	hypoxia inducible factor 1 alpha
HIF-2α	hypoxia inducible factor 2 alpha
HK2	hexokinase 2
HMG CoA	hydroxyméthylglutaryl-CoA
IDH	isocitrate dehydrogenase
IL-8	interleukin 8
LAT1	large neutral amino acid transporter
LDHA	lactate dehydrogenase A
LDL	low-density lipoprotein
LDLR	low-density lipoprotein receptor
Lw	linewidth
MAPK	mitogen-activated protein kinases
MCT	monocarboxylate transporter
MEF	myocyte enhancer factor
Mg^{2+}	cation magnesium
MHC-1	Major histocompatibility complex 1
mTORC1	mammalian target of rapamycin complex 1
MTP	mitochondrial transition pore
NADH	nicotinamide adenine dinucleotide
NADPH	nicotinamide dinucleotide phosphate
NF-κB	nuclear factor kappa-light-chain-enhancer of activated B cells
NH_4^+	ammonium ion
NMR	nuclear magnetic resonance
O_2	oxygen

OAA	oxaloacetate
OCR	Oxygen consumption rate
OXPHOS	oxidative phosphorylation
p53	tumor protein 53
PDC	pyruvate dehydrogenase complex
PDH	pyruvate dehydrogenase
PDK	pyruvate dehydrogenase kinase
PDP	pyruvate dehydrogenase phosphatase
PEP	phosphoenolpyruvate
PFK	phosphofructokinase
PFKFB3	phosphofructo-2-kinase/fructose-2,6-bisphosphatase 3
PHD	prolyl-hydroxylases
Pi	inorganic phosphate
PK	pyruvate kinase
PKM2	pyruvate kinase isoform M2
ppm	parts-per notation
PPP	pentose phosphate pathway
PUMA	p53 upregulated modulator of apoptosis
RF pulse	Pulsed radiofrequency
RNA	ribonucleic acid
ROS	reactive oxygen species
SERBP2	sterol regulatory element-binding protein-2
SHMT2	Serine hydroxymethyltransferase 2
SIRT1	NAD^+-dependent deacetylase sirtuin-1
SMCT1/SLC548	sodium-coupled monocarboxylate transporter
TCA	tricarboxylic acid
TECs	tumor endothelial cells
TEM	tumor microenvironment
TSP	trimethylsilylpropanoic acid
VEGF	vascular endothelial growth factor
VEGFR2	VEGF receptor 2
w_0	precession frequency
xCT	cysteine/glutamate antiporter

INTRODUCTION

1. Bioenergetics of cancer cells

(Adapted from Schoonjans et al. 2020)

The metabolic needs of the proliferating cancer cells significantly differ from the quiescent cells (DeBerardinis et al. 2016). To support rapid proliferation under specific microenvironmental constraints, tumor cells must undergo a metabolic reprogramming. Depending on the cancer cell type or microenvironment modification, tumor cells rely on glucose but also fatty acids, lactate and specific amino acids for their bioenergetic and biosynthetic needs (fig.1).

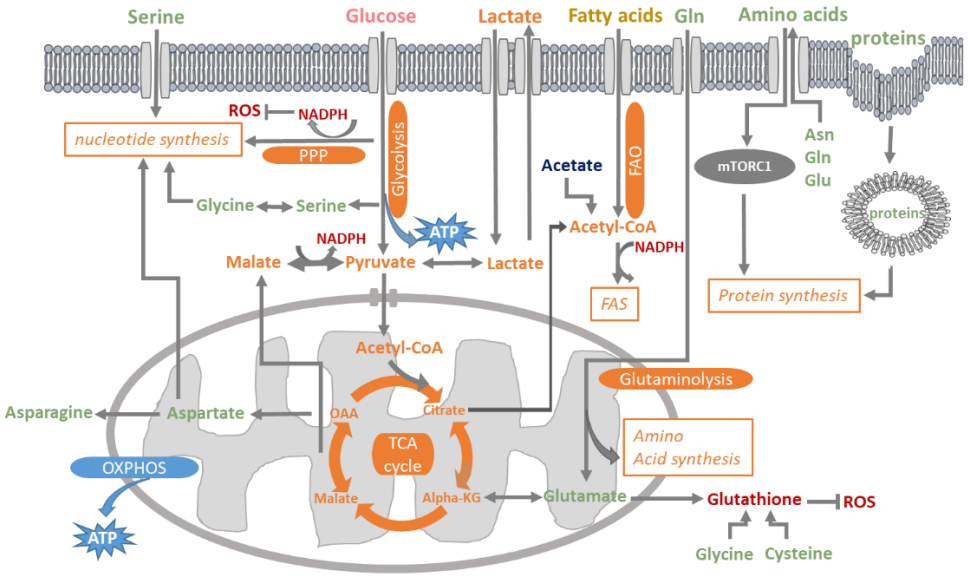

Figure 1. Bioenergetics of cancer cells. *Cancer cells can take up glucose, amino acids, fatty acids, lactate and extracellular proteins to support proliferation. Glucose metabolism through glycolysis produces ATP and carbon intermediates to sustain proliferation such as intermediates for the pentose phosphate pathway (PPP) and for*

de novo serine synthesis. PPP generates NADPH (defense against reactive species of oxygen, ROS) and is involved in nucleotide synthesis. Extracellular and de novo serine also participate in nucleotide synthesis. The end-product of glycolysis, pyruvate, can be converted into lactate or acetyl-CoA. Lactate is exported out of the cells and acetyl-CoA fuels tricarboxylic acid (TCA) cycle. In some cancer cells, lactate can be taken up and used as carbon substrate for pyruvate production. TCA cycle produces carbon intermediates for cellular proliferation such as aspartate, asparagine, glutamate and precursors for lipid synthesis. In the presence of oxygen, TCA cycle via oxidative phosphorylation (OXPHOS) produces ATP. TCA cycle can also be fueled by glutamate. Glutamate is the result of glutamine (Gln) metabolism, glutaminolysis. Glutaminolysis is also involved in amino acid synthesis and in concert with glycine and cysteine, glutathione production (defense against ROS). Cancer cells can import fatty acids from extracellular and, via fatty acid oxidation (FAO), generate ATP and acetyl-CoA. Fatty acids can also be synthesized de novo (FAS) via an acetyl-CoA sources provided from citrate or acetate. Glutamine (Gln), glutamate (Glu) and asparagine (Asn) can act as exchange substrates for antiporters that allow the entrance of extracellular amino acids. The level of intercellular amino acid regulates mTORC1 activity, which in turn regulates protein synthesis. In case of depleted nutrient medium, cancer cells can import entire protein via micropinocytosis and through lysosomal degradation release free amino acids.

1.1. Aerobic glycolysis and TCA cycle dependency

In most healthy cells, glucose is metabolized into pyruvate (glycolysis) and then oxidized in the mitochondria through tricarboxylic acid (TCA) cycle in order to produce energy via oxidative phosphorylation (OXPHOS) (fig.2a). In the absence of oxygen, only glycolysis can provide energy and pyruvate is converted into lactate in the cytosol in order which allow the replenishment

of the pool of NAD^+ which is essential to maintain a high glycolytic rate (Kim et al. 2006) (fig 2b). Alternative fuels can be provided by alanine aminotransferase which allows the reversible transamination of alanine and alpha-ketoglutarate to glutamate and pyruvate (Porporato et al. 2011). In addition, alanine can exert a negative control on pyruvate production, details on this mechanism will be explained on figure 5.

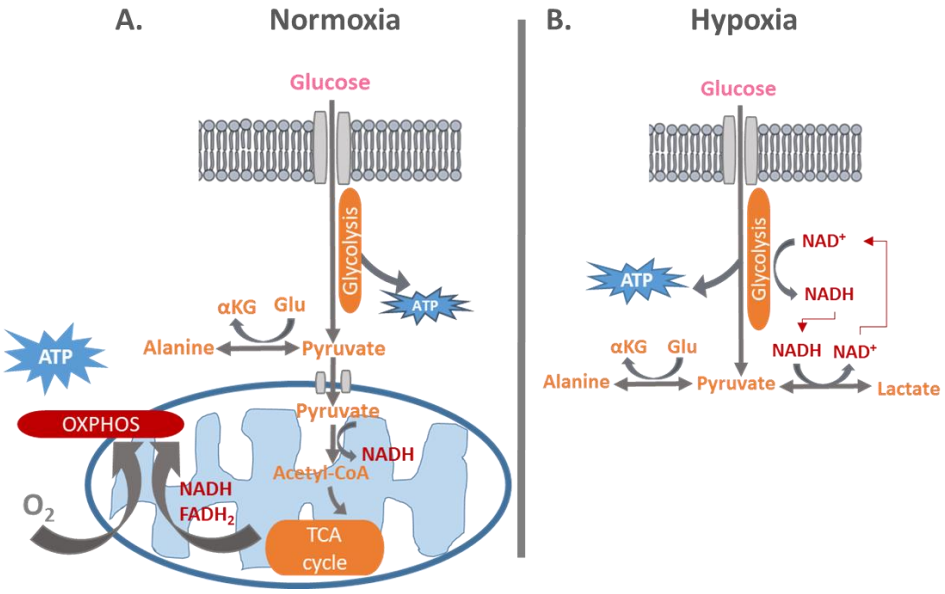

Figure 2. Glucose metabolism in normoxia and hypoxia. *A, in the presence of oxygen, glucose is oxidized in the mitochondria to produce ATP through OXPHOS. B, in the absence of oxygen, glucose is metabolized into lactate and ATP is only produced by glycolysis. Lactate production from pyruvate allows to replenish the pool of NAD^+ required for glycolysis. Reversible transamination of alanine and alpha-ketoglutarate (αKG) to glutamate (Glu) can provide alternative fuels.*

Otto Warburg observed that this physiological response to hypoxia occurs in cancer cells even in the presence of oxygen (Warburg 1956, Warburg 1956). Warburg originally explained this phenomenon, called aerobic glycolysis, by an impaired mitochondrial function in tumor cells leading to a non-coupling of glycolysis to energy production from mitochondria. However, the Warburg hypothesis has now been reassessed because only a few mutations of mitochondrial metabolic enzymes have been described in a limited number of cancer types (Laurenti et al. 2016, San-Millan et al. 2017). Moreover, recent studies have shown that cancer cell of various origins rely on mitochondrial respiration and that mitochondrial metabolism is actually necessary for tumorigenesis (Weinberg et al. 2010). Nevertheless, Warburg's observation that cancer cells consume a large amount of glucose has been validated in many cancer patients (Pereira-Nunes et al. 2020).

- Origin of the Warburg Effect

Today, it is clear that the exacerbated glycolytic flux is mainly due to an interplay between acquisition of genetic mutations and external responses to the tumor microenvironment (Cairns et al. 2011). Both can induce loss of function of tumor suppressors and activation of oncogenes that can promote the expression or activity of proteins (transporters, enzymes, cofactors) involved in glycolysis (fig.3) (DeBerardinis et al. 2016).

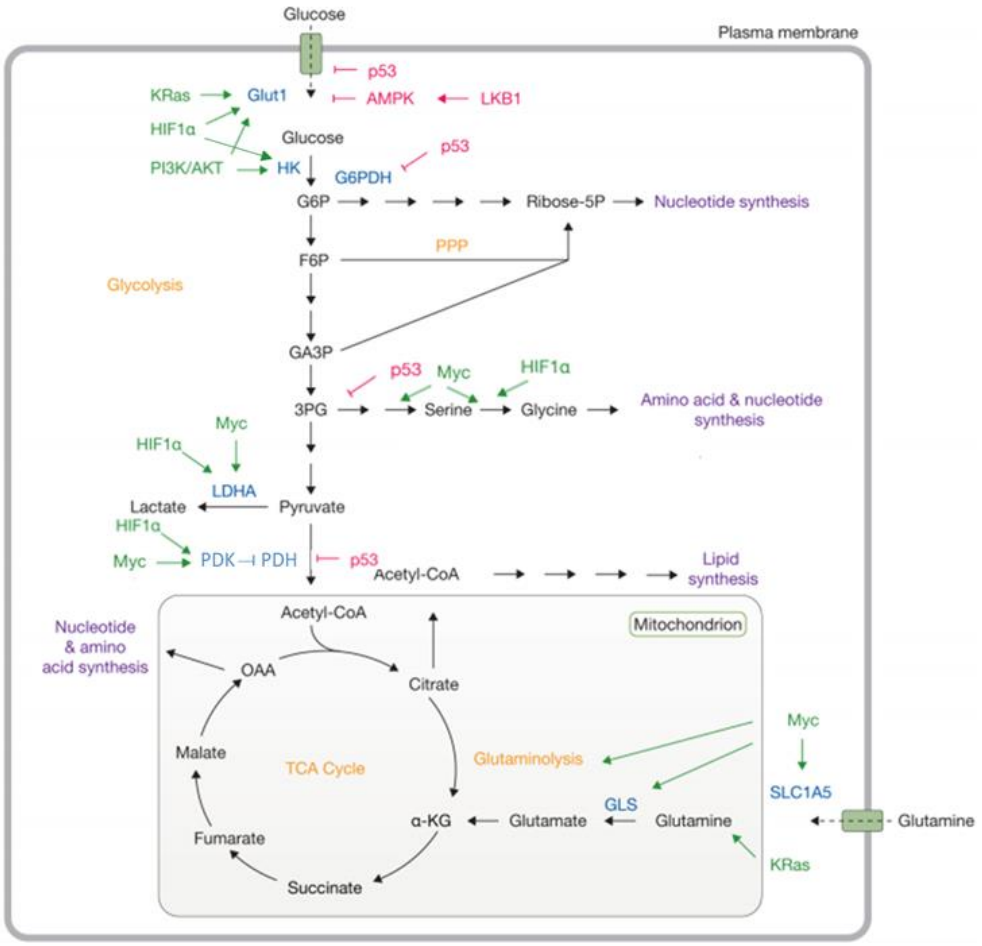

Figure 3. Influence of oncogenic and tumor suppressor signaling on cancer cell metabolism *(adapted from DeBerardinis, 2015). Oncoproteins activation (green) and loss of function of tumor suppressors (pink) regulate expression and activity of nutrient transporters, transcription factors, and metabolic enzymes (blue) which influence the acquisition and metabolism (yellow) of nutrients to support biosynthetic pathways (purple).*

The transcription factor HIF-1α (hypoxia-inducible factor 1 alpha) is a master regulator of glycolysis (Semenza 2001). HIF-1α can be stabilized directly by hypoxia through inhibition of its degradation mediated by prolyl-hydroxylases (PHD) (fig.4) (Yu et al. 2001).

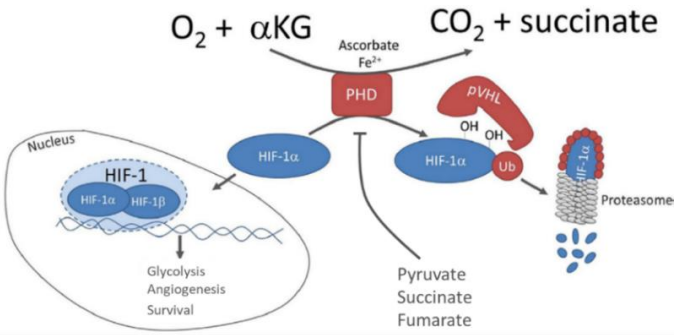

Figure 4: Regulation of HIF-1α stabilization *(adapted from Iommarini et al. 2017). In normoxia, hypoxia-inducible factor 1 alpha (HIF-1α) is hydroxylated by prolyl hydroxylase (PHD), inducing ubiquitination by the Von Hippel–Lindau tumor suppressor (pVHL) and the consequent proteasomal degradation. Pyruvate, succinate and fumarate inhibit pVHL activity. The hydroxylation reaction induces the conversion of alpha-ketoglutarate (αKG) to succinate and requires cofactors, ferrous iron and ascorbate. In hypoxia, hydroxylation cannot occur and HIF-1α dimerizes with the constitutively expressed HIF-1β, leading to an active HIF-1 complex, which activates transcription genes promoting glycolytic metabolism, angiogenesis and survival (Iommarini et al. 2017).*

Hypoxia occurs in early stages during tumor development as soon as cells become too distant from blood vessels. This leads to a hypoxia-driven activation of HIF-1α. In addition to increased glycolytic flux, HIF-1α induced angiogenic signaling to form new blood vessels. Even if normoxia is restored, the TCA cycle suppression induced by HIF-1α establishes a powerful

feedback loop to stabilize HIF-1α (Kinnaird et al. 2015). Alpha-ketoglutarate, a TCA cycle intermediate is essential for PDH activity (fig.4). Consequently, its decrease reduces PDH activity and enhances HIF-1α stabilization (Kinnaird et al. 2015). Other factors may be responsible for normoxic HIF-1α stabilization such as mutations in TCA cycle enzymes. For instance, mutation in the succinate dehydrogenase or fumarate dehydrogenase enzyme leads to an increase in succinate or fumarate concentration, which are allosteric inhibitors of PDH (Isaacs et al. 2005, Selak et al. 2005). Through the same mechanism as PDH allosteric inhibition, pyruvate is also associated to HIF-1α stabilization (Sonveaux et al. 2012). Mutation in oncogenes or tumor suppressor genes are also responsible for HIF-1α stabilization either by increasing HIF-1α expression or by inactivating HIF-1α degradation machinery (Iommarini et al. 2017). Finally, ROS and nitric oxide are also able to inhibit PDH activity in normoxia, thereby promoting HIF-1α stabilization (Li et al. 2007, Movafagh et al. 2015).

HIF-1α increases glycolytic flux by enhancing the expression of glucose transporters (Glut 1 and Glut 3) and of glycolytic enzymes insensitive to the Pasteur Effect (allosteric inhibition of key glycolytic enzymes by energetic metabolites): hexokinase 2 (HK2), phosphofructokinase 2 (PFK2) and pyruvate kinase M2 (PKM2) (fig.5) (Mathupala et al. 2001, Minchenko et al. 2002, Luo et al. 2011). PKM2 can be present as a dimer with a low affinity for phosphoenolpyruvate (PEP) or tetramer with a high activity for PEP (fig.5) (Mazurek et al. 2005). The tetramerization of PKM2 is promoted by serine and fructose-1,6 bisphosphate and allows ATP and pyruvate production. The dimeric conformation of PKM2 is induced by lactate, amino acids and lipids

and allows accumulation of glycolytic intermediates to fuel branching glycolytic pathways. HIF-1α also represses mitochondrial activity by controlling pyruvate fate (fig.5). HIF-1α decreases pyruvate entry into the TCA cycle (via PDK upregulation) and increases pyruvate conversion into lactate (via LDHA upregulation) (Koukourakis et al. 2005, Semba et al. 2016).

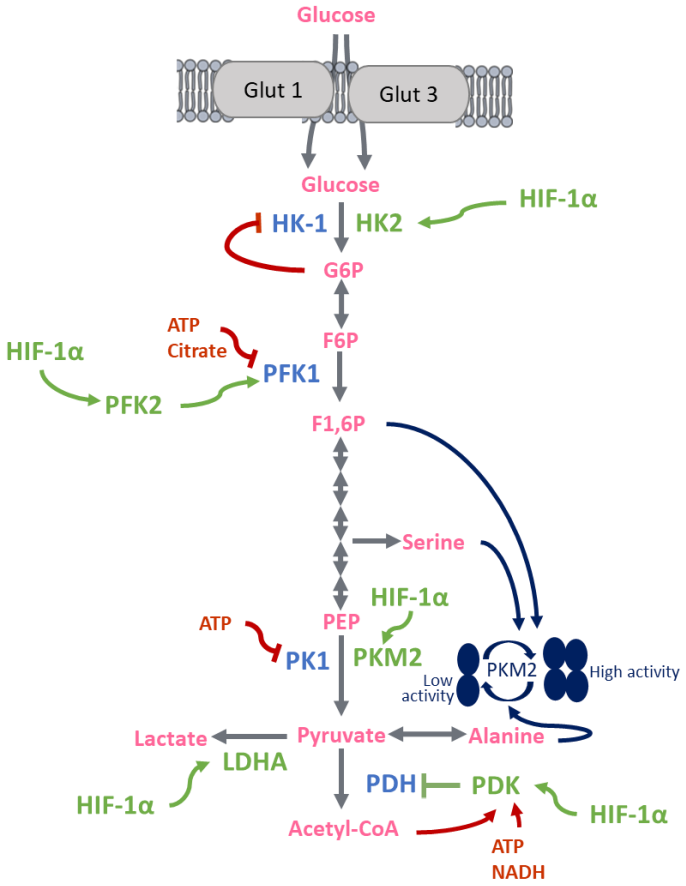

Figure 5: Regulation of glucose metabolism by HIF-1α to counteract inhibition of glycolytic enzymes mediated by energy metabolites. *ATP, citrate, glucose-6-phosphate, acetyl-CoA and NADH exert an allosteric inhibition (red arrows) on key glycolytic enzymes in order to restrain glycolytic flux when energy demand is complete. HIF-1α counteract these negative feedbacks by enhancing the expression*

of enzyme insensitive to these allosteric inhibitions (green arrows). PKM2 conformation regulates pyruvate production from PEP. Alanine induces the dimeric conformation of PKM2 which has a low activity for PEP. Serine and phosphofructose-1,6-P promote the tetrameric conformation of PKM2 which has a high activity.

Beside HIF-1α, HIF-2α isoform also plays an important role in cancer adaptation and development (Ratcliffe 2007). HIF-2α stability is regulated by the same mechanism as HIF-1α. HIF-2α also dimerizes with HIF-1β. However, the active complex HIF-2α/HIF-1β has a different pattern of targeted genes than HIF-1α. HIF-2α does not trigger the glycolytic phenotype but has been identified as a key regulator of metabolic adaptation to acidosis (Hjelmeland et al. 2011, Corbet et al. 2014). The activity of HIF-2α under acidosis will be detailed in the chapter 2.2 (metabolic reprogramming induced by extracellular acidosis).

As seen in figure 3, other oncogenes and tumor suppressors are involved in the enhancement and maintenance of the glycolytic phenotype. For instance, most glycolytic gene promoters contain consensus for the transcription factor c-Myc that is activated upon chromosomal translocations, gene amplification, and single-nucleotide polymorphisms and thereby supports glycolysis under normoxia (DeBerardinis et al. 2016). The tumor suppressor p53 is mutated or deleted in 50% of all human cancers. p53 is better known to be involved in DNA repair and apoptosis but more recently has been associated with regulation of tumor metabolism (DeBerardinis et al. 2016). p53 directly represses glucose transporters and PDK expression and is involved in the repression of several glycolytic enzymes. Consequently, loss of function of p53 favors glycolytic flux and decreases OXPHOS (Kruiswijk et

al. 2015). All of these metabolic adaptations allow tumors to continuously drive glycolysis to support part of their metabolic needs without coupling to OXPHOS.

- Consequences of the Warburg Effect

The enhancement of the glycolytic flux allows rapid glycolytic ATP production without the need for oxygen, which renders cancer cells insensitive to fluctuations in oxygen levels. The resulting increase in glycolytic intermediates supplies new precursors for biosynthetic pathways involved in nucleotides, lipids and amino acid synthesis and numerous cofactors for macromolecular synthesis. Among pivotal biosynthetic pathways branched to glycolysis are the pentose phosphate pathway (PPP), the hexosaminidase pathway and the serine pathway (fig.6) (DeBerardinis et al. 2016).

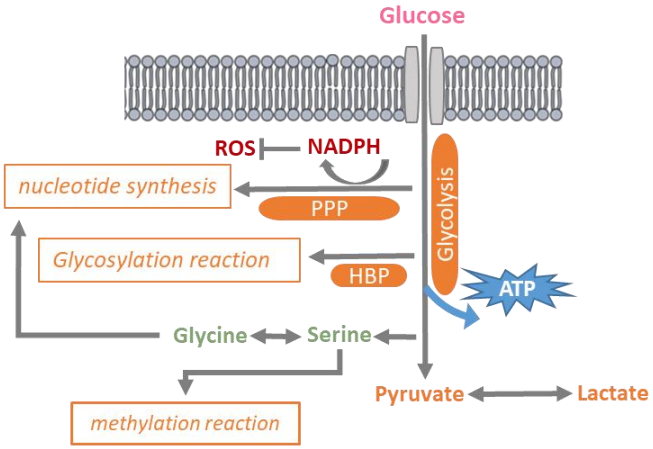

Figure 6. Biosynthetic pathways branched to glycolysis. *Glycolytic intermediates are precursors for pentose phosphate pathway (PPP), hexosamine biosynthetic pathway (HBP) and serine pathway, which provide NADPH, nucleotides and support glycosylation and methylation reaction.*

The expression or activity of PPP, HBP and serine enzymes are frequently found to be dysregulated by oncogenes or tumor suppressors (fig.3) (Boroughs et al. 2015, Chokchaitaweesuk et al. 2019).

The pentose phosphate pathway (PPP) produces NADPH, a source of reducing equivalents against the toxicity of reactive oxygen species (ROS) and ribose-5-phosphate for nucleotide synthesis (fig.6) (Jiang et al. 2014). The irreversible oxidative branch of the PPP consumes the first glycolytic intermediate, the glucose-6-phophate to produce 2 molecules of NADPH and ribulose-5-phosphate. Ribulose-5-phosphate is then used by the non-oxidative branch of the PPP to produce ribose-5-phosphate. The non-oxidative branch of the PPP can reversibly convert ribose-5-phosphate into the glycolytic intermediate glyceraldehyde-3-phosphate and fructose-6-phosphate. Serine pathway also contributes significantly to the NADPH pool, supports the synthesis of purines and sustains methylation reaction (fig.6) (Yang et al. 2016). This pathway will be described more extensively in chapter 1.2 (amino acid metabolism, serine metabolism)

The hexosamine biosynthetic pathway (HBP) metabolizes the glycolytic intermediate fructose-6-phosphate along with glutamine, uridine-5'-triphosphate and acetyl-CoA to produce the amino sugar UDP-GlcNAc (uridine diphosphate N-acetylglucosamine) (Akella et al. 2019). Since HBP utilizes macromolecules from major metabolic pathways (nucleotide, lipid, glutamine and glucose metabolism), modulation of bioenergetic preferences can affect downstream protein glycosylation reactions and thereby impact on a variety of cellular processes. These post-translational modifications can

either activate or inactivate protein functions (Akella et al. 2019). For instance, glycosylation of c-Myc, a well-known tumor oncogene, results in its activation (Chou et al. 1995). Glycosylation of phosphofructokinase 1 inhibits its activity and thereby stimulates glycolytic flux into the PPP (Yi et al. 2012).

Here above, we have described involvement of glucose metabolism in cancer focusing on the Warburg effect. However, cancer cells also rely on mitochondrial respiration and mitochondrial metabolism is necessary for tumorigenesis (Weinberg et al. 2010). The observation that mitochondria are still active in many cancers is explained by the fact that these organelles (which are at the crossroad of many essential metabolic pathways) can be fueled by other nutrients than glucose (DeBerardinis et al. 2016). Like glycolytic intermediates, fatty acid and amino acid can provide TCA cycle intermediates for anabolic pathways (Ahn et al. 2015). In addition, metabolic pathways can regulate signaling by controlling post-translational modification of proteins (see above) as well as via epigenetic regulation (Su et al. 2016, Wu et al. 2019). How amino acids and fatty acids sustain metabolic needs and control signaling in cancer cells will be detailed in the next paragraphs.

1.2. Amino acid metabolism

In addition to the increased glucose consumption, various cancer types exhibit an increased demand for specific amino acids and become dependent either on an exogenous supply or on an upregulated *de novo* synthesis (Lukey et al. 2017).

- Glutamine metabolism

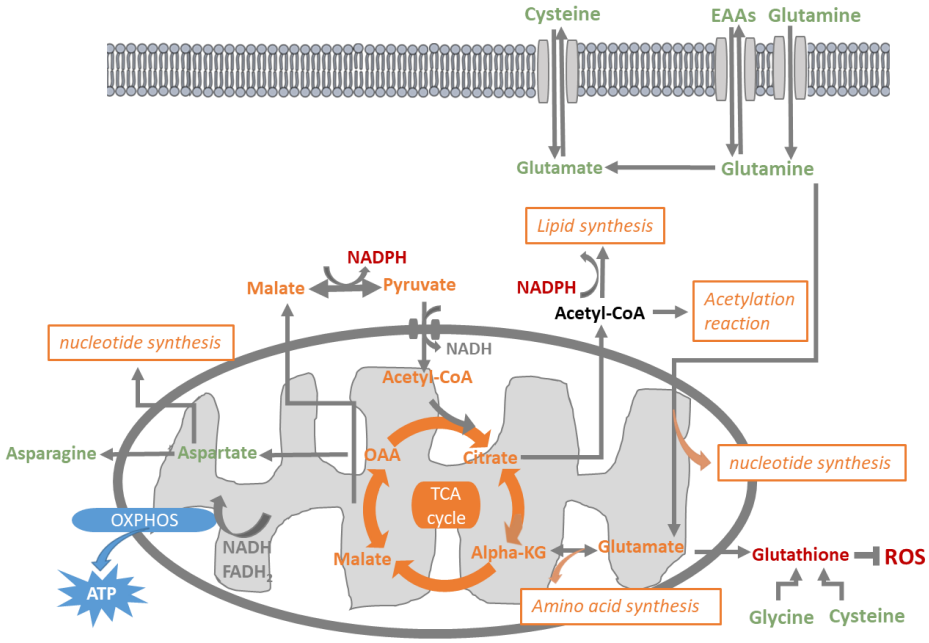

Figure 7. Metabolism of glutamine and main contributions to cell bioenergetics. *Glutamine enters into the cell and can contribute to nucleotide synthesis or be converted to glutamate. Glutamate and glutamine can be exchanged for other amino acids (EAAs and cysteine). Glutamate participates in glutathione synthesis. Glutamate is converted to α-ketoglutarate (alpha-KG) which fuels the TCA cycle. NADH and $FADH_2$ generate ATP via OXPHOS. Malate can exit the TCA cycle and produce pyruvate and NADPH. Oxaloacetate (OAA) can be converted to aspartate and participate in nucleotide synthesis. Citrate supports lipid synthesis (FAS). Acetyl-CoA supports acetylation reaction and fuels lipid synthesis.*

This non-essential amino acid is the most abundant amino acid present in the plasma and is used by the cell for energy generation and biomass production (Altman et al. 2016). Glutamine enters into the cells via many transporters, such as SLC1A5 which is upregulated in several cancer types

(Bhutia et al. 2015). Glutamine is metabolized through glutaminolysis to generate glutamate and subsequently alpha-ketoglutarate (alpha-KG) that fuels the TCA cycle (fig.7) (DeBerardinis et al. 2016). Glutamate can be converted to alpha-KG by glutamate dehydrogenase (GLUD) or aminotransferases. GLUD by-product is NH_4^+ and aminotransferase by-products are other amino acids (Altman et al. 2016). Two different routes can be used by the TCA cycle to metabolize the alpha-ketoglutarate: the canonical oxidative decarboxylation pathway and the reductive carboxylation pathway. The oxidation of alpha-ketoglutarate provides electron donor (NADH and $FADH_2$) to generate ATP through electron transport chain (ETC). TCA cycle intermediates are cataplerotic substrates: malate can be converted into pyruvate and produces NADPH, oxaloacetate (OAA) can be metabolized into aspartate to support asparagine and nucleotide synthesis. On the other hand, the reduction of alpha-ketoglutarate leads to citrate which supports fatty acid synthesis. In addition, glutamine via its conversion into glutamate is an important source of nitrogen, which supports the production of amino acids and the biosynthesis of nucleotides (Altman et al. 2016). Glutamine can be exported via efflux through LAT1 antiporter, which is coupled with the import of essential amino acids (EAAs) (Pavlova et al. 2016). By being exchanged for amino acids, glutamine contributes to mTORC1 activation. mTORC1 is a major positive regulator of cell growth. Consequently, increased glutamine uptake and metabolism can stimulate mTORC1 activity (Altman et al. 2016). Glutamate can also induce cysteine uptake by acting as an exchange substrate for the cysteine antiporter xCT (Pavlova et al. 2016). As glutamate and cysteine are two major components of glutathione, glutamine

metabolism is also involved in anti-oxidant defenses through glutathione neutralization of ROS. Glutamine is also involved in regulation of post-translational modification of proteins and epigenetics control. Indeed, glutamine is a substrate for the HBP and therefore may modulate protein glycosylation. In addition, glutamine can contribute to the acetyl-CoA pool and consequently is involved in histone and protein acetylation (Cluntun et al. 2017). Because of the diversity of fate, glutamine represents an ideal substrate for the development of cancer cells. Experimental studies have confirmed its pivotal role. In 2007, Yuneva *et al.* already described that some cancer cells were sensitive to glutamine depletion (Yuneva et al. 2007). Several experimental ^{13}C-NMR studies have shown that glutamine is used to replenish TCA cycle in cancer instead of glucose (DeBerardinis et al. 2007, Fan et al. 2013, Jones et al. 2015, Altman et al. 2016). In different cancer cell lines, it has been demonstrated that glutamine supports OXPHOS and that OXPHOS remains the largest quantitative contributor for ATP production (Le et al. 2012, Fan et al. 2013). In glioblastoma, it has been shown that glutamine also serves as a carbon source for biosynthetic pathways. First, the decarboxylation of glutamine leads to pyruvate production through the malic enzyme, consistent with NADPH production. Pyruvate replenishes TCA cycle intermediates during citrate export while NADPH serves as an electron donor for reductive reaction in lipid synthesis. Second, glutamine decarboxylation feeds the production of oxaloacetate that supplies anabolism as oxaloacetate can be converted into aspartate, a required precursor for the synthesis of nucleotides (DeBerardinis et al. 2007).

More recently, glutamine has been identified as a major source of citrate in cancer cells when the TCA cycle function is altered by hypoxia (Metallo et al. 2011). In these circumstances, glutamine preferentially undergoes reductive metabolism to produce citrate through the mitochondrial TCA cycle, then can be converted into acetyl-CoA for lipid synthesis (Metallo et al. 2011, Mullen et al. 2011, Wise et al. 2011, Zhang et al. 2014). This reductive metabolism also exists in the cytoplasm due to the expression of a cytosolic isoform of isocitrate dehydrogenase (IDH1), the enzyme converting alpha-KG into isocitrate. Some studies reported circumstances where reductive and canonical metabolism of glutamine co-exist, depending on the tumor microenvironment or mutations of oncogenes regulating the mitochondrial (McGuirk et al. 2013, Corbet et al. 2016). This ability to easily switch from one mode to another mode of glutamine metabolism offers tumor cells a metabolic plasticity advantage to rapidly adapt to new environmental constraints.

- Serine metabolism

Besides glutamine, the availability of other amino acids is also a limiting factor for cancer cell proliferation (Kory et al. 2018). Many cancer cells are dependent on serine, a non-essential amino acid involved in several metabolic processes that are crucial for cell growth (Yang et al. 2016). Serine can be synthesized de novo via a glycolysis-diverting pathway: the glycolytic intermediate 3-phosphoglycerate (3PG) is converted into serine following a three-step enzymatic reaction (fig6.) (Amelio et al. 2014). Metabolic studies have shown that cancer cells may use as much as 50% of glucose-derived carbon in serine biosynthesis and downstream metabolism (Pavlova et al.

2016). The *de novo* synthesis of serine also produces NADH and requires the nitrogen of glutamate that generates alpha-ketoglutarate. This highlights an important interplay between glutamine, TCA cycle and serine pathway. Serine can also be imported from the extracellular medium via different transporters (Yang et al. 2016). After glucose and glutamine, serine is the third most consumed metabolite in mammalian cells (Frezza 2016, Hosios et al. 2016).

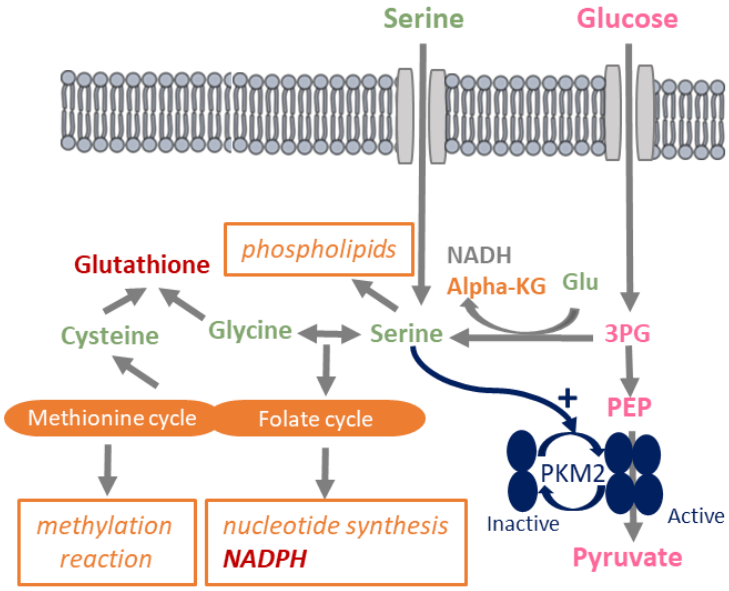

Figure 8. Metabolism of serine and principal downstream bioenergetics. *Serine can be synthesized de novo from 3-phosphoglycerate (3PG) (with production of NADH and alpha-KG) or can be imported from the extracellular media. Serine is involved in phospholipid production and can be converted into glycine. Glycine and serine support folate and methionine cycle, which participate in nucleotide synthesis, methylation reaction and NADPH and glutathione production. Serine is involved in the control of glycolytic flux by promoting the active tetrameric conformation of PKM2.*

As shown in figure 8, serine, through its conversion into glycine, is a major donor of one-carbon unit to the folate cycle which is essential for nucleic acid synthesis and contribute to NADPH regeneration (Yang et al. 2016). Methyl groups derived from one-carbon metabolism provide a major source of substrates for post-translation methylation modifications. Consequently, serine is involved in methylation of histone and DNA which influence the epigenetic control of gene expression (Kim et al. 2018).

Of note, anti-folate chemotherapy is currently used in cancer treatment (Yang et al. 2016). Through cysteine and glycine synthesis, serine is involved in the production glutathione. Serine is also involved in the production of phospholipids such as sphingolipids and phosphatidylserine. Serine can regulate glycolytic flux through activation of pyruvate kinase isoform M2 (PKM2), which catalyzes the last step of glycolysis (fig.8). Reduced serine availability lowers PKM2 activity resulting in the accumulation of glycolytic intermediates. In various cancer types, the enzymes of *de novo* serine synthesis and folate cycle enzymes were found to be overexpressed by several oncogenes (fig. 3) (Yang et al. 2016).

- Role of other amino acids

To sustain their need for amino acids, cancer cells have developed means to increase either the import or the biosynthesis of these amino acids. By acting as an exchange substrate for antiporter LAT1, glutamine is involved in the import of many essential amino acids (Pavlova et al. 2016). Fuchs *et al.* demonstrated that the expression of LAT1 was increased in several cancer types and that the expression of this antiporter could be directly correlated

with tumor growth (Fuchs et al. 2005). The metabolism of glucose, serine and glutamine is involved in the biosynthesis of all non-essential amino acids (fig.9) (Zhang et al. 2017). These amino acids are essential for protein synthesis and are important fuels supporting biosynthetic pathways (fig.9).

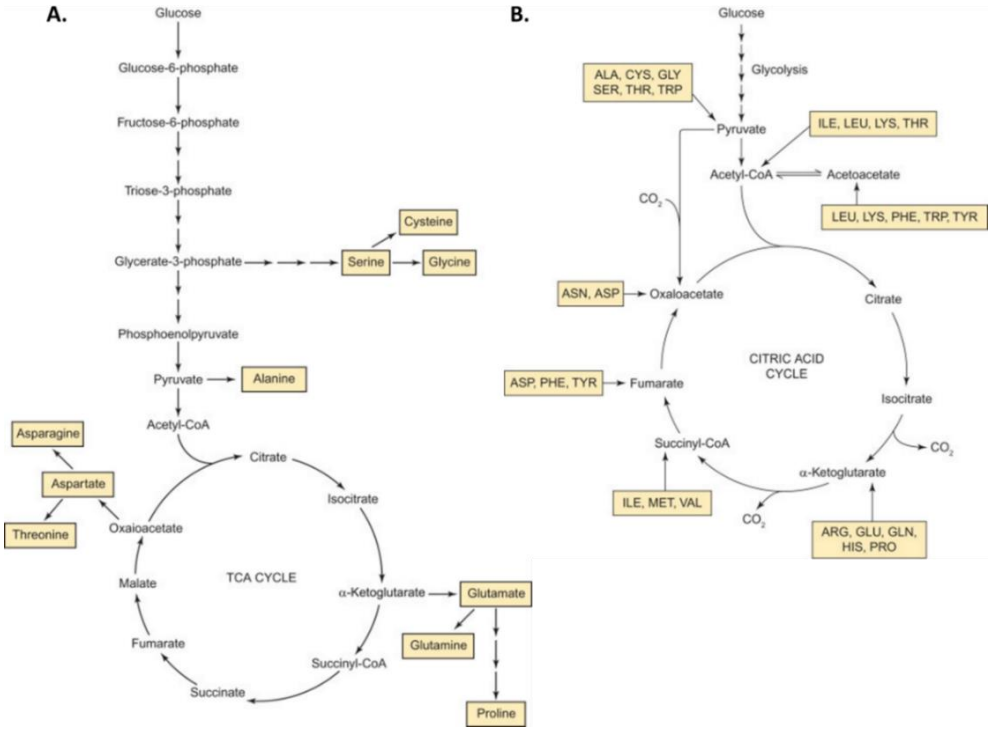

Figure 9. Synthesis of non-essential amino acids and amino acids catabolism *(Litwack, G, 2008). A. Non-essential amino acid production: serine, glycine and cysteine are produced from the glycolytic intermediate 3PG as well as alanine, which is produced from pyruvate. Aspartate, asparagine and threonine are produced from the TCA intermediate OAA as well as glutamate, glutamine and proline, which are produced from alpha-KG. B. The catabolism of essential and nonessential amino acids can fuel TCA cycle and glycolysis.*

Glycine, glutamine, aspartate, serine and methionine represent sources of nitrogen and one-carbon donors for nucleotide synthesis. Through glutathione synthesis and NADPH production, amino acids also regulate ROS homeostasis. Catabolism of branched-chain amino acids (BCAAs; valine, leucine, and isoleucine), threonine and lysine can fill the acetyl-CoA pool and support lipid synthesis as well as protein acetylation. Through their influence on methionine cycle, methionine, serine, and glycine regulate methylation reaction (Lieu et al. 2020).

Specific amino acids participate in various critical cellular functions. For instance, nitric oxide is produced by arginine metabolism and promotes angiogenesis (Lieu et al. 2020). Krall *et al*. observed that asparagine level regulates the uptake of amino acids and mTORC1 activity. More specifically, asparagine regulates the serine uptake and influences the serine metabolism as well as nucleotide synthesis (Krall et al. 2016). The asparagine biosynthesis is the result of glutamine metabolism into aspartate which is then converted into asparagine. Sullivan *et al.* demonstrated that a major role of glutamine oxidation for respiration was to provide access to electron acceptors to support aspartate biosynthesis. They further demonstrated that aspartate supported cancer proliferation through its contribution to nucleotide synthesis (Sullivan et al. 2015). These data highlight the importance of the *glutamine-aspartate-asparagine* axis in cancer proliferation. In many tumor cells, some non-essential amino acids become essential because of the high metabolic demand (such as glutamine and serine) or mutations in specific metabolic enzymes (Geck et al. 2016). For example, arginine auxotrophic tumors have been described. These tumors cannot synthesize arginine due

to a lack of argininosuccinate synthase (Geck et al. 2016). This feature is of potential interest for cancer therapy since healthy cells do not need extracellular sources of non-essential amino acids.

In the absence of glutamine and other amino acids, cancer cells have developed a third way to obtain proper resources via the micropinocytosis of extracellular proteins, phagocytosis of apoptotic bodies and entosis of living cells (Pavlova et al. 2016, Zhang et al. 2017). After lysosomal degradation, cancer cells recover free amino acids and may therefore survive in unfavorable environment (fig.10).

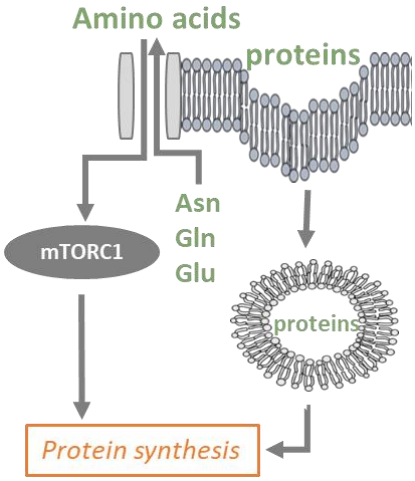

Figure 10. Extracellular amino acid import. *Cancer cells can import amino acids via specific antiporter (with exchange of other amino acids) or through proteolytic scavenging. In this case, extracellular proteins or live/dead cells are engulfed and digested in lysosomes to release free amino acids. Amino acids regulate mTORC1 activity and support protein synthesis.*

1.3. Fatty acid synthesis and oxidation

Lipids are important building blocks for producing new cells. They are major components of membranes, are able to fuel TCA cycle and are also involved in lipidation reactions and cellular signaling (DeBerardinis et al. 2016). Fatty acids can be obtained from extracellular media or synthesized *de novo* (fig.11).

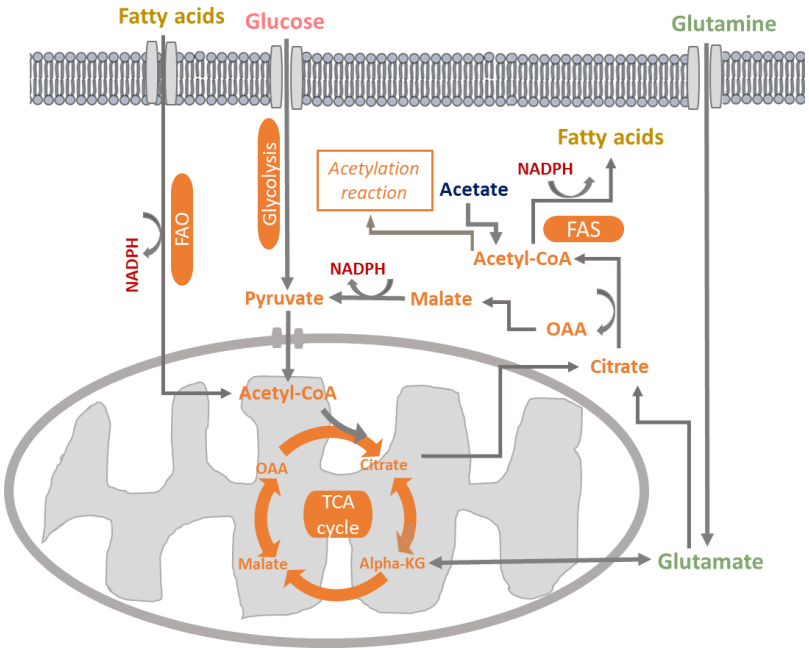

Figure 11: Fatty acid synthesis and oxidation. *Glucose, glutamine and acetate can support fatty acid synthesis (FAS) through mitochondrial and cytosolic acetyl-CoA production. Mitochondrial acetyl-CoA is exported to the cytoplasm through the shuttle citrate-malate-pyruvate. Extracellular lipids can be taken up from the environment. Lipids oxidation through fatty acid oxidation (FAO) also generate mitochondrial acetyl-CoA. Acetyl-CoA supports acetylation reaction and fuels TCA cycle.*

Fatty acid synthesis requires a source of acetyl-CoA and the reducing factor NADPH. Depending on the microenvironment and the availability, glucose, glutamine or acetate are the major source of acetyl-CoA while the NADPH mainly comes from PPP (DeBerardinis et al. 2016). Acetate can be taken up from the environment or provided by intracellular sources (Rohrig et al. 2016). Acetyl-coA can be either produced in the mitochondria or in the cytoplasm (fig.11). The cytosolic production of acetyl-CoA is supported by TCA cycle glutamine reductive carboxylation and by ACSS1-dependent metabolization of acetate (Metallo et al. 2011, Lakhter et al. 2016). Mitochondrial production of acetyl-CoA is supported by TCA cycle fueling of glucose and glutamine, by fatty acid oxidation, by ACSS2 or ACSS3-dependent metabolization of acetate and by oxidative degradation of some amino acids (Pietrocola et al. 2015, Schug et al. 2015, Zhang et al. 2020). To support fatty acid synthesis which occurs in the cytoplasm, mitochondrial acetyl-CoA can be exported to the cytosol through the citrate-malate-pyruvate shuttle (fig.11) (Pietrocola et al. 2015). To achieve this, mitochondrial acetyl-CoA is condensed with oxaloacetate to form citrate. Citrate is exported out of the mitochondria via citrate carrier and converted back into acetyl-CoA through ATP citrate lyase with concomitant production of oxaloacetate. This shuttle allows the exchange of several metabolic intermediates between the cytosol and mitochondria since cytosolic oxaloacetate can be metabolized into malate with consumption of NADH. Cytosolic malate can be transported back into the mitochondria to replenish TCA cycle and produces NADH or be converted into pyruvate with production of NADPH (Pietrocola et al. 2015).

While the *de novo* synthesis of fatty acids is low in most healthy cells, tumorigenesis is associated with high lipid synthesis (Pavlova et al. 2016). In the presence of abundant extracellular nutrients and oxygen, most tumors rely on *de novo* fatty acid production (Boroughs et al. 2015). Moreover, the three major enzymes involved in fatty acid synthesis (ATP citrate lyase, acetyl-CoA carboxylase and fatty acid synthase) are frequently upregulated in various cancer types (Pavlova et al. 2016). However, under some conditions such as acidosis, cancer cells need to import lipids from the extracellular environment (Corbet et al. 2016). Imported fatty acids can be stored into lipid droplets and serve as energy reserve to fulfill metabolic needs during the invasion process (Corbet et al. 2020). Imported lipids can also be metabolized into acetyl-CoA through fatty acid oxidation and acetyl-CoA can supply TCA cycle (fig.11.). Acetyl-CoA is also involved in protein acetylation reactions and modulates gene expression levels by epigenetic controls of histone acetylation (Corbet et al. 2016). Of note, upon oxidation, fatty acids can supply more than twice as much ATP per mole than oxidation of glucose or amino acids (Boroughs et al. 2015). To resume, like amino acid metabolism, cancer cells have developed various mechanisms to exploit lipid metabolism in order to sustain growth in hostile microenvironment

2. Microenvironment drives tumor metabolic plasticity

(Adapted from Schoonjans *et al.* 2020)

The tumor microenvironment (TME) is a dynamic network composed of cancer cells, stromal cells and extracellular matrix but also contains a complex mixture of signaling molecules (Arneth 2019). Stromal cells include many different types of cells including -among others- vascular and lymphatic endothelial cells, fibroblasts and infiltrating immune cells such as macrophages and lymphocytes. Tumors cells interact with these cancer-associated cells within the extracellular matrix and, in return, TME offers tumor-promoting conditions. These stromal cells, for instance fibroblasts and macrophages, that are activated by cancer cells are called cancer-associated fibroblasts (CAFs) and tumor-associated macrophages (TAM) (fig.12).

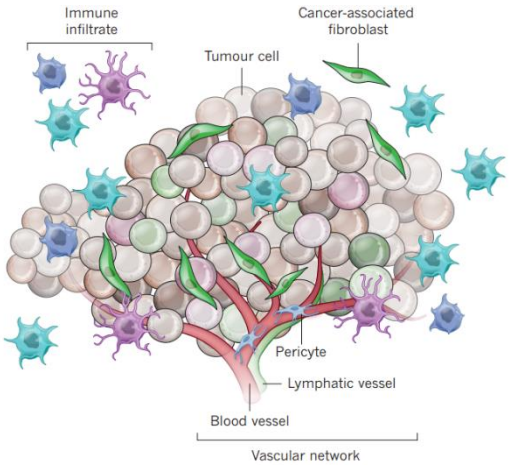

Figure 12: Tumor cells are surrounded by stromal cells (Junttila et al. 2013). *The TME is composed of a heterogenous mixture cancer cells and of stromal cells (vascular and lymphatic endothelial cells, cancer-associated fibroblasts and immune cells).*

Still abnormal and heterogeneous TME imposes constraints on fast-growing tumors. Limited access to mature vasculature leads to local hypoxia, accumulation of metabolic wastes and acidification and nutrient deprivation (Corbet et al. 2017). These constraints in turn induce profound metabolic

rewiring in tumors (vs. healthy tissues) but also within a given tumor with distinct metabolic preferences according to the tumor areas (fig.13).

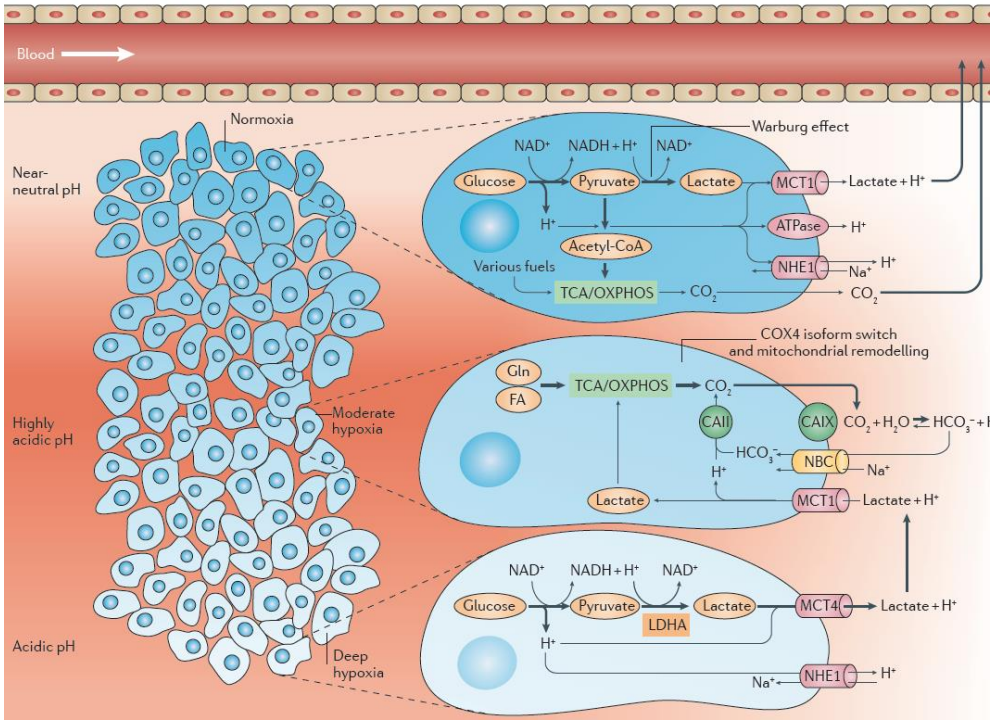

Figure 13: pH, oxygen levels and nutrient availability fluctuate inside the tumor microenvironment *(Corbet et al. 2017). Cancer cells close to blood vessels rely on glucose and other available bioenergetics to fuel glycolysis and OXPHOS. Downstream products, lactate, H^+ and CO_2 are efficiently washed-out into the bloodstream. When cancer cells start to be distant from blood vessels and enter in a moderate hypoxic environment, glutamine (Gln) and fatty acids (FA) fuel OXPHOS. After diffusion, CO_2 is not easily washed-out and is converted to H^+ and HCO_3^-, which generate a highly acidic environment. In regions of deep hypoxia, cancer cells only rely on glucose to fuel anaerobic glycolysis. Exported lactate and H^+ are substrates for cancer cells in the moderate hypoxic region reducing their acidification impact in deep hypoxia region.*

2.1. Hypoxia enhances metabolic plasticity

Hypoxia takes place when cancer cells have limited access to oxygen or when the balance between oxygen supply and consumption is disrupted. Several factors contribute to the occurrence of tumor hypoxia including chronic hypoxia (diffusion-limited hypoxia and hypoxemic hypoxia) and acute hypoxia (due to temporal fluctuations in red blood cell flux) (Sonveaux 2008, Bayer et al. 2012). The main physiological response to hypoxia is the stabilization of the transcription factor HIF-1α (Nakazawa et al. 2016). As explained in the first chapter of the introduction, HIF-1α increases glycolytic flux, prevents oxidative mitochondrial activity and enhances angiogenesis. In addition to decrease mitochondrial respiration, the decrease in acetyl-CoA entering into TCA cycle affects other metabolic pathways as it reduces the level of TCA cycle intermediates required for biomass production such as non-essential amino synthesis acids and fatty acid synthesis (Nakazawa et al. 2016). Therefore, hypoxic cancer cells exhibit an increase in glutamine consumption to compensate for the decrease in glucose contribution to TCA cycle (Nakazawa et al. 2016). As previously described, both oxidative and reductive glutamine metabolism can sustain TCA cycle. It has been shown that HIF-1α can shift glutamine metabolism from oxidative to reductive carboxylation to support lipid synthesis (Metallo et al. 2011).

There is increasing evidence that, under hypoxia, cancer cells rely on carbon sources other than glutamine and glucose (Eales et al. 2016). Under hypoxia, several cancer cells lines increased their uptake of extracellular lipids (Kamphorst et al. 2013). Hypoxia upregulates an enzyme involved in acetate

metabolism (ACSS2, acetate to acetyl-CoA) (Schug et al. 2015). As a consequence, a large fraction of fatty acid carbon is derived from acetate (Kamphorst et al. 2014). Overall, specific adaptations induced by hypoxia in acetate metabolism and/or fatty acid uptake influence the fuel choice (Kamphorst et al. 2013, Schug et al. 2015, Li et al. 2020). The acetate assimilation to maintain lipogenesis together with the increased uptake of fatty acid support the rapid proliferation of tumor cells under hypoxia (Kamphorst et al. 2013, Kamphorst et al. 2014, Schug et al. 2015). Serine metabolism under hypoxia was also investigated by Ye *et al*. They found that the expression of SHMT2, the enzyme that converts serine into glycine in mitochondria, was induced under hypoxia through HIF-1α. They also observed that depletion of this enzyme in hypoxic cells increased ROS levels, led to cell death *in vitro* and decreased tumor growth *in vivo*. They concluded that this enzyme was crucial to connect serine metabolism to mitochondrial redox control of cancer and to maintain cell survival (Ye et al. 2014).

Hypoxia is heterogeneous in solid tumors, a feature that can enhance metabolic cooperation between different microenvironment and cell types. For example, De Bock et al. demonstrated that tumor vascular endothelial cells (ECs) rely on glycolysis rather than on oxidative phosphorylation for ATP production. This allows oxygen to permeate further into the tumor instead of being directly consumed by proximal ECs (De Bock et al. 2013). Another example of metabolic cooperation is the symbiosis existing between hypoxic and oxygenated cancer cells within a tumor (fig.13) (Sonveaux et al. 2008): the lactate released by highly hypoxic glycolytic cancer cells is metabolized by less hypoxic cancer cells. As a consequence, glucose can diffuse through

the oxygenated tumor cell and fuel glycolysis of distant, hypoxic tumor cells. Hypoxia also drives angiogenesis and this will be detailed in chapter 4.

2.2. Metabolic reprogramming induced by extracellular acidosis

The increase in glycolytic flux leads to the production of protons in part from ATP hydrolysis. Protons need to be exported outside the cells to avoid cytoplasm acidity and to maintain cellular function. Therefore, cancer cells have developed different mechanisms to export protons outside the cell. It has been shown that under hypoxia, HIF-1α upregulates plasma membrane ion pumps and transporters leading to extracellular medium acidification (Taddei et al. 2013). Lactate and H^+ are exported in the extracellular medium through the MCT4 transporter. Protons can also be exported outside the cells by Na^+/H^+ exchangers and H^+-ATPases (Pillai et al. 2019). Of note, oxygenated areas are also involved in extracellular acidification because CO_2 produced by cellular respiration diffuses outside the cell and is hydrated in the extracellular medium in bicarbonate and proton (Corbet et al. 2017). The disorganized tumor vasculature prevents an efficient wash-out of H^+ released into the extracellular medium and contributes to its acidification (Corbet et al. 2017). Extracellular acidosis has been largely described promoting cancer cell migration, invasion and metastasis (Boedtkjer et al. 2020). Acidosis also plays a role in tumor metabolism reprogramming (fig.14) (Corbet et al. 2017).

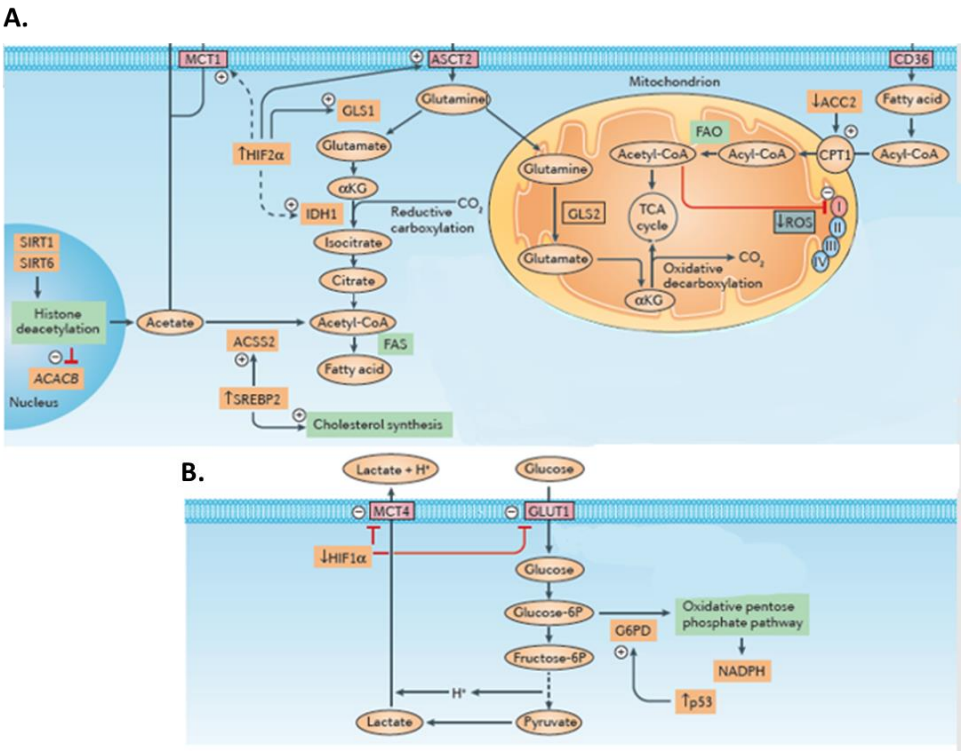

Figure 14. Metabolic reprogramming induced by extracellular acidosis *(adapted from Corbet and Feron 2017c). Extracellular acidosis induces changes in histone acetylation via the activity of sirtuins (SIRT1/6). The result is a decrease in HIF-1α and ACC2 and an increase in HIF1-2α and acetate. A. HIF1-2α increases glutamine import and metabolism and upregulates MCT1. SERBP2, also enhanced by acidosis, increases acetate metabolism into acetyl-CoA. Acetyl-CoA from acetate and reductive metabolism of glutamine support fatty acid synthesis (FAS). Due to downregulation of ACC2 (via deacetylation by sirtuin of the gene that encodes ACC2, ACACB), FAS and fatty acid oxidation (FAO) occur concomitantly under acidosis. FAO and glutamine oxidation support OXPHOS. By mitochondrial protein hyperacetylation, acetyl-CoA restrains complex I activity to limit ROS production. B. The decrease in HIF-1α expression induced by acidosis reduces glycolytic activity by decreasing glucose transport and lactate and proton efflux. Acidosis activates p53,*

which contributes to the enhancement of the pentose phosphate pathway (PPP). PPP produces NADPH for FAS.

In 2008, Chen et al. performed a genome-scale gene expression study in breast cancer to measure response to lactic acidosis. They observed that low-risk breast cancer patients exhibited a preference for aerobic respiration and a repression of glycolysis genes expression (Chen et al. 2008). In another study, Chen demonstrated that acidosis abolished stabilization of HIF-1α (Tang et al. 2012). In 2013, Lamonte et al. performed stable-isotope tracers of glucose, glutamine and palmitate under acidosis. They observed that acidosis redirects glucose away from glycolysis, increases respiratory metabolism and p53 activity (fig.14) (Lamonte et al. 2013). They also found that acidosis promoted an increase in glutamine uptake and consumption leading to the ATP generation. They measured an increase in fatty acid oxidation, which, together with glutaminolysis, increased ROS production. Interestingly, p53 activation by acidosis redirected glucose away from glycolysis towards the oxidative branch of the PPP to produce NADPH resulting in ROS neutralization (fig.14) (Lamonte et al. 2013). To study metabolic remolding induced by long-term exposure to acidosis, the team of Olivier Feron and Cyril Corbet developed a model of cancer cells chronically adapted to acidic pH (pH 6.5) (Corbet et al. 2014). Different cancer cell lines from various origins have been cultured in media buffered a pH 6.5 during several weeks. Acid-adapted cells were obtained when the proliferation rate of the cells maintained in the acidic medium was similar to that of parental cells (cultured at pH 7.4). With this model, Corbet et al. described that chronic exposure to acidosis leads to metabolic reprograming towards glutamine

and fatty acid metabolism (fig.14) (Corbet et al. 2014, Corbet et al. 2016). The change in expression of HIF-1α and HIF-2α, mediated by NAD^+-dependent activation of the deacetylase sirtuin, was the main driver of the glutamine metabolism shift. The upregulation of HIF-2α supported the expression of transporters and enzymes involved in glutamine metabolism while the reduction in HIF-1α accounted for a decrease in glycolytic turnover. Glutamine through reductive carboxylation was shown to contribute to fatty acid synthesis and changes in histone acetylation allowed concomitant fatty acid oxidation (FAO) (i.e. from fatty acids imported from the extracellular media). Interestingly, these authors also showed that acetylation of mitochondrial complex I reduced ROS production in these conditions of active stimulation of the TCA cycle. More recently, Corbet *et al.* demonstrated that acidosis favors the formation of lipid droplets used as sources of energy during metastases (Corbet et al. 2020). Another study has shown that chronic acidosis increases acetate metabolism. It was found that extracellular acidic pH triggered activation of SREBP2 by stimulating its nuclear translocation and binding to its targets, namely ACSS2 that promotes conversion of acetate into acetyl-CoA (Kondo et al. 2017). Consequently, acetate also contributes to the acetyl-CoA pool in acidosis. In summary, in order to reduce proton production, cancer cells shift their metabolism away from glycolysis and rely on glutamine and fatty acid metabolism. Even if hypoxia and acidosis are often considered as a whole and often present similar adaptation, some metabolic reprogramming are specific to each hallmark. Moreover, different studies demonstrated that areas of hypoxia and acidosis do not overlap in all tumors (Corbet et al. 2017).

2.3. How cancer cells escape to nutrient deprivation

Even if acidosis and hypoxia can regulate cell preferences in nutrients, the presence of nutrients themselves is a limiting factor for cell function. While some tumors regions are well vascularized, some others are poorly perfused leading to decreased availability of oxygen and of exogenous nutrients. Nutrient availability also fluctuates during tumor development. It has been established that, when tumors become deprived of nutrients, they decrease their demand in ATP in order to keep an adequate ATP/ADP ratio to drive unfavorable reactions (DeBerardinis et al. 2016). The mTOR pathway, which controls cell proliferation, regulates this energy demand. Indeed, under nutrient-rich conditions, mTORC1 promotes cell growth by stimulating biosynthetic pathways and repressing autophagy. On the opposite, when amino acid level is low, mTORC1 is inhibited and cell proliferation is consequently reduced while autophagy is activated (Rabanal-Ruiz et al. 2017, Kim et al. 2019). Moreover, Palm *et al*. demonstrated that the mTORC1 inhibition in a nutrient depleted microenvironment led to an increased micropinocytosis and lysosomal degradation resulting in free amino acid liberation (Palm et al. 2015). In response to specific nutrient limitations, cancer cells can shift their metabolism to other sources of energy. Polet *et al*. demonstrated that glutamine deprivation in leukemia cells led to the upregulation of the serine pathway independently from glucose metabolism. They observed that glutamine depleted medium induced the upregulation of serine metabolism enzymes (Polet et al. 2016). Another example of metabolic plasticity induced by specific food deprivation is provided by the glutamine

metabolism that is increased when using a glucose depleted medium (Le et al. 2012).

Cancer cells may also benefit from a symbiosis with other cells in the microenvironment (Lyssiotis et al. 2017). By-products of one type of cell could serve as a carbon source for another type of cell. The prototypical example is the lactate-based metabolic symbiosis: lactate released by hypoxic cells is taken up and consumed by more oxidative cancer cells thereby sparing glucose that can reach hypoxic cancer cells in larger amounts. (Sonveaux et al. 2008, De Bock et al. 2013) (fig. 15).

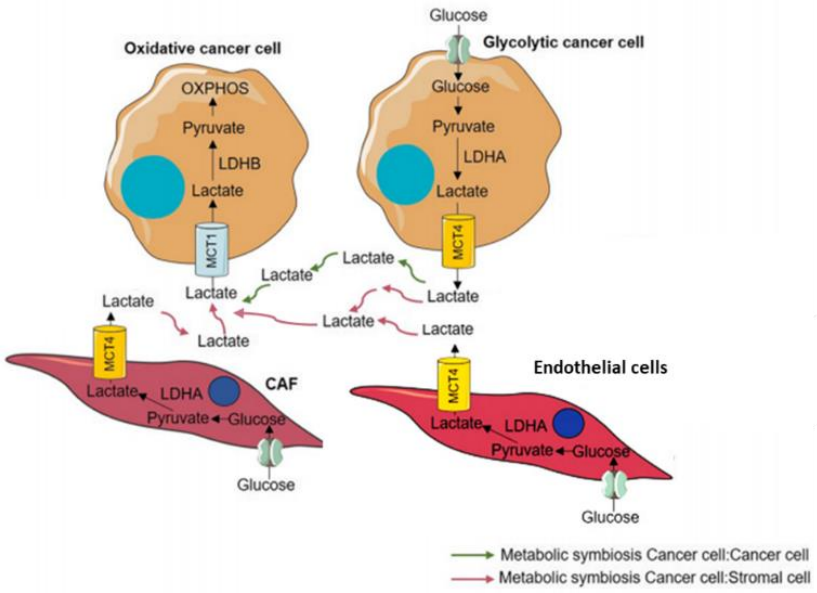

Figure 15: Metabolic symbiosis involving lactate metabolism (adapted from Mendes et al. 2020). *Glycolytic cancer cells, endothelial cells and cancer-associated fibroblasts (CAFs) export lactate which is imported by oxidative cancer cells to fuel TCA cycle (Mendes et al. 2020).*

Independently from hypoxia, lactate shuttle was also reported between cancer-associated fibroblasts (CAFs) and cancer cells, it was named the Reverse Warburg Effect. Cancer cells induce an oxidative stress in CAFs by secreting ROS, which triggers aerobic glycolysis through HIF-1 α and NF- κ B stabilization. The resulting increase in lactate production and export is used by cancer cells to sustain their metabolic needs (fig.15) (Fu et al. 2017).

In a more recent study, researchers observed that ovarian cancer cells secrete lysophosphatidic acid, which accounts for the induction of aerobic glycolysis in normal fibroblasts thereby promoting the transition to CAFs (Radhakrishnan et al. 2019). Moreover, other studies have documented that, depending on the cancer type, cancer cells can corrupt CAFs to produce specific metabolites to support their bioenergetic needs. For instance, in pancreatic cancer, pancreatic cancer-associated fibroblasts excrete alanine upon exposure to pancreatic cancer cells. Alanine is taken up by pancreatic cancer cells and used to fuel TCA cycle. Moreover, alanine can outcompete glucose and glutamine to fuel metabolism and decrease tumor dependency to glucose and glutamine, which are limited in the pancreatic tumor microenvironment (Kamphorst et al. 2015, Sousa et al. 2016). In ovarian tumors, CAFs instead produce glutamine to fuel ovarian cancer cells (Yang et al. 2016). CAFs are actually proposed to consume glutamate and lactate, the waste products of ovarian cancer cells, in order to produce glutamine (Tajan et al. 2016). In a similar way, in glutamine-restricted microenvironment, astrocytes produce glutamine for glioblastoma (Tardito et al. 2015) and adipocytes produce glutamine for pancreatic cancer cells (Meyer et al. 2016).

3. Dichloroacetate to target tumor metabolism

The exacerbated glycolytic flux is an enticing target for anti-cancer treatments (Gatenby et al. 2004, Porporato et al. 2011). Among glycolytic modulators, inhibitors of pyruvate dehydrogenase kinase (PDK) have received particular attention (Kroemer et al. 2008, Saunier et al. 2016, Golias et al. 2019). PDK inactivates the enzyme pyruvate dehydrogenase (PDH). The active PDH converts pyruvate to acetyl-CoA that fuels the tricarboxylic acid cycle (TCA). Therefore, the inhibition of PDK reactivates PDH leading to a redirection of glucose metabolism from cytoplasmic glycolysis to mitochondrial oxidation (fig.15) (Bonnet et al. 2007).

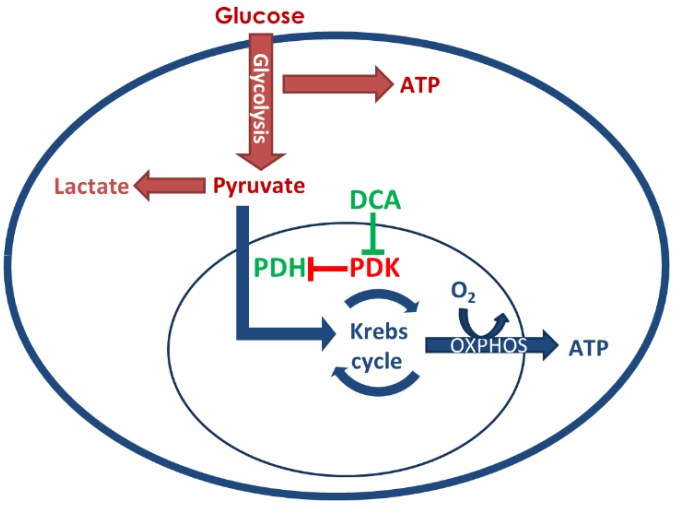

Figure 16: Dichloroacetate (DCA) shifts metabolism from glycolysis to glucose oxidation. *DCA inhibits PDK and consequently allows pyruvate to fuel the TCA cycle and decreases lactate production.*

3.1. Inhibition of PDK by dichloroacetate

Dichloroacetate is the conjugate base of dichloroacetic acid, it will be named DCA along this work. DCA was first described as a PDK inhibitor by Whitehouse et al., in 1973 (Whitehouse et al. 1973). DCA enhances pyruvate mitochondrial oxidation and reduces lactate production. Since DCA was discovered as a metabolic modulator, numerous studies have been performed in order to fully characterized the therapeutic action of DCA.

- Biodistribution and metabolism of DCA

DCA is a by-product of water chlorination and a metabolite of industrial solvents that makes chronic exposure inevitable. Currently, toxicological studies of DCA exposure in atmosphere and chlorinated drinking water do not support the hypothesis that exposure to DCA from environmental sources represents a hazard to humans. Human toxicity has so far been limited to reversible effects on the nervous system and the liver (Stacpoole 2011, Stacpoole 2017, Tataranni et al. 2019).

DCA therapeutic potential began to be studied by Stacpoole et al., in 1970 (Stacpoole et al. 1970). In the last 30 years, DCA has been mainly used to treat congenital and acquired forms of lactic acidosis. In parallel, toxicity, metabolism and pharmacokinetics of DCA have also been investigated (Stacpoole 1989, Stacpoole et al. 1992, Stacpoole et al. 1992, Stacpoole et al. 1998). DCA is a small molecule (151 Da) with a pKa of 1.48. DCA is rapidly absorbed by the gastrointestinal tract and is distributed to multiple tissues throughout the body with a bioavailability of 100%. In patients treated for lactic acidosis, DCA exerts a systemic lactate-lowering effect within 60 min of

a single oral or intravenous dose of 10 mg/kg (Stacpoole et al. 1998). Because DCA is ionized at physiological pH, it cannot cross the plasma membrane by diffusion. Due to its structure, Stacpoole *et al.*, first hypothesized that DCA crosses both plasma and mitochondrial membranes via the monocarboxylate and pyruvate transporters respectively (Kankotia et al. 2014). In 2011, Babu *et al.*, demonstrated that the sodium-coupled monocarboxylate transporter 1 (SMCT1/SLC5A8) has a high affinity for DCA and was responsible for cellular DCA uptake (Babu et al. 2011). DCA is dechlorinated to glyoxylate by cytosolic and mitochondrial glutathione transferase zeta 1 (GSTZ1). The GSTZ1 enzyme was first identified as a hepatic enzyme but GSTZ1 transcripts were consecutively found in kidneys, testes, heart, brain and other human tissues (James et al. 2017). The plasma half-life of an initial dose of DCA is around 1 hour and increases with dose repetition because DCA inhibits its own metabolism via inactivation of GSTZ1. Among human beings, there are known polymorphisms in *GSTZ*, which may account for differences in the ability to metabolize DCA. Used at therapeutically doses (10 to 50 mg/kg daily), DCA has a good tolerability and safety although it can produce a reversible peripheral neuropathy in adults (Kankotia et al. 2014).

- Mechanism of action of DCA on PDK

DCA is a structural analogue of pyruvate (fig.17), that is known to act as an allosteric inhibitor of PDK (Stacpoole 1989).

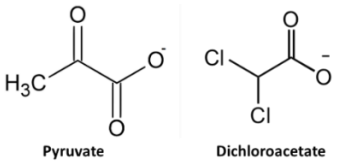

Figure 17. Chemical structure of pyruvate and dichloroacetate.

Each PDK isoform has two domains of about equal size (fig.18). The N-terminal regulatory domain binds PDH via the lipoyl-binding site and contains the pyruvate-binding site. The C-terminal catalytic domain contains ATP/ADP-binding site where phosphoryl transfer occurs (Patel et al. 2014). DCA acts on the pyruvate-binding site of PDK and inhibits the catalytic activity of the kinase(Papandreou et al. 2011).

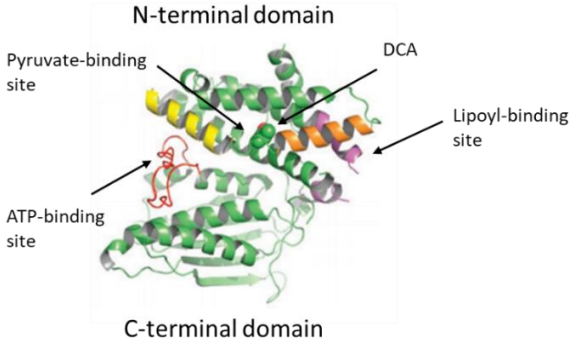

Figure 18: Binding of the pyruvate analog DCA induces conformational changes in PDK1 *(adapted from Milne 2013). Upon binding of DCA, PDK1 enhances small movements of helices 6 (orange) and 7 (yellow). Movement of this helical rod may induce cross-talk between the ATP-binding site (red), the lipoyl-binding site (magenta), and the pyruvate/DCA-binding site.*

There are four isoforms of PDK (PDK1-4) which vary in terms of tissue distribution, kinetic activity and sensitivity to DCA. PDK2 is the isoform that is the most sensitive to DCA, PDK3 the most resistant and PDK1 and PDK4 have an intermediate sensitivity (Papandreou et al. 2011). PDK2 is ubiquitously expressed in tissues, other isoforms have a tissue-specific expression (Kankotia et al. 2014). In several diseases such as cancer, expression of PDK isoforms is altered (Papandreou et al. 2011).

PDK phosphorylates and inactivates PDH. PDH is one of the three enzymes of the pyruvate dehydrogenase complexes (PDC). PDC is a multienzyme complex with the core structure formed by 48 subunits of dihydrolipoamide acetyltransferase (E2) and 12 subunits of dihydrolipoamide dehydrogenase-binding protein (E3BP) (Golias et al. 2019) (fig.19). 20-30 subunits of pyruvate dehydrogenase (E1) are attached to the subunit binding domains of E2 and 6-12 subunits of dihydrolipoamide dehydrogenase (E3) are attached to E3BP. Regulatory PDK and PDP (pyruvate dehydrogenase phosphatase) are also part of this shell, binding to lipoyl domains (L1, L2 and L3) of E2 and E3BP.

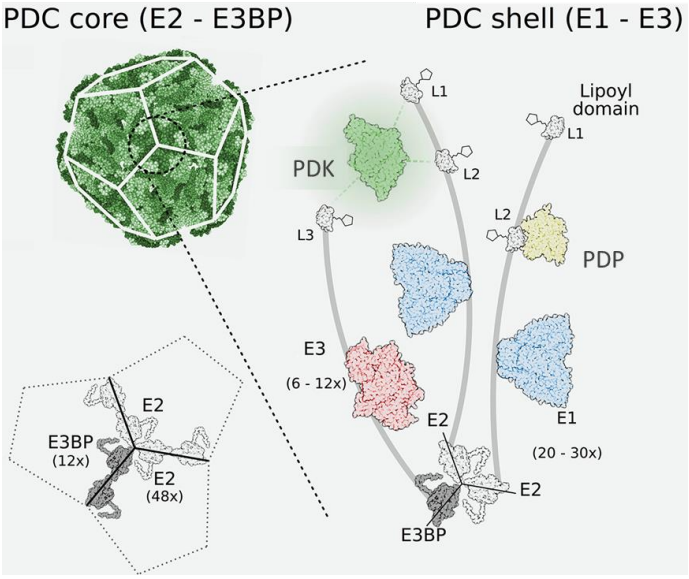

Figure 19: Schematic presentation of domains and components of the PDC *(adapted from Golias et al., 2019). PDC core is constituted by several copies of E2 and E3BP subunits to which several copies of E1 and E3 subunits are bound. PDK and PDP bind the lipoyl domains (L1, L2 and L3) of E2 and E3BP.*

PDH (E1) presents 3 serine phosphorylation sites (fig.20) although the phosphorylation of one residue is sufficient to inactivate the enzyme (Papandreou et al. 2011). The four isoforms of PDK have different kinetics parameters of phosphorylation, PDK2 possesses the greatest activity (Saunier et al. 2016). The activity of PDK is stimulated by ATP, NADH and acetyl-CoA and is inhibited by ADP, NAD^+, CoA and pyruvate (fig.20) (Saunier et al. 2016).

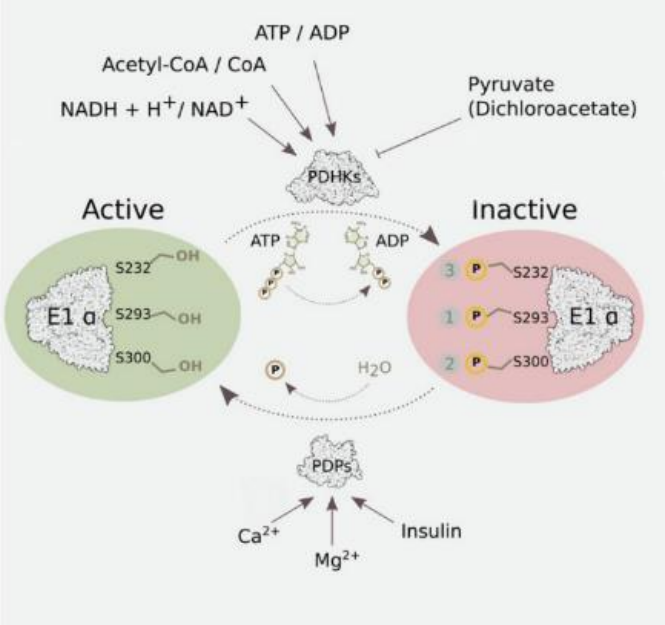

Figure 20. Regulation of PDH activity *(adapted from Golias et al., 2019). PDK and PDP regulate the PDH activity (E1α subunit of PDC). PDK inhibits PDH by phosphorylating PDH serine residues and PDP activates PDC by dephosphorylating these sites. Ratios of PDC end-products/substrates regulate PDK activity and pyruvate or dichloroacetate allosterically inhibit PDK. PDP is activated by insulin, Ca^{2+} and Mg^{2+} ions.*

PDP is responsible for PDH dephosphorylation and thus reactivation. There are two isoforms of PDP with similar rates of dephosphorylation. PDPs are activated by Ca^{2+} and Mg^{2+} ions, and insulin (Saunier et al. 2016).

PDC is located into the mitochondrial matrix and catalyzes the irreversible oxidative decarboxylation of pyruvate into Acetyl-coA, CO_2 and NADH (Papandreou et al. 2011). Through its action on PDH, PDK inhibits the conversion of pyruvate into Acetyl-CoA. DCA inhibits PDK and thus activates PDH thereby redirecting pyruvate into the mitochondria and reducing lactate production (Kankotia et al. 2014). In other words, DCA induces a shift from glycolysis to oxidative phosphorylation (OXPHOS).

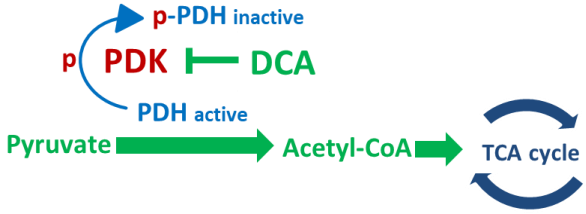

Figure 21. PDK inhibition by DCA enhances pyruvate conversion into acetyl-CoA. *PDK phosphorylates and inactivates PDH. Active unphosphorylated PDH metabolizes pyruvate into acetyl-CoA which can fuel TCA cycle. By inhibiting PDK, DCA activates PDH and allows pyruvate conversion into acetyl-CoA.*

3.2. Anti-cancer action of DCA

PDH phosphorylation by PDK is highly regulated in cancer. In various cancer cell lines, it has been shown that the expression of PDK1 and PDK3 is up-regulated by HIF-1 α (Kim et al. 2006, Papandreou et al. 2006, Lu et al. 2008). In the Burkitt's lymphoma cell line, c-Myc binds to PDK1, PDK2 and PDK3

promoters, suggesting that it could play a role in PDK expression (Li et al. 2003). Another study documented that p53 negatively regulates PDK2 in different cancer cell lines (Schroder et al. 2010). Moreover, numerous studies have measured an upregulation of one or more isoforms of PDK depending on the tumor type, PDK overexpression being associated with poor prognosis (Zhang et al. 2015, Saunier et al. 2016, Golias et al. 2019). Post-translational regulation of PDK1 has also been reported with the demonstration that oncogenic tyrosine kinases are able to phosphorylate PDK1 and enhance its kinase activity (Hitosugi et al. 2011). Altogether these data indicate that the activity and expression of PDK are strongly regulated by oncogenic signaling, making it a potential attractive target for anti-cancer therapy.

In 2007, Bonnet *et al*. showed that DCA, through PDK inhibition, reduces cancer cell proliferation via the induction of oxidative stress and apoptosis in various cancer cell types but not in healthy cells (Bonnet et al. 2007). Since this first study, more than 200 preclinical studies have been performed studying the anti-cancer action of DCA in mice bearing (most often) human tumors (Stacpoole 2017).

- Proliferation inhibition and apoptosis induction

By reversing aerobic glycolysis, DCA decreases glycolytic intermediates available for biosynthetic pathways, in particular for the pentose phosphate pathway (Sutendra et al. 2013). This reduction in building blocks from glycolysis was proposed to account for the anti-proliferative effects of PDK inhibition (De Preter et al. 2016). In addition, by reactivating the

mitochondrial activity, DCA reverses the suppression of mitochondria-dependent apoptosis (fig.22) (Michelakis et al. 2008, Sutendra et al. 2013).

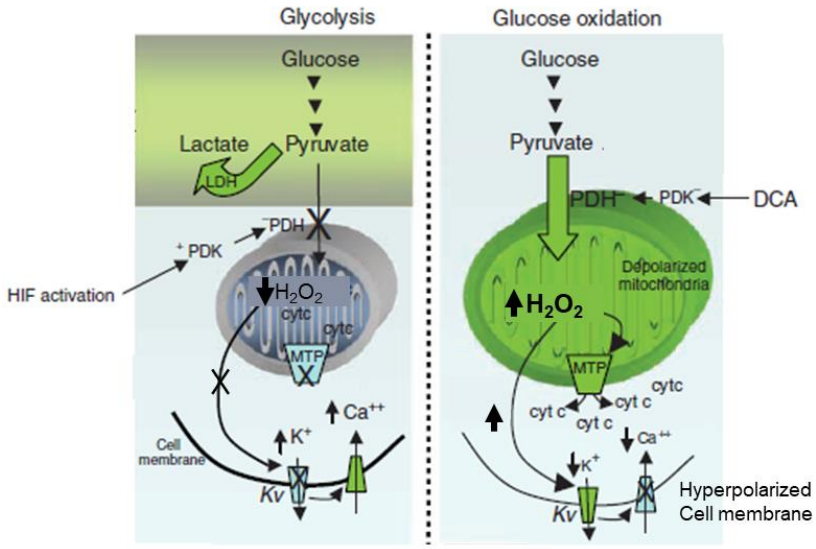

Figure 22: DCA reverses apoptosis resistance induced by the glycolytic phenotype *(adapted from Michelakis, 2008). By increasing glucose oxidation, DCA enhances TCA cycle activity and mitochondrial H_2O_2 production leading to depolarization of mitochondrial membrane which in turn activates voltage- and redox-sensitive mitochondrial transition pore (MTP). Activation of MTP allows export of the pro-apoptotic factor cytochrome-c which triggers apoptosis. The increase of H_2O_2 reduces intracellular potassium ions and calcium ions which further enhances apoptosis induction (Michelakis et al. 2008).*

This is explained by the increased acetyl-CoA production and TCA cycle activity, promoting the formation of NADH and $FADH_2$, and a stimulated flux of electrons in the mitochondrial respiratory chain. DCA thus leads to a progressive decrease in the mitochondrial membrane potential and an increase in ROS production which in turn activate voltage- and redox-

sensitive mitochondrial transition pore (MTP). Pro-apoptotic activators, like apoptosis-inducing factor and cytochrome c are then released from the mitochondria upon MTP opening. The translocation of pro-apoptotic factors from the mitochondria to the cytoplasm induces apoptosis through the activation of caspases signaling. In addition, translocated ROS are able to activates Kv1.5 potassium ion channels present on the plasma membrane. Because intracellular potassium ions exert a tonic inhibition on caspases, the increase efflux of potassium ions from the cell relieves this inhibition, further enhancing apoptosis. The expulsion of potassium ions hyperpolarizes the plasma membrane which inhibits voltage-dependent Ca^{2+} entry. The decreased intracellular Ca^{2+} level inhibits the activation of NFAT (nuclear factor of activated T cells), which further increases Kv1.5 expression; creating a positive feedback loop ultimately resulting in reduced tonic inhibition of caspases (Michelakis et al. 2008).

Morfouace *et al*., reported another mechanism of apoptosis induction by DCA. These authors observed that DCA reactivates OXPHOS in cancer stem cells without ROS production and consecutive anti-cancer apoptosis. They demonstrated that DCA induces a Bax-dependent apoptosis via the increased expression of Foxo3 and p53. By inducing Foxo3 and p53 expression, DCA enhances the overexpression of BH3-only proteins (Bad, Noxa, and Puma), which in turn facilitates Bax-dependent apoptosis (Morfouace et al. 2012).

Pro-apoptotic effect of DCA is not always observed in *in vitro* studies. DCA can induce cytostatic effects (ie, no cell death) depending on cancer cell types

and/or DCA concentrations. Several studies have documented that DCA concentrations lower than 5 mM inhibit cancer cell proliferation without inducing apoptosis (Sun et al. 2011, Delaney et al. 2015, Harting et al. 2017).

- Extracellular acidosis reduction and metastasis inhibition

The second major impact of DCA on tumor metabolism is the reduction of lactate production and the buffering of H^+ by dehydrogenases located in the mitochondria. Therefore, lactate and H^+ efflux is reduced as well as extracellular acidosis (Kankotia et al. 2014). Since the extracellular acidic pH resulting from a high glycolytic turnover facilitates the breakdown of the extracellular matrix required for cancer cell invasion, reduction in tumor acidosis could be, in part, responsible for the anti-metastatic effect of DCA observed in some *in vivo* studies (Michelakis et al. 2010, Sun et al. 2010, Kolesnik et al. 2015).

- Angiogenesis inhibition

Besides these direct metabolic effects, it has been observed that DCA decreases tumor angiogenesis (Michelakis et al. 2010, Duan et al. 2013, Sutendra et al. 2013, Sutendra et al. 2013, Kinnaird et al. 2016). Several studies that reported a reduction in tumor angiogenesis after DCA treatment also documented inhibition of HIF-1α within the tumor tissue (Michelakis et al. 2010, Sutendra et al. 2013, Kinnaird et al. 2016). DCA has actually been reported to inhibit HIF-1α both *in vitro* and *in vivo* by either increasing the production of alpha-ketoglutarate (a cofactor of PHD) or by increasing p53 activity (that competes with HIF-1α for the same co-transcription factor) in response to ROS production (Michelakis et al. 2010, Sutendra et al. 2013,

Kinnaird et al. 2016) (Sutendra et al. 2013). Through HIF-1α degradation, DCA reduces the expression of HIF-1α target genes including pro-angiogenic effectors such as vascular endothelial growth factor (VEGF) (Sutendra et al. 2013). However, a direct effect of DCA on endothelial cells, which trigger angiogenesis, has never been properly investigated. The rationale behind the interest of studying a direct action of DCA on endothelial cells will be detailed in chapter 4 (metabolism in tumor angiogenesis).

- Lipid metabolism dysregulation

In 1978, Stacpool *et al.*, observed that DCA lowers plasma cholesterol and triglyceride levels in diabetics rats but also in diabetic and hypercholesterolemia patients (Stacpoole et al. 1978). Later, they discovered that DCA administration decreases HMGCoA reductase activity (the rate-limiting enzyme in cholesterol biosynthesis) in liver and leukocytes (Stacpoole 1989). This inhibition leads to a reduction in total and low-density lipoproteins (LDL) cholesterol.

More recently, Khan *et al.* (Khan et al. 2017) elucidated another non-exclusive mechanism of DCA-dependent regulation of LDL cholesterol. They found that DCA increases low-density lipoprotein receptor (LDLR) expression and thus LDL intake in different hepatic and leukemic cell lines in response to enhanced expression of ERK5, a redox MAPK. ERK5 activates the transcription factor MEF2 that upon interaction with cognate binding sites within LDLR promoter stimulate its expression (Khan et al. 2017).

- Enhancement of anti-tumor immunoreactivity

Two different mechanisms link DCA to immune modulations in cancer, either through enhancement of MHC-1 expression or upon reduction of extracellular acidosis.

In leukemia cells, it has been shown that DCA, by reactivating OXPHOS, increases MHC-1 expression. Researchers identified that the forced respiration induced by DCA leads to increased levels of ERK5 which in turn increases MHC-1 expression (Charni et al. 2010).

The acidic microenvironment driven by highly glycolytic cancer cells also exerts an immunosuppressive function. Interestingly, it has been observed that DCA promotes immune stimulation through the inhibition of lactate and proton accumulation (Ohashi et al. 2013).

3.3. DCA in combined therapies

In many studies, DCA potentiates the effect of other anti-cancers therapies such as chemotherapeutic agents, radiation therapy and targeted therapies. More than 50 reports have been listed in the following reviews (Kankotia et al. 2014, Stacpoole 2017, Tataranni et al. 2019). In most of them, DCA overcomes resistance to radiation or chemotherapy through mitochondrial activity reactivation and enhancement of apoptosis. There is a strong association between PDK overexpression and chemoresistance explaining why DCA increases chemosensitivity in different cancer types (Tataranni et al. 2019).

For instance, in a study of hypoxia-induced chemoresistance in gastric cancer, researchers observed that the levels of HIF-1α and PDK-1 were higher in-patients who showed recurrence after chemotherapy (Xuan et al. 2014). They found that the expression of PDK-1 was positively correlated with HIF-1α expression. Moreover, they observed *in vitro* that PDK-1 expression was higher under hypoxia. Finally, they observed that DCA treatment was able to re-sensitize resistant gastric cancer cells through the alteration of glucose metabolism (Xuan et al. 2014). These results suggest that metabolic changes induced by hypoxia, such as higher PDK-1 expression, could be a marker of chemoresistance as well as a target for DCA therapy. DCA has also been studied in combination with bevacizumab, an anti-angiogenic drug (Kumar et al. 2013). Kumar et al. showed that glioblastoma cells that were rendered resistant to anti-angiogenic therapy (after long-term exposure to bevacizumab) enhanced HIF-1α-related gene expression and consequently presented a shift from mitochondrial respiration to glycolysis. They showed that DCA reversed this shift induced by bevacizumab, highlighting the plasticity of tumor metabolism in response to therapeutic agents. These two studies underline the ability of DCA to counteract drug resistance induced by HIF-1α and the benefit of combining it with other anti-cancer agents.

DCA was also studied in combination with metabolic agents. For instance, the combination of DCA with metformin, a metabolic drug that inhibits mitochondrial respiration, shows promising results in anti-cancer therapies. Metformin suppresses tumor growth in different cancers via the inhibition of complex 1 which disrupts oxidative phosphorylation and subsequently increases glycolytic metabolism (Ward et al. 2017). Metformin is thus leading

to excessive lactate production and glucose consumption that may be opposed by DCA administration, suggesting a potential benefit of combining metformin with DCA. Different studies on glioblastoma, ovarian, lung and breast cancers have actually confirmed that DCA enhanced cytotoxicity of metformin via the reduction of metformin-mediated lactate accumulation (Haugrud et al. 2014, Li et al. 2016, Ward et al. 2017, Kolesnik et al. 2020). In addition, DCA in combination with metformin enhances oxygen consumption and ROS production suggesting an increase of TCA cycle fueling by acetyl-CoA (Choi et al. 2014). Another recent study combined DCA with arginase in auxotroph tumors to arginine (Verma et al. 2019). Verma *et al.* observed that this drug combination synergistically reduced tumor growth both *in vitro* and *in vivo*. They observed an increase in the expression of genes involved in cell cycle and p53 signaling but the underlying mechanism is still unknown (Verma et al. 2019).

3.4. DCA in cancer clinical trials

There are a few published clinical trials related to the use of DCA as a single agent in cancer therapy. DCA was first tested in a small clinical trial with five GBM patients for up to 15 months. Patients were treated with a starting dose of 12.5 mg/kg orally twice daily for 1 month and then the dose was increased to 25mg/kg orally twice daily. After that, a dose de-escalation protocol was followed, decreasing the dose by 50% when dose-limiting toxicity occurred. Peripheral neuropathy was the only apparent toxicity and when the dose was decreased to 6.25 mg/kg, none of the patients experienced such neuropathy. One patient died from brain edema complications 3 months after DCA

therapy. After 15 months of DCA treatment, the four others patients had stable disease and all were still alive at 18 months (Michelakis et al. 2010). Another phase 2 clinical trial on patients with metastatic breast cancer and advanced stage non-small cell lung cancer (NSCLC) had to be closed earlier, after seven patients enrolled, for safety concerns. DCA 6.25 mg/kg was administered orally twice daily. The only breast cancer patient had a stable disease after 8 weeks, quickly followed by progression in the brain. For the six other patients with advanced NSCLC, two patients had disease progression prior to the first scheduled scans. Two patients withdrew consent within a week of enrollment, one after experiencing a pulmonary embolism and the other to enroll in hospice care. Within 1 week of initiating DCA, one patient died suddenly of unknown cause and one experienced a fatal pulmonary embolism. Researchers conclude that patients with previously treated advanced NSCLC did not benefit from oral DCA (Garon et al. 2014). A phase 1 trial with personalized, *GSTZ1* genotype – based DCA dosing in 8 adults with recurred brain tumors evaluated that chronic DCA administration was well tolerated, without major neurotoxicity (Dunbar et al. 2014). Another phase 2 trial in myeloma has evaluated associations between *GSTZ1* genotyping, DCA response and peripheral neuropathy on six patients. Researchers observed that patients with low activity promoter genotype showed the strongest response, but also the most severe neuropathy. They suggest that identifying the maximum tolerated DCA dose regarding *GSTZ1* genotyping could be useful to achieve maximum benefit from DCA treatment (Tian et al. 2019). Additionally, different case reports have been published. In one patient with recurrent metastatic melanoma, DCA therapy

resulted in regression and stabilization for over 4 years' duration (Khan et al. 2017). In another patient, DCA therapy resulted in tumor stabilization of stage 4 colon cancer for a period of nearly 4 years (Khan et al. 2016). One patient with non-Hodgkin's lymphoma showed complete remission after four months of DCA auto-medication. The patient remains tumor-free after 2 years of continuous DCA usage (Flavin 2010). Finally, a phase 2 trial of DCA in combination with cisplatin and radiation in 50 patients with head and neck squamous cell carcinoma is still ongoing (NCT01386632).

3.5. Derivatives of DCA

In order to increase DCA efficacy on cancer cells and to decrease the toxicity of DCA, several DCA derivatives have been developed (James et al. 2017, Tataranni et al. 2019). The efficacy of two of them, Mito-DCA and Mitaplatin, have shown promising results on cancer cells. Mito-DCA, a fusion of a lipophilic cation to three DCA molecules was reported to facilitate transport across mitochondrial membrane and to exceed DCA in potency against some human prostate cancer cell lines (Pathak et al. 2014). Mitaplatin is a fusion of one molecule of cisplatin and two molecules of DCA. After crossing the plasma membrane, mitaplatin becomes reduced and releases DCA and cisplatin that attack DNA. Upon exposure to mitaplatin, an increase in apoptosis was observed in several human cancer cell lines, but not in healthy human cells with an IC_{50} value more than 8 times lower than IC_{50} values for DCA (Dhar et al. 2009, Xue et al. 2012).

4. Metabolism in tumor angiogenesis

4.1. Glycolytic switch to angiogenic switch

Hypoxia induces both a glycolytic switch and an angiogenic switch that both contribute to tumor progression (fig.23) (Porporato et al. 2011).

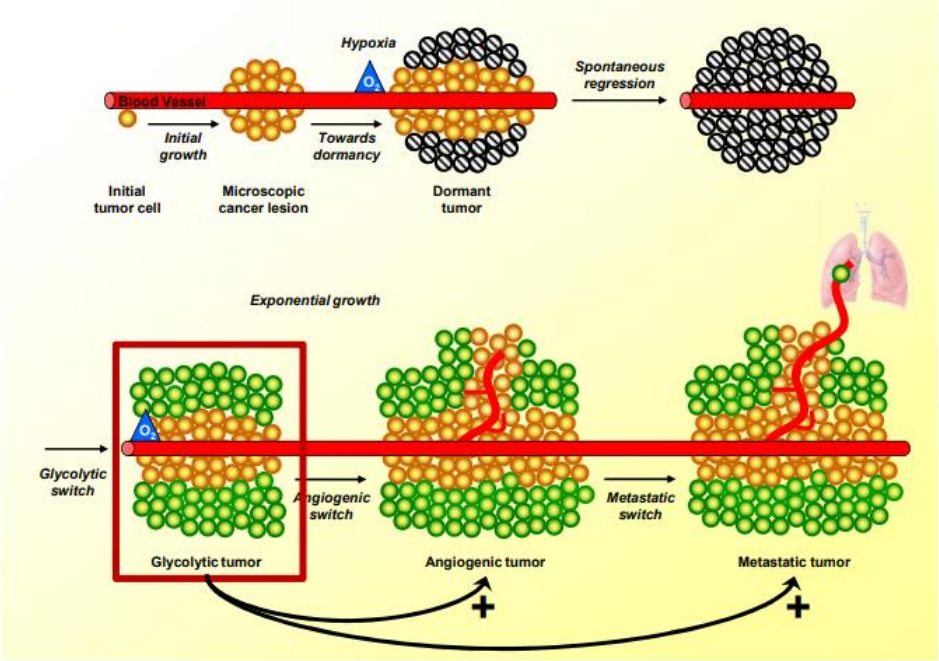

Figure 23: Glycolytic switch promotes angiogenic switch *(Sonveaux P). Cancer cells that acquired genetic mutations to over proliferate need to adapt to hypoxia in order to continue to growth far from blood vessels. The glycolytic switch, initially induced by hypoxia, allows a dormant tumor to enter into an exponential growth phase. Glycolytic tumors acquire the ability to trigger angiogenesis inducing an angiogenic switch leading to a more aggressive phenotype able to metastasize.*

In hypoxic cancer cells, HIF-1α is stabilized. In addition to the promotion of glycolytic metabolism, HIF-1α increases the expression of pro-angiogenic

growth factors such as vascular endothelial growth factor (VEGF) which are secreted in the tumor microenvironment. Pro-angiogenic growth factors enhance vessels sprouting to extend the vasculature towards the tumor and supply the growing tumor with oxygen and nutrients. Pro-angiogenic growth factors can also be secreted by non-cancerous cells present in the hypoxic tumor microenvironment such as tumour-associated macrophages (fig.24) (Wong et al. 2017).

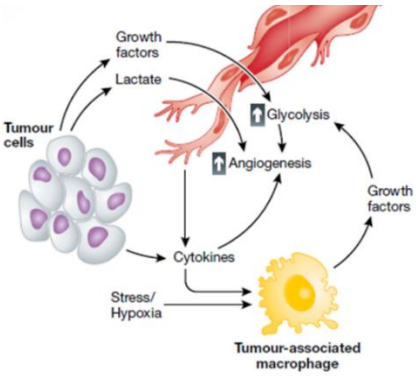

Figure 24. Tumor microenvironment triggers angiogenesis *(adapted from Wong et al. 2017). Glycolytic cancer cells produce pro-angiogenic growth factors and lactate. The hypoxic environment also increases the release of growth factors by tumor-associated macrophages. These factors trigger angiogenesis through ECs activation and enhancement of glycolytic flux in ECs.*

VEGF is a main driver of the angiogenic process. VEGF binds VEGF receptor 2 (VEGFR2) on ECs and induces an intracellular signaling cascade leading to ECs proliferation and migration (Fitzgerald et al. 2018). ECs line blood vessels and ensure delivery of oxygen and nutrients to surrounding tissues. Another driver of angiogenesis is the lactate released by glycolytic cancer cells (fig.25). ECs and oxidative cancer cells can uptake lactate and convert it into pyruvate which leads to HIF-1α stabilization through allosteric inhibition of PHD (the enzyme involved in HIF-1α degradation). In oxidative cancer cells, HIF-1α stabilization enhances VEGF production. In ECs, PHD inhibition by pyruvate stabilizes HIF-1α and nuclear factor-κB (NF-κB) that enhance the expression

of VEGF-receptor and induce an autocrine pro-angiogenic signaling through bFGF (indirectly controlled by HIF-1) and IL-8 (NF-κB target gene product) (fig.25). Moreover, lactate conversion into pyruvate generates $NADH+H^+$ which can produce ROS through metabolization by NAD(P)H oxidase. ROS can then reinforce PHD inhibition and increase activation of NF-κB (Vegran et al. 2011, Dhup et al. 2012, Sonveaux et al. 2012).

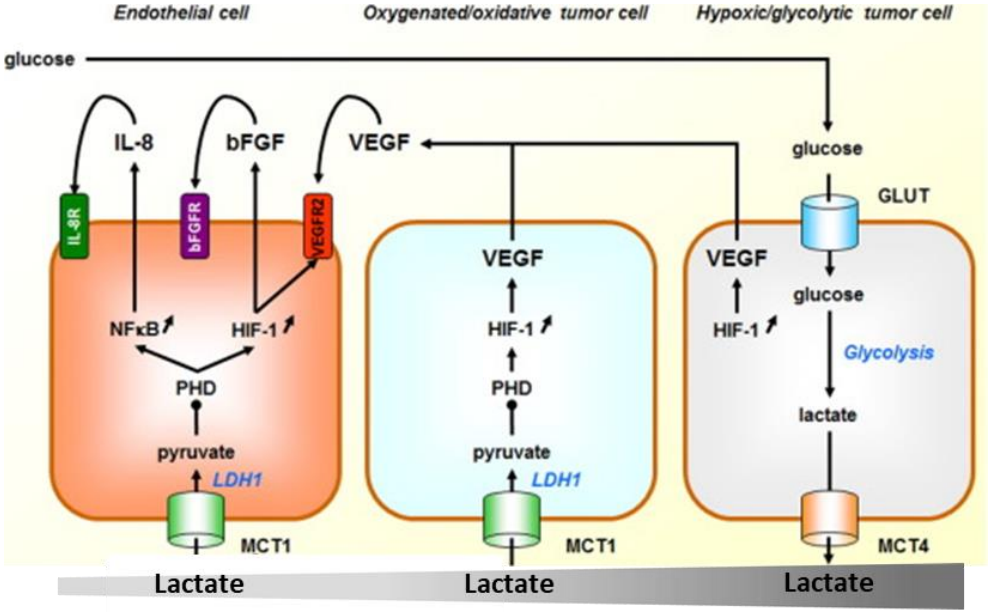

Figure 25. ECs activation by angiogenic signaling *(adapted from Spugnini et al., 2015). HIF-1α signaling in hypoxic tumor cells enhances lactate and VEGF secretion. Lactate can be taken up by oxidative tumors cells or by ECs and converted into pyruvate. In oxidative cells, pyruvate inhibits PHD which enhances VEGF production by HIF-1α. In ECs, pyruvate enhances the expression of VEGF-receptor (through HIF-1α stabilization) and an autocrine pro-angiogenic signaling through bFGF (indirectly controlled by HIF-1α) and IL-8 (NF-κB target gene product).*

Upon stimulation by pro-angiogenic factors, ECs are able to sprout to extend the vasculature (angiogenesis). Although angiogenesis is a physiological process, the over-expression of pro-angiogenic factors in cancer leads to a pathological process where blood vessels are functionally and structurally abnormal. Newly formed tumor vessels are immature, irregularly shaped and leaky resulting in irregular blood flow creating new hypoxic regions and thus more angiogenic factors production. Poor perfusion induces chemotherapeutic resistance and discontinued mural ECs facilitate tumor cells dissemination and promotion of metastases (Carmeliet 2005, Wong et al. 2017).

4.2. Metabolic reprogramming of tumor endothelial cells

To form new blood vessels, ECs metabolism is upregulated to sustain this high energy and biomass-demanding processes (Li et al. 2019). Quiescent ECs have a basal glycolytic metabolism and upon simulation by different factors such as VEGF and bFGF, the expression of several glycolytic proteins in ECs (including GLUT1, LDHA, PFKFB3 and HK2) is upregulated allowing increased glucose uptake and glycolytic flux (Wong et al. 2017) (fig.26) (Li et al. 2019). For the same reasons as cancer cells, high rate of glycolysis in proliferating ECs protects against fluctuations in the level of oxygen, allows rapid ATP production and generates precursors for biomass synthesis (Wong et al. 2017). In proliferative ECs, pentose phosphate pathway and serine pathway are also involved in biomass production and in redox homeostasis (Polet et al. 2013, Teuwen et al. 2019).

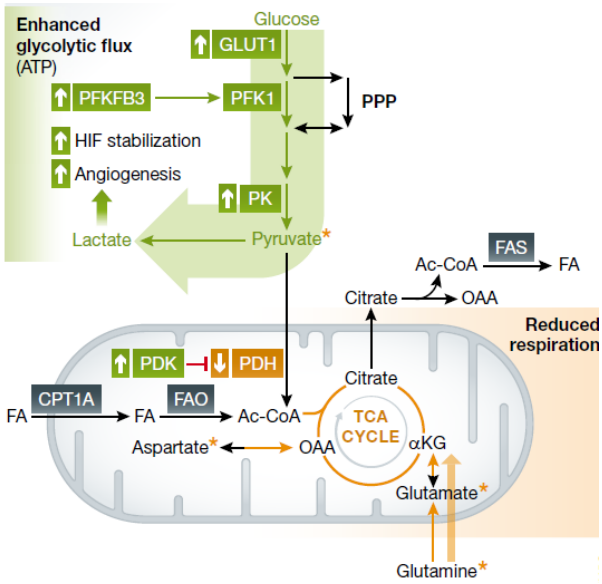

Figure 26. ECs metabolism adaptation to angiogenic signaling *(adapted from Wong et al. 2017). Angiogenic signaling increases glycolytic flux through enhancement of the expression of several glycolytic enzymes (GLUT1, PFKFB3, PK, PDK). Glycolytic intermediates fuel the pentose phosphate pathway (PPP). ECs also utilize fatty acids (FA) and glutamine to sustain TCA cycle.*

Glycolytic flux in tumor ECs (TECs) is higher than glycolytic flux in healthy proliferative ECs and more glycolytic intermediates are derived from serine and PPP pathways (Li et al. 2019). This is probably due to a combination of hypoxia-dependent increased glycolysis and the secretion of pro-angiogenic/pro-glycolytic growth factors (Wong et al. 2017). Even if glycolysis is crucial for ECs proliferation, mitochondria are still functional and participate in energy and biomass production (fig.26) (Li et al. 2019). It has been shown that glutamine is also essential for ECs proliferation and migration especially by replenishing mitochondrial tricarboxylic acid (TCA) cycle (Huang et al. 2017, Kim et al. 2017). TCA cycle intermediates are

involved in the synthesis of nucleotides, proteins and fatty acids. For instance, oxaloacetate, a TCA cycle intermediate, can be metabolized into aspartate and then into asparagine. Both are nitrogen donors for protein synthesis. *Huang et al.* have shown that asparagine promotes ECs growth by activating signaling pathways involved in protein and nucleotide synthesis (Huang et al. 2017). Citrate, another TCA cycle intermediate, contributes to ECs fatty acid synthesis (Fitzgerald et al. 2018). On the other hand, fatty acid oxidation (FAO) also sustains TCA cycle and nucleotide synthesis in proliferative ECs (Schoors et al. 2015, Bruning et al. 2018). Impairment in this pathway leads to defects in ECs proliferation but not migration, meaning that FAO is involved in biomass production rather than in energy production (Schoors et al. 2015, Bruning et al. 2018).

It is important to note that even if cancer cells and TECs share many similarities in terms of metabolic paths, the origin of the reprogramming differs fundamentally. In cancer cells, intrinsic genetic mutations and adaptation to external stimuli from the tumor microenvironment drive the increase in cell proliferation and then the glycolytic switch. In ECs, glycolytic metabolism is increased only by external stimuli (VEGF, lactate, hypoxia) and ECs can switch back to a quiescent status when the stimulation is reduced (Li et al. 2019).

4.3. Anti-angiogenic therapies: past and future

The first generation of anti-angiogenic therapies were based on vascular endothelial growth factor (VEGF) blockade. These therapies have shown limited results due to upregulation of alternative proangiogenic signaling pathways (Fitzgerald et al. 2018, Li et al. 2019). There is now a growing interest to target TECs directly through their metabolism, which is, as we described above, dysregulated during tumor angiogenesis (Li et al. 2019). The dependency of proliferating ECs on glucose, glutamine and FAO for energy and biomass production opens new opportunity for anti-angiogenic treatments (Polet et al. 2013). Inhibition of the glycolytic activator PFKFB3 has already been shown to promote ECs quiescence and to induce tumor vessel normalization and thereby improve vessel perfusion (Cantelmo et al. 2016).

In 2017, in a study on flow-induced metabolic reprogramming in ECs, Wu et al. showed that the pyruvate dehydrogenase kinase enzyme 1 (PDK-1) was involved in the enhancement of the glycolytic metabolism (Wu et al. 2017). They demonstrated that HIF-1α increased glycolytic enzymes but also PDK-1 expression leading to a reduction in mitochondrial respiratory capacity. Using DCA, they further showed that PDK-1 inhibition partially rescued ECs respiration strongly suggesting that PDK is an attractive target to reduce EC proliferation.

5. Magnetic resonance spectroscopy to measure cancer cell metabolism and oxygen consumption

During this PhD thesis, we measured the metabolic profile and plasticity of several cell lines. For that purpose, we used two techniques of magnetic resonance spectroscopy that we will briefly introduce here. ^{13}C nuclear magnetic resonance (NMR) spectroscopy gives us information about cellular metabolic fluxes while electron paramagnetic resonance (EPR) spectroscopy allows us to measure cellular oxygen consumption.

5.1. ^{13}C NMR spectroscopy to follow glucose and glutamine metabolism

- NMR basics

NMR is based on the magnetic properties of some atomic nuclei. Nucleus can be considered as a charged rotating particle, which is called a spin. Each atom has a specific nuclear spin value I, which depends on its nuclear structure (number of protons and neutrons). I is the nuclear spin value which characterizes the intrinsic quantum mechanical property of nuclei and can have a value multiple of 1/2 or can be zero (fig.27).

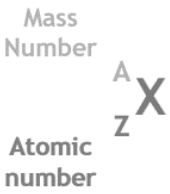

A odd	I = n/2	I = 1/2 : ^{1}H, ^{31}P, ^{13}C I = 3/2 : ^{11}B
A peer & Z odd	I = n	I = 1 : ^{2}H, ^{14}N I = 3 : ^{10}B
A & Z peers	I = 0	I = 0 : ^{12}C, ^{16}O

Figure 27. The nuclear spin of an atom depends on its atomic structure. *Atoms with an odd mass number (A) have a semi-integer I value. Atoms with an odd proton number (Z) and a peer A number have an integer I value. Atoms with peers A and Z number have zero I value.*

As the spin is a moving charge, it is characterized by a magnetic moment $\vec{u}$. There are $2\mathrm{I} + 1$ energy states for a nucleus, corresponding to the number of directions that the magnetic moment can adopt in an external magnetic field ($\overrightarrow{B_0}$). ^{12}C atoms have a spin of 0 (fig.27) and can take only one orientation. Consequently, nuclear magnetic resonance, which measures the transition to one state of energy to another, on this nucleus is not applicable. Only nuclei with an I value that differs from zero have magnetic proprieties. ^{13}C atoms, which have a spin value of ½, has two energy states and can have two possible orientations when an external magnetic field is applied. Spins precess around the magnetic field and are distributed between the two possible energy levels: the lowest energy state (parallel to $\overrightarrow{B_0}$) and the highest energy state (antiparallel to $\overrightarrow{B_0}$). A larger number of spins will be in the state of lower energy, leading to a net magnetization $\vec{M}$ parallel to $\overrightarrow{B_0}$ (fig.28).

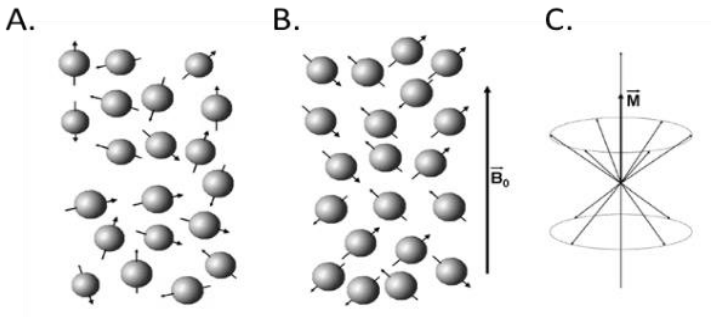

Figure 28. Basic principles of magnetic resonance for a spin ½ *(Akoka). A. In absence of magnetic field, spins are randomly oriented. B. When a magnetic field ($\overrightarrow{B_0}$) is applied, spins precess around $\overrightarrow{B_0}$, more spins are aligned in parallel to $\overrightarrow{B_0}$ and less spins are aligned antiparallel to $\overrightarrow{B_0}$. C. The vector sum of all the nuclear magnetic moments (nuclear magnetization, $\overrightarrow{M}$) is then non-zero and oriented in the direction of the $\overrightarrow{B_0}$ field.*

This difference of nuclei repartition between the two energy states is proportional the precession frequency (ω_0) of the nucleus. The precession frequency depends on intrinsic nuclear property (gyromagnetic ratio, y) and on the magnetic field strength: $\omega_0 = \gamma \, . \, \overrightarrow{B_0}$.

As the net magnetization $\vec{M}$ is very small compared to the applied magnetic field to $\overrightarrow{B_0}$, it is not observable when it is parallel to $\overrightarrow{B_0}$. In order to observe the magnetization, a second magnetic field $\overrightarrow{B_1}$ is transitory applied perpendicularly to $\overrightarrow{B_0}$. $\overrightarrow{B_1}$ is an excitation pulse (RF pulse) rotating at the same precession frequency as ω_0. The energy of the RF pulse is absorbed by the nuclei and spins go from one energy state to the other state and precess around the direction of $\overrightarrow{B_1}$. Consequently, the RF pulse flips $\vec{M}$ away from $\overrightarrow{B_0}$ toward $\overrightarrow{B_1}$ direction (flip angle) and reduces the net magnetization along $\overrightarrow{B_0}$

axis (fig.29). The flip angle depends on the duration and the intensity of the RF pulse.

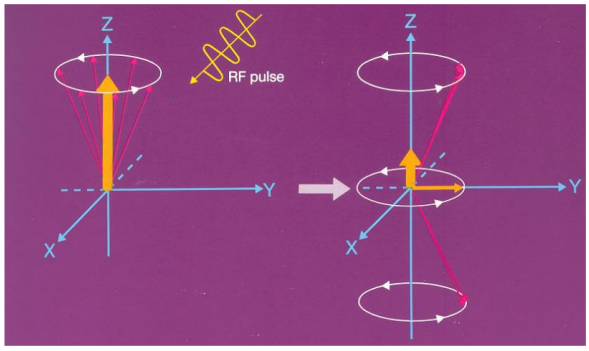

Figure 29. RF pulse effects on the magnetization *(Chavhan 2007). RF pulse decreases the magnetization along the z-axis and establishes a new magnetization in the xy plan.*

When the RF pulse is stopped, $\vec{M}$ gradually returns (relaxation) to its equilibrium position, parallel to $\overrightarrow{B_0}$. A detector placed in the transversal plan detects the temporal evolution of the rotating magnetization, which decreases in the transversal plane and increases in the $\overrightarrow{B_0}$ direction (fig.30).

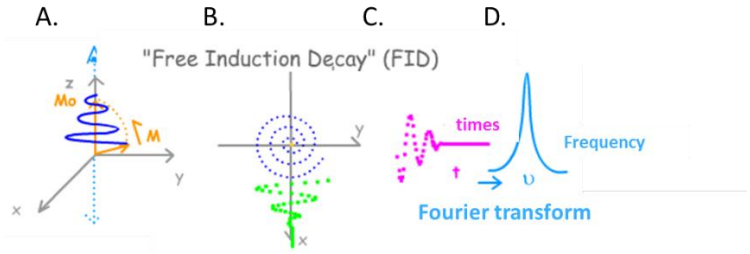

Figure 30. NMR signal detection*. Spin relaxation over time (A. seen from above along the vertical axis z, B, seen in the xy plane), which gives the free induction decay (FID) signal (C.). The signal over times (FID) is converted in a signal over frequency thanks to the Fourier transform (D.).*

(http://www.unice.fr/cdiec/cours/rmn_web/rmn_theorie/c_theorie.htm)

Consequently, the energy emission occurs in the form of sinusoidal waves decreasing over time and provides the free induction decay (FID) signal. The NMR spectrum is obtained by the used of the Fourier transform, which converts the signal over time (FID) into a signal over frequency (fig.30). When the spins have relaxed, a second identical RF pulse is applied, then stopped, and signals are accumulated to get a larger signal-to-noise ratio (Akoka , Chavhan 2007).

- ^{13}C NMR to measure cellular metabolism

^{13}C-NMR spectroscopy can be used to measure the metabolism and metabolic fate of different substrates such as glucose-$^{13}C_6$ or glutamine-$^{13}C_5$. NMR presents a lower sensitivity than mass spectroscopy (MS), which is currently more commonly used to study metabolic fluxes (Emwas 2015). However, NMR offers several advantages to assess metabolic fluxes. NMR samples are reusable allowing multiple analysis whereas MS samples are destroyed after one analysis. Reproducibility in NMR experiments is higher than MS since there is no batch effect (I.e., no interaction with the machine). Finally, NMR can be used for whole tissues samples analyses and for *in vivo* studies making findings more easy to translate into the clinic. The use of a ^{13}C-labeled substrate improves the sensitivity of detection because ^{13}C natural abundance is 1,11% and has a low gyromagnetic ratio. However, having a low natural abundance can be considered as an advantage to observe metabolic fluxes since it allows (together with the use of a labeled substrate) to specifically track downstream metabolites.

Each different ^{13}C atom of a molecule has a specific absorption frequency depending on its chemical environment. The presence of electrons around a nucleus forms an electronic shield that reduces the magnetic field perceived by the nucleus: the magnetic field perceived by the nucleus will be weaker than the real applied magnetic field. Electropositive compounds around a nucleus increase the electronic shield of the nucleus and consequently decrease the absorption frequency (shielding effect). Electronegative compounds decreased the electronic shield and increased the absorption frequency (unshielding effect).

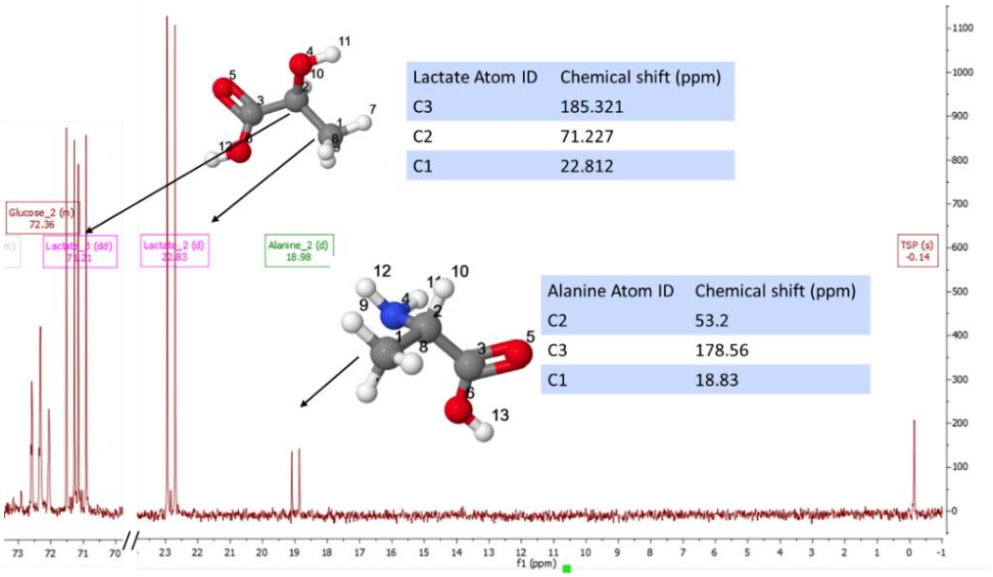

Figure 31. Representative spectrum of intracellular metabolites of HCT-116 cancer cells incubated for 24 hours with media containing 10mM glucose-$^{13}C_6$. *Signals of TSP (natural abundance), alanine ($^{13}C1$), lactate ($^{13}C1$ and $^{13}C2$) and glucose ($^{13}C2$) are visible. Tables show the assigned chemical shift of each ^{13}C of lactate and alanine regarding their atom ID (http://www.bmrb.wisc.edu/).*

For instance, the carbon 3 of lactate (fig.31) has two atoms of oxygen in its chemical environment. Oxygen is more electronegative than carbon and consequently the carbon 3 of lactate is less shielded than the carbon 2, which has one atom of oxygen in its chemical environment. These two carbons have different electronic shields and will have different absorption frequencies since the magnetic field perceived is different. In the NMR spectrum, the carbon 3 will have a higher absorption frequency than the carbon 2.

Instead of using absorption frequency, NMR spectroscopists use the chemical shift (δ) to assign each ^{13}C present in molecules. Chemical shifts are expressed in ppm (parts-per million), which is independent of the magnetic field. The chemical shift of a nucleus is the difference in resonance frequency of the nucleus (ω) and a standard (ω_{ref}), compared to the frequency of the standard: $\delta = ((\omega - \omega_{ref}) \times 10^6)/\omega_{ref}$. For instance, in the table of lactate chemical shift in figure 31, we can see that carbon 3 of lactate has a higher chemical shift (δ= 185 ppm) than the carbon 2 (δ = 71ppm) since carbon 3 is less shielded and has a higher absorption frequency than carbon 2.

In biological media, TSP (trimethylsilylpropanoic acid) is often used as a standard since silicon is more electropositive than carbon. Consequently, silicon increases the electronic shield of the three methyl groups. Of note, the three methyl groups have the same chemical environment and consequently the same chemical shift, thus the amplitude of the signal is multiplied by 3. Because these ^{13}C are more shielded than any other ^{13}C of cellular metabolites, their absorption frequency is the lowest. All the ^{13}C metabolites have a higher absorption frequency and consequently a higher chemical shift

(fig.31). The chemical shifts of each ^{13}C of metabolites are searchable in databases such as the bmrb database (http://www.bmrb.wisc.edu/) (tables fig.31).

Each carbon also interacts with their neighbor carbons inside the molecule, which is called spin-spin coupling. Each signal is composed of several peaks depending on the number of direct covalent links with another carbon (fig.31). For instance, the carbon 3 of lactate (fig.31) has a covalent link with another carbon (C2), which gives a signal composed of two peaks, a doublet (d). The carbon 2 of lactate has a covalent link with 2 carbons (C1 and C3), which gives a signal composed of four peaks, a doublet of doublet (dd). Consequently, each ^{13}C signal is composed of a specific number of peaks, which helps for the signal assignment, the matching of the signal to the corresponding ^{13}C.

5.2. Quantification of cellular oxygen consumption by EPR spectroscopy

The cellular oxygen consumption can be measured using EPR spectrometry. EPR allows the study of species containing unpaired electrons, such as oxygen which has two unpaired electrons. EPR is based on the same principles as NMR, but EPR detects spins of unpaired electrons instead of nuclear spins like in NMR.

The electron possesses a quantic number of electronic spin of ½. Therefore, in a magnetic field, magnetic moments can have two different orientations: parallels and antiparallel to the magnetic fields. As in NMR, each orientation

refers to a particular state of energy and the resonance will be obtained by irradiation of the sample with a frequency wave specific to the electron. The irradiation will excite the electron to the upper level of energy when the applied field is equal to the field for the resonance. The energy absorption is detected by a detector, which will give the signal intensity over the magnetic field. The amplitude of the EPR signal is proportional to the concentration of the detected paramagnetic species. EPR signal is presented in first derivative rather than in absorption curve. An important feature of the EPR signal is the linewidth (the peak to peak splitting along the magnetic field axis) of the signal, which is inversely proportional to the relaxation time (fig.32.a).

Oxygen is a triplet radical, which possesses two unpaired electrons. However, it is impossible to directly perform EPR spectroscopy on dissolved oxygen because of the fast relaxation of the electron spin. An indirect measure is possible because O_2 can act as relaxing agent. Through collision with a paramagnetic probe, oxygen reduces the relaxation time of the probe, which increases the linewidth of the probe. The linewidth is therefore proportional to the concentration of O_2 in the cellular sample. To measure oxygen consumption by cells, a stable paramagnetic sensor, for example a nitroxide, is introduced in a cellular suspension in a closed environment. Monitoring changes in EPR linewidths over time in such a system provides the measurement of the oxygen consumption rate (OCR).

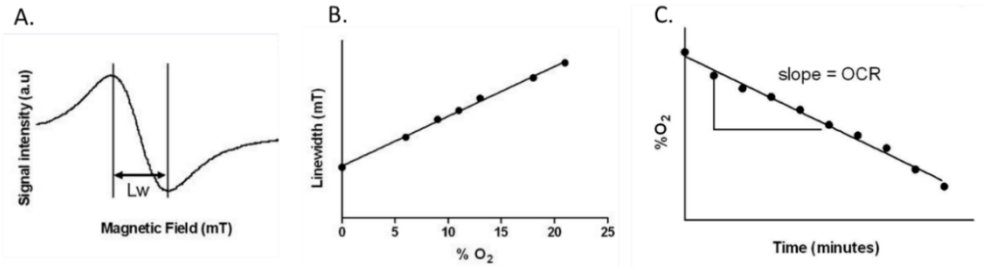

Figure 32: In vitro oxygen consumption *(adapted from Danhier et al., 2013). A. ^{15}N-PDT EPR spectrum first derivative, the linewidth (Lw) is proportional to O_2 %. B. Calibration curve of the Lw as function of O_2 concentration. C. The slope of O_2 % over time curve gives the oxygen consumption rate (OCR) of the sample.*

AIMS OF THE THESIS

1. Rationale and general aim

Among all glycolytic enzymes, the enzyme pyruvate dehydrogenase has several unique metabolic characteristics that give it high potential as metabolic target against cancer. Regarding clinical data, PDK upregulation over expression is associated with cancer aggressiveness but also chemotherapy resistance. When looking at cellular mechanism of action, PDK has the ability to control pyruvate fate and thereby enhances the Warburg effect while decreasing mitochondrial ROS production and subsequent apoptosis induction. Therefore, PDK inhibition has the potential to attenuate the Warburg effect but also to induce cell death through redirection of pyruvate into the mitochondria and subsequent increase in ROS production. Since the first discovery that DCA reduces cancer proliferation, numerous studies have investigated the underlying mechanisms to better understand its anti-cancer action. Today, it is clear that DCA redirects glycolytic flux back into the mitochondria. Consequently, there is a decrease in glycolytic intermediates to sustain proliferation and an increase in mitochondrial-dependent apoptosis. However, *in vivo* studies do not always observe an effect of DCA on tumor growth. PDK inhibition may lack efficacy because tumor metabolism continuously adapts to new constraints in the tumor microenvironment. Due to its mode of action, DCA should target cancer cells that are dependent on glycolysis associated with efflux of lactate and protons, which leads to extracellular acidosis. However, extracellular acidosis has never been considered as a potential modulator DCA activity. On the

other hand, the success of anti-cancer treatments that target tumor metabolism is not only dependent on cancer cells response but also on the interaction of the drug with the surrounding tumor microenvironment. Even if several reports have shown that oxidative healthy cells were not impacted by DCA, stromal cells that also rely on glycolysis are present within the tumor microenvironment and could be affected by DCA.

The aim of the thesis was therefore to investigate the anti-cancer action of DCA taking into account different aspects of the tumor microenvironment. We evaluated the impact of extracellular acidosis on the efficacy of DCA using a long-term selection of cancer cells able to proliferate under acidic conditions. We have also explored a potential action of DCA on endothelial cells, which are known to be dependent on glycolysis to perform angiogenesis. Moreover, several studies have shown that DCA reduces angiogenesis but a direct effect on endothelial cells has never been investigated. In these two models, we investigated tumor metabolic plasticity after DCA treatment with a special focus on the glutamine metabolism.

2. Specific aims

2.1. Unraveling the impact of acidosis-induced metabolic reprogramming in tumor cells exposed to DCA

The first objective of this thesis was to explore the role of extracellular acidosis on the DCA efficacy. On the one hand, because of its mode of action, DCA should theoretically target aggressive glycolytic tumors. On the other hand, the extracellular acidosis associated with glycolysis is responsible for a metabolic shift, redirecting metabolism away from glycolysis. Therefore, this

metabolic reprogramming could decrease the sensitivity to DCA because these extracellular acidosis-adapted cancer cells are less dependent on glycolysis. Considering these theoretical contradictory effects, we aimed to examine how acidic pH influences the effects of DCA on the bioenergetics and proliferation of cancer cells.

2.2. Exploring the effects of PDK inhibition by DCA on endothelial cells

The second objective of this thesis was to study the impact of DCA on non-cancerous cells present in the tumor microenvironment, namely ECs. Previous studies reported that DCA decreased tumor angiogenesis. Authors postulated that this effect was mediated by a paracrine signaling induced by DCA. In cancer cells DCA decrease HIF-1 activity resulting in a reduced expression of HIF-1α target genes including pro-angiogenic factors. Besides this cancer cells mediated effect, a direct effect of DCA through a metabolic reprogramming of ECs has never been considered. However, in 2017, a study on flow-induced metabolic reprogramming in ECs, showed that HIF-1α increased PDK-1 expression in ECs. Researchers observed that PDK-1 expression was involved in the upregulation of the glycolytic metabolism of proliferative ECs. Therefore, we investigated the impact of DCA exposure on endothelial cells.

RESULTS

1. INFLUENCE OF ACIDOSIS-INDUCED METABOLIC REPROGRAMMING ON DCA RESPONSE

Acidosis-induced metabolic reprogramming in tumor cells enhances the anti-proliferative activity of the PDK inhibitor dichloroacetate

Schoonjans, C. A., Joudiou, N., Brusa, D., Corbet, C., Feron, O., & Gallez, B. (2020). Cancer Letters, 470, 18-28.

For supplementary methodology information, see methodology section on ^{13}C fluxomic methodology and on acid-adapted cancer cells models (page 139).

Cancer Letters 470 (2020) 18–28

Contents lists available at ScienceDirect

Cancer Letters

journal homepage: www.elsevier.com/locate/canlet

Original Articles

Acidosis-induced metabolic reprogramming in tumor cells enhances the anti-proliferative activity of the PDK inhibitor dichloroacetate

C.A. Schoonjans[a,b], N. Joudiou[c], D. Brusa[d], C. Corbet[b], O. Feron[b], B. Gallez[a,*]

[a] Université Catholique de Louvain (UCLouvain), Louvain Drug Research Institute, Biomedical Magnetic Resonance Research Group, Brussels, Belgium
[b] Université Catholique de Louvain (UCLouvain), Institut de Recherche Expérimentale et Clinique, Pole of Pharmacology and Therapeutics, Belgium
[c] Université Catholique de Louvain (UCLouvain), Louvain Drug Research Institute, Nuclear and Electron Spin Technologies, Brussels, Belgium
[d] Université Catholique de Louvain (UCLouvain), Institut de Recherche Expérimentale et Clinique, Flow Cytometry Platform, Belgium

ARTICLE INFO

Keywords:
pHe
13C-NMR
Glycolysis inhibition
Metabolic plasticity
Bioenergetics

ABSTRACT

Altered metabolic pathways in cancer such as exacerbated glycolytic flux and increased glutamine metabolism are promising targets for anti-cancer therapies. While commonly observed in glycolytic tumors, extracellular acidosis has never been considered as a potential modulator of anti-metabolic drug activity such as dichloroacetate (DCA). Using cancer cells from various origins selected for their ability to proliferate under acidic conditions, we found that DCA exerts greater inhibitory effects on the growth of these acid-adapted cells than in parental cells. Moreover, daily DCA administration to mice led to a significant decrease in tumor growth from acid-adapted cells but not from parental cells. 13C-tracer studies revealed that DCA induced a double metabolic shift, diminishing glycolysis and increasing intracellular glutamine in acid-adapted cells. As a consequence, DCA reduced the pentose phosphate pathway activity more extensively and increased apoptosis in acid-adapted cells. Finally, the combination of DCA with a glutaminase inhibitor significantly enhanced the cytotoxic effects of DCA. Overall, the interplay between acidosis and DCA exposure leads to metabolic reprogramming that considerably alters cellular fitness.

1. Introduction

Glucose fermentation through glycolysis even in the presence of oxygen (aerobic glycolysis) is a common feature of malignant tumors and is associated with cancer aggressiveness and invasion [1,2]. This exacerbated glycolytic flux is an enticing target for treatments because of their specificity to cancer cells. Indeed, upregulated glycolysis is described as an effective way for cancer cells to support rapid proliferation, an adaptation that is not present in most normal cells [3,4]. To date, clinical studies with glycolysis inhibitors have provided encouraging data [5,6] but efforts are still needed to identify which tumors will benefit from these treatments. Among glycolytic modulators, inhibitors of pyruvate dehydrogenase kinase (PDK) have received particular attention [7–9]. PDK inactivates the enzyme pyruvate dehydrogenase (PDH) by phosphorylation. The active unphosphorylated PDH converts pyruvate to acetyl-CoA that fuels the tricarboxylic acid cycle (TCA). Therefore, the inhibition of PDK reactivates PDH leading to a redirection of glucose metabolism from cytoplasmic glycolysis to mitochondrial oxidation [10].

It has been repeatedly observed that dichloroacetate (DCA), a PDK inhibitor currently tested in clinical studies (i.e. Trial ID: NCT01386632 and ACTRN12615000226505), decreases the proliferation of various cancer cells lines [11–14]. DCA reverses aerobic glycolysis leading to a decrease in lactate production. In addition, by reactivating the mitochondrial function, DCA reverses the suppression of mitochondria-dependent apoptosis [12,15]. Finally, DCA decreases glycolytic intermediates available for anaplerosis, in particular through the pentose phosphate pathway [12]. Consequently, this reduction of building blocks from glycolysis accounts for the anti-proliferative effects of PDK inhibition [16]. Besides these direct metabolic effects, it has been shown that DCA decreases HIF-1 alpha activity and increases p53 activity resulting in decreased glucose uptake, tumor angiogenesis, tumor perfusion and tumor growth [12,17,18]. In addition, a survey of studies on DCA from Papandreou et al. highlighted that DCA was more effective *in vivo* than *in vitro* [19]. These observations suggest that factors of the tumor microenvironment may modulate the efficacy of DCA.

Because the exacerbated glycolytic flux in tumor leads to extracellular acidosis, it is crucial to investigate the effect of cell adaptation to acidosis on DCA activity [20,21]. Indeed, besides its contribution to tumor genomic instability and invasiveness [22–24], extracellular

* Corresponding author. Biomedical Magnetic Resonance, UCLouvain, Avenue Mounier 73.08, B-1200, Brussels, Belgium.
E-mail address: bernard.gallez@uclouvain.be (B. Gallez).

https://doi.org/10.1016/j.canlet.2019.12.003
Received 19 September 2019; Received in revised form 20 November 2019; Accepted 1 December 2019

acidosis can lead to tumor metabolic reprogramming [25–27]. For example, it was recently demonstrated that a long-term exposure of cancer cells to acidic pH leads to a metabolic reprogramming towards glutamine metabolism at the expense of the glycolytic metabolism [28,29].

The aim of our study was to unravel the role of extracellular acidosis on the efficacy of DCA. On one hand, because of its mode of action, DCA should theoretically target aggressive glycolytic tumors. On the other hand, the extracellular acidosis associated with glycolysis is responsible for a metabolic shift from glycolysis to glutamine metabolism: this metabolic reprogramming could render cells adapted to low extracellular pH (pHe) less sensitive to DCA because they are less dependent on glycolysis. Considering these theoretical contradictory effects, we aimed to examine how acidic pH influenced the effects of DCA on the bioenergetics and proliferation of cancer cells. We used a long-term selection of cancer cells able to proliferate under acidic conditions [28]. We first observed that DCA was more effective in acidic pH-adapted cells compared to their native counterparts in reducing cell viability, cell proliferation and tumor growth. To dissect the mechanisms responsible for this enhanced effect, we assessed the uptake of DCA by the tumor cells, the PDK isoforms abundance and the phosphorylation of PDH by PDK. Via ^{13}C NMR spectrometry, we measured metabolic shifts induced by DCA in glucose and glutamine metabolism. To further investigate the link between metabolic shift and their action on growth and proliferation, we measured pentose phosphate pathway activity and mitochondrial dependent apoptosis. Finally, we assessed the relevance of our results by performing a combined therapy with DCA and glutaminase inhibitors. Overall, we discovered that the metabolic plasticity observed under acidosis can be exploited to enhance the activity of PDK inhibitors.

2. Material and methods

2.1. Cell culture and reagents

All cell lines were acquired from the American Type Culture Collection (ATCC, Manassas, VA, USA). Cells were stored according to the supplier's instructions and used within 6 months after defrosting frozen aliquots. SiHa cervix cancer cells and HCT-116 colon cancer cells were maintained in DMEM supplemented with 10 mM of glucose, 2 mM of glutamine (Sigma-Aldrich, Saint-Louis, MO, USA), 10% heat-inactivated FBS (Thermo Fisher Scientific, Waltham, MA, USA) and with 25 mmol/L of both PIPES and HEPES to adjust pH to 7.4 or 6.5. Acidic pH-adapted tumor cells were established as previously described by Corbet et al. [28]. Briefly, SiHa and HCT-116 cell lines were cultured in DMEM medium (supplemented with 10 mM of glucose, 2 mM of glutamine, 10% heat-inactivated FBS and with 25 mmol/L of both PIPES and HEPES) buffered at pH 6.5. 72 h of incubation in the 6.5 medium led to a significant inhibition of tumor cell growth. Tumor cells were maintained in this medium (repeatedly renewed) for 8–10 weeks until they completely recovered and grew at the same rate as parental cells. Dichloroacetate (DCA) and 6-Aminonicotinamide (6-AN) were purchased from Sigma-Aldrich and were directly dissolved in culture media. Bis-2-(5-phenylacetamido-1,3,4-thiadiazol-2-yl)ethyl sulphide (BPTES) was purchased from Sigma-Aldrich and first dissolved in DMSO and then diluted in culture media.

2.2. Cell density

Cell density was assessed by using the Presto Blue reagent (Thermo Fisher Scientific, Waltham, MA, USA) according to manufacturer's instructions. Four cancer cell types were analyzed: parental cells cultured at a pH of 7.4 or acutely exposed to an acidic pH (pH 6.5; 48h) and chronically acid-adapted cells cultured at a pH 6.5 or exposed to a pH 7.4 for 24 or 48 h. Cells were treated with 0, 5 or 10 mM of DCA. For the combined study, cells were treated with 0, 1 or 5 mM of DCA in presence or not of 10 μM BPTES. 48 h after, 10% Presto Blue reagent was added to each well. After 1 h at 37°-C, fluorescence intensity (λ_{exc}/λ_{em} = 544/612 nm) was measured using a plate reader (SpectraMax M2e, Molecular Devices), which allowed the quantification of cell viability by using the reducing power of living cells.

2.3. Cell proliferation

Cell proliferation was assayed with a 5-bromo-2′-deoxyuridine (BrdU)-ELISA based kit (Roche, Bâle, Switzerland) following the provider's instructions. Cells were treated with 0, 5 or 10 mM of DCA. After treatment for 48 h, cells were incubated in the presence of BrdU for 2 h. The amount of BrdU incorporated in the cells was assessed by measuring the absorbance at 370 nm using a plate reader (SpectraMax M2e, Molecular Devices), which allowed the quantification of DNA synthesis in replicating cells.

2.4. Western blotting analyses of PDK isoforms and PDH phosphorylation

Whole cell lysates were collected and subjected to immunoblot analysis as previously described [30]. Primary antibodies: PDHK1 (1:1000,#3820, Cell Signaling, Danvers, MA, USA), phospho-PDHE1-A (1/1000, #ABS204, Millipore, Burlington, MA, USA), PDK1 (1/1000, #3205, Cell Signaling), PDK2 (1/1000, WH0005164M2, Sigma), PDK3 (1/1000, NBP1-32581, Novus, Saint Charles, MO, USA) and PDK4 (1/1000, NBP1-07047, Novus). Gel loading was normalized with a HSP90 antibody (1/1000, 610419, BD Bioscience, San Jose, CA, USA).

2.5. ^{13}C NMR spectroscopy measurement of intra/extracellular metabolites

Intra- and extracellular metabolites were measured with ^{13}C nuclear magnetic resonance (NMR) via the use of ^{13}C-labeled tracers. 1×10^6 cells were seeded in 100 mm dishes for Glucose-$^{13}C_6$ tracer experiments and 2×10^6 cells were seeded in 150 mm dishes for Glutamine-$^{13}C_5$ tracer experiments (two dishes per condition). After 24 h, cells were cultured with or without 5 mM DCA and with DMEM supplemented with either 10 mmol/L of D-Glucose-$^{13}C_6$ (CLM-1396, Euriso-top, Saint-Aubin, France) and 2 mmol/L of unlabeled L-glutamine, or 10 mmol/L of unlabeled D-glucose and 2 mmol/L of L-Glutamine-$^{13}C_5$ (CC1050P1, Cortecnet, Voisins-le-Bretonneux, France). 24h after treatments, extracellular media were collected and polar cellular metabolites were extracted using dual phase extraction procedure adapted from Teng et al. [31]. Briefly, a mixture of methanol, chloroform and water in the volume ratio 2:2:1 was used to generate two-phase extracts after centrifugation. The upper aqueous phase containing polar metabolites was collected. The solvent was completely removed using a vacuum concentrator. The sample was reconstituted in 600 μl sodium phosphate buffer with 10% deuterium oxide containing 0.75 wt % 3-(trimethylsilyl)propionic-2,2,3,3-d_4 acid (TSP) (Sigma-Aldrich, 293040). For extracellular metabolites, 540 μl of media was used and 60 μl of deuterium oxide containing 0.75 wt % TSP was added. ^{13}C NMR spectra of cellular extracts and media were acquired on a 600 MHz Bruker NMR equipped with a broadband cryoprobe. The acquisition time was 0.8 s with 1024 repetitions for Glucose-$^{13}C_6$ tracer and 2048 repetitions for L-Glutamine-$^{13}C_5$ and 10 s of interpulse delay (1D sequence with inverse gated decoupling using 30° flip angle). Spectrum analysis, assignment and quantification were performed with Topspin and MestReNova software. For Glutamine-$^{13}C_5$ tracer extra dishes were seeded for protein normalization (Pierce™ BCA Protein Assay Kit, Thermo Fisher).

2.6. Measurement of oxygen consumption rate

The effect of DCA on oxygen consumption rate (OCR) was evaluated on parental and acid-adapted cell lines via a X-band Electron Paramagnetic Resonance (EPR) spectrometer operating at 9 GHz

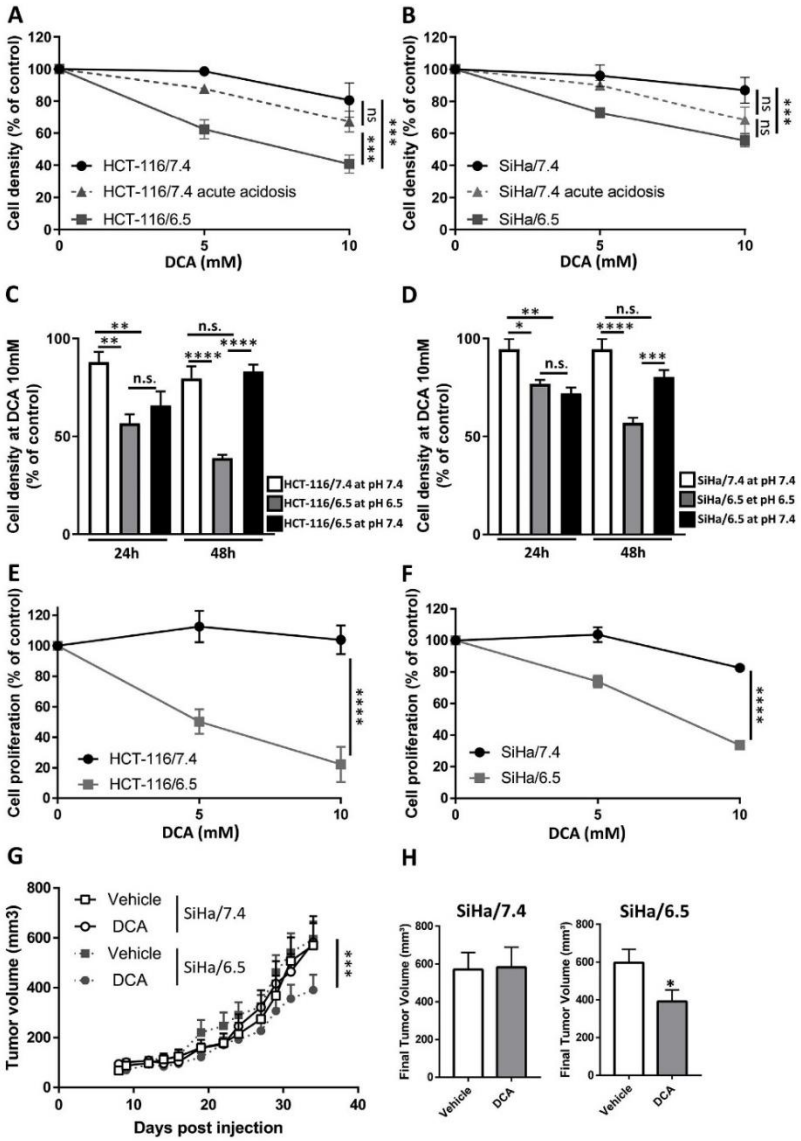

Fig. 1. Chronic acidosis enhances the growth inhibitory action of DCA. A-B, effect of increasing doses of DCA (0-5-10 mM) on cell density (A, HCT-116 cells and B, SiHa cells) after 48 h exposure (n = 3). C-D, acid adapted cells were incubated at pH 7.4 for 24 and 48 h. Cell density measurement (C: HCT-116 cell lines and D: SiHa cell lines) after DCA treatment (10 mM, 24 and 48 h) of parental (white), acid-adapted cells (gray) and acid-adapted cell cultured at pH 7.4 (black) (n = 3). E-F, effect of increasing doses of DCA (0-5-10 mM) on cell proliferation (E, HCT-116 cell lines and F, SiHa cell lines) after 48 h exposure (n = 3). G, tumor growth of SiHa parental and SiHa acid-adapted xenografts in nude mice (n = 8–10) treated daily with or without DCA (100 mg/kg). H, Final tumor volume of SiHa/7.4 and SiHa/6.5 xenografts. Statistical analysis: Two-way ANOVA Sidak's multiple comparisons test (A–G) and unpaired *t*-test (H). *p < 0.05, **p < 0.01, ***p < 0.001, ****p < 0, 0001.

(Bruker EMXplus) as previously described [32]. Cells were incubated with 5 mM of DCA for 24h; after trypsinization, cells were resuspended in cell growth medium at a concentration of 2.5×10^6 cells/mL. 100 μL of cell suspension were mixed with 100 μL of 20% w/v of dextran in 0.9% NaCl solution and 6 μL of 0.2 mM ^{15}N-PDT, which served as oxygen sensor. A 75 μL-glass capillary tube (Hirschmann Labogeräte) was filled with the cell suspension, sealed and inserted into a quartz tube, then placed into the EPR cavity. The cavity was continuously flushed with a gas mixture (400 l/h) at 37 °C throughout the spectra acquisition. EPR spectra were acquired every 60 s, and pO_2 values were obtained by measuring the peak to peak EPR signal linewidths, which was then converted into pO_2 by means of a calibration curve. Oxygen consumption rate (OCR) was then calculated as the slope of pO_2 over time curve.

2.7. DCA uptake measurement

Cells were treated with or without 5 mM DCA. 24 h after treatment, extracellular media was collected and proteins were extracted and quantified (Pierce™ BCA Protein Assay Kit, Thermo Fisher Scientific) for sample normalization. Collected extracellular media was processed and analyzed by ^{13}C NMR spectroscopy as described in the previous section. DCA chemical shift of the carbon from the carboxylic group was found at 173.56 ppm.

2.8. NADPH and NADP$^+$ measurements

Cells were treated with or without 5 mM DCA and with or without 0.1 mM 6-aminonicotinamide (6-AN) for 48 h. NADPH and NADP$^+$ levels were detected individually from 12,000 harvested cells using the NADP/NADPH-Glo Assay kit (Promega, Leiden, Netherlands) according to manufacturer's instructions.

2.9. Flow cytometry

After treatment with or without 10 mM DCA for 48 h, cells were rinsed with PBS, detached with trypsin and resuspended in fresh media. EBioscience™ Annexin V Apoptosis Detection Kit APC (Invitrogen™, Thermo Fisher Scientific) was used for the determination of the percentage of living, apoptotic and dead cells following provider's instructions. The cells were distinguished between alive (double negative) and dead: early/medium apoptotic (AnnV + DAPI−), late apoptotic (AnnV + DAPI+). Flow cytometric data were acquired using a BD FACS Canto II flow cytometer and processed with FlowJO software. FACS analysis by FlowJo was processed for each cell line separately. At least 20,000 events were analyzed for each sample.

2.10. Mass spectrometry

Cells were washed with PBS before adding culture media containing 2 mM L-[U–^{13}C]glutamine tracer for 24 h. Tumor cells were rinsed in cold 0.9% NaCl and snap-frozen in liquid nitrogen. Mass spectrometry measurements (^{13}C isotope analysis and absolute quantification of intracellular metabolites) were then performed by the Metabolism Core in the Sanford Medical Discovery Institute (La Jolla) [33].

2.11. In vivo tumor growth

Animal studies were undertaken in accordance with Belgian and the Université catholique de Louvain ethical committee regulations (agreement numbers 2018/UCL/MD/021). A total of 2.10^6 native SiHa cells or acidic pH-adapted SiHa cells were inoculated subcutaneously into the right flank of six-week-old female NMRI nude Mice (Janvier, Le Genest-Saint-Isle, France). Tumors were measured three times per week with an electronic caliper. When they reached a mean diameter of 5 mm, DCA in PBS (100 mg/kg) or PBS alone was injected daily intraperitoneally.

2.12. Statistical analysis

Data are expressed as mean ± SEM (standard error of the mean). The number of experiments and the statistical test used are given in each figure caption. All data were analyzed with the GraphPad Prism 8.0 software.

3. Results

3.1. Chronic acidosis enhances the growth inhibitory action of DCA

We first examined whether extracellular acidosis could influence the effects of DCA on cancer cell growth. We investigated possible changes on cell density and cell proliferation under DCA treatment in acid-adapted HCT-116 and SiHa cancer cells in comparison to native (parental) counterparts. The effect of increasing doses of DCA on cell density was significantly more pronounced in acid-adapted cells compared to corresponding parental cells (Fig. 1A–B). In contrast, in cells acutely exposed to acidosis, DCA did not induce any significant effect on cell density: cell density was not significantly different between parental cells under physiological pH and under acute acidic pH (Fig. 1A–B). We investigated the reversibility of the increased sensitivity to DCA resulting from chronic exposure to acidic pH. For that purpose, HCT-116/6.5 and SiHa/6.5 cells were cultured at pH 7.4 for 24 and 48 h. After 24 h of DCA treatment at pH 7.4, there was no significant difference between acid-adapted cells cultured at pH 6.5 and 7.4. However, after 48 h h, acid-adapted cells cultured at pH 7.4 presented the same sensitivity to DCA than parental cells (Fig. 1 C-D). The effect of increasing doses of DCA on cell proliferation was also significantly more pronounced in acid-adapted cells compared to corresponding parental cells (Fig. 1E–F). Exposition to 10 mM DCA induced a reduction in cell proliferation by 78% and 66% in acid-adapted HCT-116 and SiHa cells, respectively but either was not or barely effective in parental cells. To assess the therapeutic relevance of our *in vitro* experiments, we monitored the *in vivo* effect of DCA on the growth of tumors obtained by injection of parental or acid-adapted SiHa cells in mice. Daily administration of DCA (100 mg/kg) had no effect on parental SiHa tumors. In contrast, DCA treatment led to a significant decrease in tumor growth obtained from acid-adapted SiHa cells (Fig. 1G–H).

3.2. The higher uptake of DCA and the lower expression in PDK isoforms in acid-adapted cells account for the larger decrease in PDH phosphorylation

We first confirmed that the effects observed on cell density and proliferation were related to PDK inhibition, i.e. to a decrease in phosphorylated PDH. For both cell lines exposed to 5 mM DCA, a decrease in phosphorylated PDH was observed, and this reduction was more important in acid-adapted cells compared to parental cells (Fig. 2A). Of note, in untreated SiHa cells, the basal level of phosphorylated PDH was lower in acid-adapted cells compared to parental cells (Fig. 2A, right panel). We further explored the possible mechanisms responsible for this higher activity of DCA in acid-adapted cells. We first found that the DCA uptake, as quantified by ^{13}C NMR spectrometry, was significantly higher in acid-adapted cells than in parental cells (Fig. 2B). We also quantified the expression of the four different PDK isoforms in parental and acid-adapted cells. We observed that, except for PDK1 in HCT-116 cells, the abundance of each PDK isoform was reduced in acid-adapted cells compared to parental cells (Fig. 2C). This reduction in the pool of PDK as well as the higher uptake of DCA in acid-adapted cells is very likely to contribute to the larger decrease in PDH phosphorylation induced by DCA in acid-adapted cells.

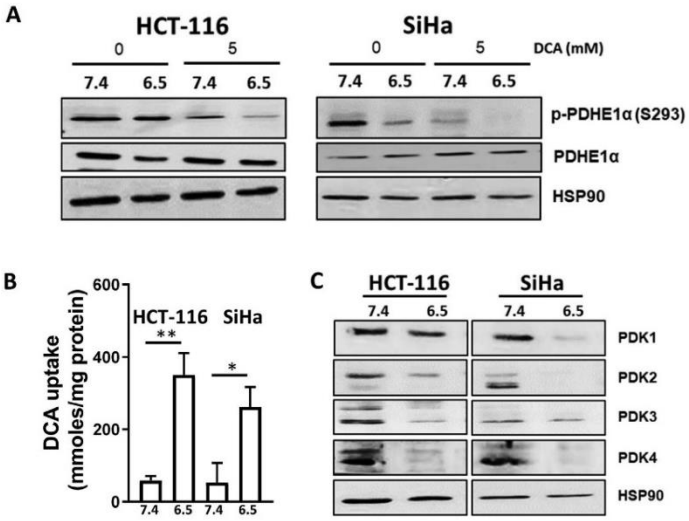

Fig. 2. Higher uptake of DCA and lower PDK abundance in acid-adapted cells account for the DCA-induced decrease in phosphorylated PDH. A, representative immunoblotting of phosphorylated and total form of PDH in SiHa, HCT-116 parental cell lines and acid–adapted cells after exposure to 0 or 5 mM of DCA for 24 h (n = 3). B, DCA uptake after exposure to 5 mM DCA for 24 h (n = 4) of SiHa and HCT-116 cell lines as well their adapted-cells. One-way ANOVA Sidak's multiple comparisons test, *p < 0.05, **p < 0.01. C, representative immunoblotting of the four PDK isoforms in SiHa, HCT - 116 cell lines and their pH 6.5 (n = 2).

3.3. The "glycolysis to oxidative" metabolic shift induced by DCA is larger in acid-adapted cells

^{13}C NMR spectrometry was further used to assess the effect of DCA on glucose metabolism in parental and acid-adapted cells. These two parental cell lines are known to present different metabolic profiles. The glucose consumption is two times higher in HCT-116 than in SiHa cells (8 μmol/10^6 cells vs 4 μmol/10^6 cells) and lactate secretion is two times lower in SiHa than in HCT-116 cells (7 μmol/10^6 cells vs 16 μmol/10^6 cells [28]. In Fig. 3B, we also measured the lactate production that was two times higher in HCT-116 than in SiHa cells. Consequently, the HCT-116 cell line is more glycolytic than the SiHa cell line. We monitored the fate of D-Glucose-$^{13}C_6$ in parental and acid-adapted cells, exposed or not to 5 mM DCA, for lactate and alanine production (Fig. 3A). We observed that the basal lactate production from glucose was significantly lower in acid-adapted cells compared to parental cells (Fig. 3B), confirming that acid-adapted cells are less glycolytic as previously shown in our laboratory [28,29]. When exposed to DCA 5 mM, we observed the expected reduction in lactate production from glucose (Fig. 3A, C). This result was observed in all parental and acid-adapted cancer cells. Interestingly, we observed that the relative decrease in lactate production from glucose was significantly more important in acid-adapted cells than in parental cells (Fig. 3C). In parental HCT-116 cells, we also observed that DCA treatment reduced the production of alanine, a metabolite produced by reductive amination of pyruvate (Fig. 3D). In SiHa cells, the very low basal glycolytic flux prevented the detection of alanine. Finally, an increase in OCR was observed in all cell lines except in SiHa parental cell line. This increase in OCR was more important in acid-adapted cells than in parental cells (Fig. 3E).

3.4. DCA-induced oxidative shift accounts for the growth inhibitory action of DCA through reduction of PPP activity and enhancement of apoptosis

De Preter et al. previously demonstrated that the inhibition of glycolysis by DCA controlled proliferation through reduction in pentose phosphate pathway (PPP) [16]. To bridge this gap between the proliferation assays and glycolytic flux measured in parental and acid-adapted cells, we evaluated the PPP flux by measuring the NADPH/NADP ratio after treatment using DCA and/or using 6-aminonicotamide (6-AN), a specific inhibitor of the PPP [33,34]. We observed that DCA had no influence on NADPH/NADP ratio in parental cells (Fig. 4A), but significantly reduced this ratio in acid-adapted cells. Interestingly, 6-AN also slightly reduced the NADPH/NADP ratio depending on the cell type (Fig. 4A). Most importantly, there was no significant difference between cells treated with DCA or 6-AN. Moreover, no additional decrease was observed when cells were simultaneously exposed to DCA and the PPP inhibitor, 6-AN. Overall, these results suggest that the decrease in NADPH production in acid-adapted cells is linked to a reduction in the PPP.

In addition to DCA anti-proliferative effects, we also observed that DCA exposure led to a decrease in cell density. Therefore, we investigated the effect of DCA exposure on apoptosis and cell death with flow cytometry. 10 mM DCA exposure for 48 h induced an increase in early and late apoptotic cells in acid-adapted HCT-116 cells, but not in parental cells (Fig. 4B–C). In acid-adapted SiHa cells, DCA exposure did not increase the proportion of early apoptotic cells but increased the proportion of late apoptotic/dead cells. In contrast, DCA exposure did not increase early apoptosis nor cell death in SiHa parental cells.

3.5. DCA exposure exacerbates glutamine metabolism in acid-adapted cells

We used L-Glutamine-$^{13}C_5$ tracer to measure glutamine metabolism (glutamate, malate and aspartate production from glutamine) by ^{13}C NMR spectrometry (Fig. 5A). We first observed that the glutamine uptake (determined from residual extracellular glutamine concentration after 24h) was higher in acid-adapted cells than in parental cells (Fig. 5B). Interestingly, for both cell lines the intracellular concentration of glutamine was higher in acid-adapted cells than in parental cells (Fig. 5C). DCA also increased intracellular glutamine concentration in acid-adapted cells but not in parental cells. No significant change in glutamate concentration was observed after DCA treatment, except for HCT-116 acid-adapted cells (Fig. 5D). Contrarily to the effect observed in parental cells, exposure to 5 mM DCA induced a significant increase

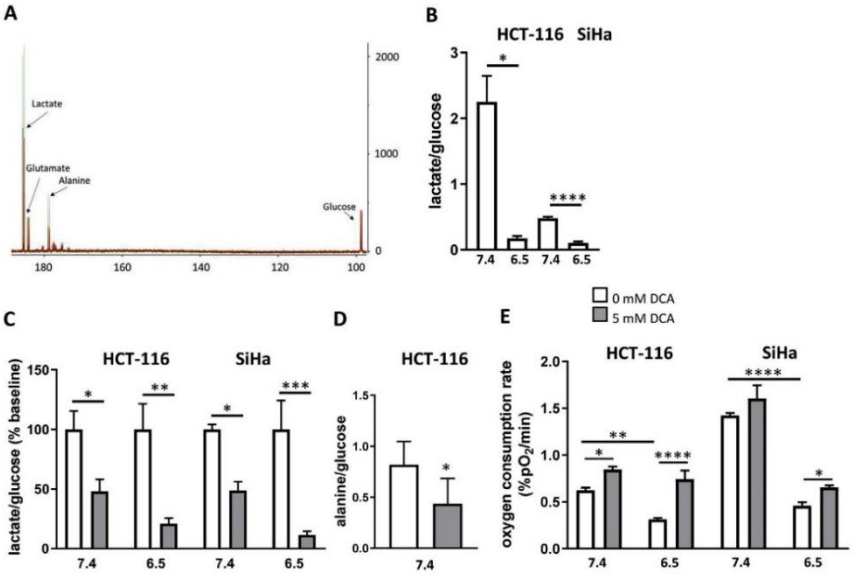

Fig. 3. The "glycolysis to oxidative" shift induced by DCA is larger in acid-adapted cells. A-D, Tumor cells were exposed during 24h to 10 mM of glucose-$^{13}C_6$ with or without 5 mM of DCA. Intra- and extracellular metabolites were measured by ^{13}C NMR spectroscopy (n = 5). A, representative spectra of intracellular metabolites of HCT-116 parental cells with zero (green) or 5 mM of DCA (red). B, lactate production from glucose in control conditions (0 mM DCA); results are expressed as ratio of total lactate (sum of intra-and extracellular lactate) on intracellular glucose. C, Baseline-corrected lactate production from glucose highlighting the larger effect of DCA in acid-adapted cells. D, alanine production from glucose (ratio of intracellular alanine on intracellular glucose). E, Oxygen consumption rate measured in parental HCT – 116, SiHa cell lines and their corresponding acidic-adapted cells, treated with or without 5 mM DCA for 24h (n = 3). Statistical analysis: paired *t*-test (D) and Two-way ANOVA (B, C, E) (Sidak's multiple comparisons test) *p < 0.05, **p < 0.01, ***p < 0.001, ****p < 0. 0001. (For interpretation of the references to colour in this figure legend, the reader is referred to the Web version of this article.)

in malate production from L-Glutamine-$^{13}C_5$ in acid-adapted cells (Fig. 5E). We also observed that the intracellular concentration of aspartate (produced from L-Glutamine-$^{13}C_5$) was increased in parental cells exposed to DCA 5 mM (Fig. 5F). As aspartate is produced by oxaloacetate, an intermediate of TCA cycle, this supports a stimulatory effect of DCA on glutamine metabolism in parental cells maintained at neutral pH. Using ^{13}C NMR, we failed to detect aspartate in acid-adapted cells. Finally, with mass spectrometry, we observed that the production of pyruvate from glutamine, a reaction involving another intermediate of the TCA cycle, namely malate, was more important in acid-adapted SiHa cells compared to parental SiHa cells (Fig. 5G).

3.6. The combination of DCA with a glutaminase inhibitor enhances the cytotoxic effect of DCA in acid-adapted cells

As DCA increased glutamine utilization, we hypothesized that stronger cytotoxic effects could be obtained by the association of DCA to an inhibitor of the glutamine pathway. For this purpose, we combined DCA with BPTES, an inhibitor of glutaminase-1 which converts glutamine into glutamate. We observed that in parental and acid-adapted cells, the combination DCA and BPTES significantly enhanced the growth inhibitory action of DCA (Fig. 6), an effect that was much more pronounced in acid-adapted cells.

4. Discussion

At first sight, the higher DCA-induced toxicity on tumor cells chronically exposed to acidosis compared to parental cells (Fig. 1) looks paradoxical considering that those cells are more prone to use glutamine and fatty acids at the expense of the glycolytic metabolism [28]. This unexpected observation prompted us to dissect the mechanisms responsible for this DCA effect which revealed an exquisite interplay between acidosis, pyruvate dehydrogenase and mitochondria at the origin of this enhanced anti-cancer activity.

We first observed a larger decrease in PDH phosphorylation in acid-adapted cells (Fig. 2A), an effect consistent with the PDK inhibition induced by DCA. Both the higher uptake of DCA and the lower expression of PDK isoforms observed in acid-adapted cells account for this enhanced PDK inhibition (Fig. 2B–C). It has been suggested that the uptake of DCA is mediated by monocarboxylate transporter and traverses the mitochondrial membranes via pyruvate transporter systems [11]. In addition, MCT1 (monocarboxylate transporter 1) is upregulated in tumor cells chronically exposed to acidosis [28]. However, in our case, the MCT1 blocker AR-155858 [35] and the MPC (mitochondrial pyruvate carrier) blocker 7ACC2 [36] did not affect DCA-induced cytotoxicity (data not shown). While DCA is mostly present under the ionized deprotonated form at pH 6.5 and 7.4 (due to its low pKa, 1.35), the proportion of neutral protonated form is about ten times higher at pH 6.5 compared to pH 7.4, a factor that could contribute to a higher diffusion of DCA through the cell membrane. However, the sole increase in DCA uptake cannot account for the increase in toxicity as we did not observe any significant difference in cell density between parental cells under physiological pH and cells acutely exposed to acidic pH under acute acidic (Fig. 1A–B). The increase in DCA concentration

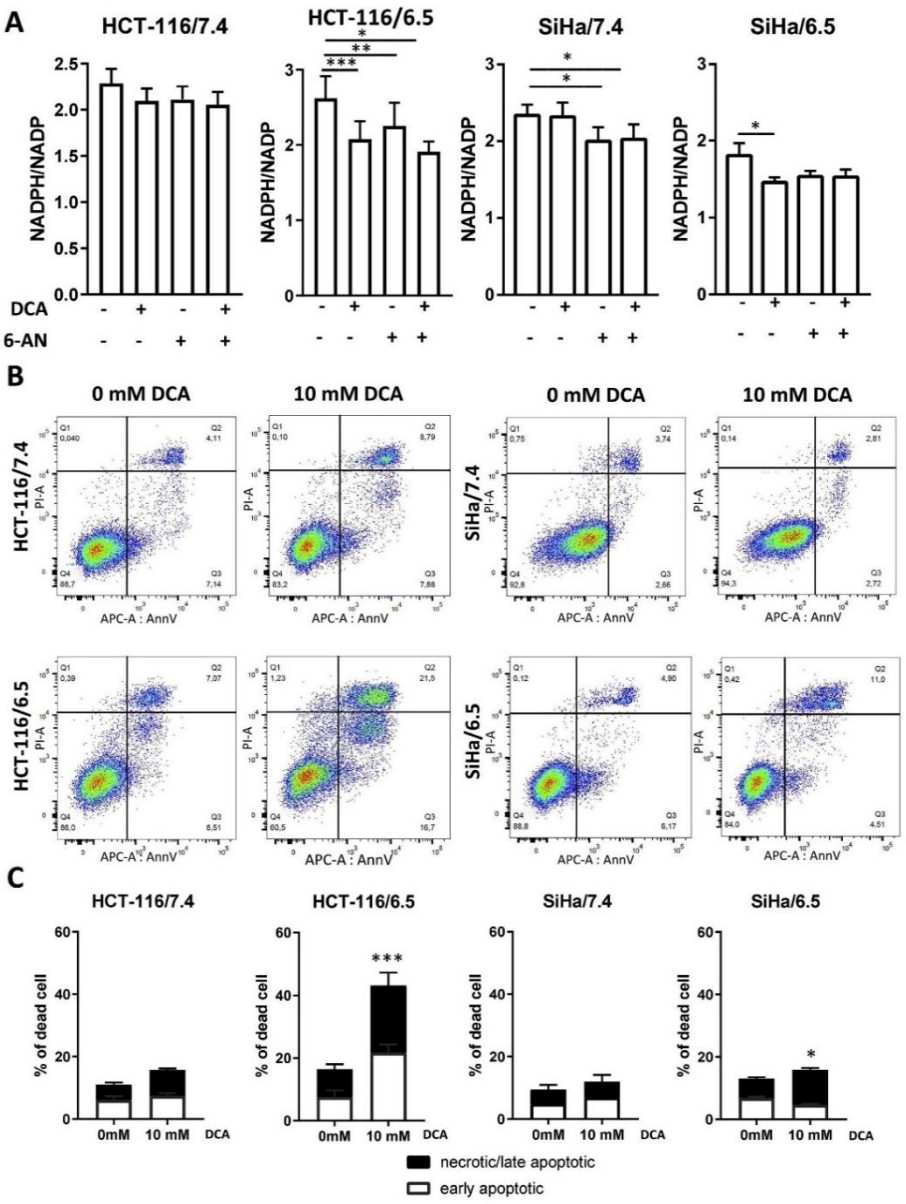

Fig. 4. DCA decreases PPP activity and enhances apoptosis in acid-adapted cells, but not in parental cells. A, NADPH/NADP measurements (n = 3) in HCT - 116, SiHa cell lines and their pH 6.5 – adapted cells treated with or without DCA (5 mM, 48h) and with or without 6-AN (100 μM, 48h). B, representative AnnexinV/PI flow cytometry plots of HCT-116 parental and acid-adapted cells and SiHa parental and acid-adapted cells, treated with or without 10 mM of DCA for 48h. C, histograms of percentage of apoptotic and dead cells. Statistical analysis: One-way (A) or Two-way ANOVA (Sidak's multiple comparison test) (C), *$p < 0.05$, **$p < 0.01$, ***$p < 0.001$.

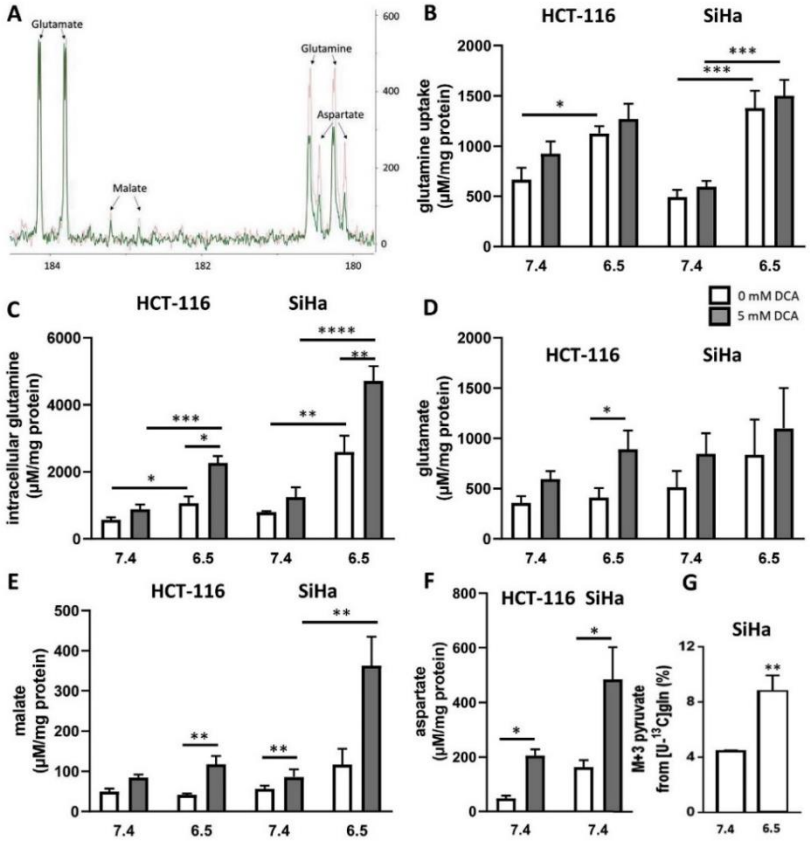

Fig. 5. Glutamine utilization is higher in acid-adapted cells leading to an increase in pyruvate production. A-F, SiHa and HCT-116 tumor cells were exposed during 24h to 2 mM Glutamine-^{13}C5 with or without 5 mM DCA. Intra- and extracellular metabolites were measured by ^{13}C NMR spectroscopy (n = 4) and result were normalize by total protein mass (mg). A, representative spectra of intracellular metabolites of HCT-116 parental cells with zero (green) or 5 mM of DCA (red). B, glutamine uptake. C, intracellular glutamine concentration. D, intracellular glutamate concentration. E, intracellular malate concentration. F, intracellular aspartate concentration. G, relative abundance of pyruvate mass isotopomers in parental and acidic acid-adapted SiHa cells cultured for 72 h with glutamine-5-^{13}C. Statistical analysis: Two-way ANOVA Sidak's multiple comparisons test (B–F) and paired *t*-test (G). *p < 0.05, **p < 0.01, ***p < 0.001, ****p < 0, 0001. (For interpretation of the references to colour in this figure legend, the reader is referred to the Web version of this article.)

coincided with a lower abundance of PDK isoforms observed in acid-adapted cells (Fig. 2C). This downregulation of PDKs could be due to alterations in the transcription factor HIF1-alpha activity. Corbet et al. have indeed previously demonstrated that acid-adapted cells present a downregulation of HIF-1 alpha [28] and other studies have shown that PDK1 and PDK3 are upregulated by HIF-1 alpha [37–39]. To our knowledge, the regulation of PDK2 and PDK4 by HIF-1 alpha has not been studied yet. The decrease in target enzyme together with higher concentration of the inhibitor may easily explain the larger decrease in PDH phosphorylation, a phenomenon usually associated with the re-activation of the transformation of pyruvate into acetyl-CoA. In our study, although the basal production of lactate was lower in acid-adapted cells compared to parental cells (Fig. 3B), we found that DCA induced a larger decrease in glycolytic flux (i.e., a larger relative reduction in lactate/glucose ratio) and an increase in oxidative phosphorylation (as evidenced by a net increase in OCR) in acid-adapted cells (Fig. 3). One may thus hypothesize that the low residual glycolytic metabolism in acid-adapted cancer cells renders them highly sensitive to the effects of DCA that completely shifts the glucose metabolism towards oxidative phosphorylation.

We further analyzed the consequences of this metabolic shift on cell proliferation and viability. It has been previously demonstrated that DCA controlled proliferation through reduction in PPP activity in MDA-MB-231 cell line [16]. DCA decreased PPP activity in acid-adapted cells, but not in parental cell lines (Fig. 4A), an effect that is consistent with the anti-proliferative effect of DCA in acid-adapted cells. Moreover, DCA has been described as a reactivator of mitochondrial apoptosis. By increasing the flux of pyruvate into the TCA cycle, it has been demonstrated that DCA enhanced mitochondrial membrane depolarization, which resulted in a release of pro-apoptotic mediators in the

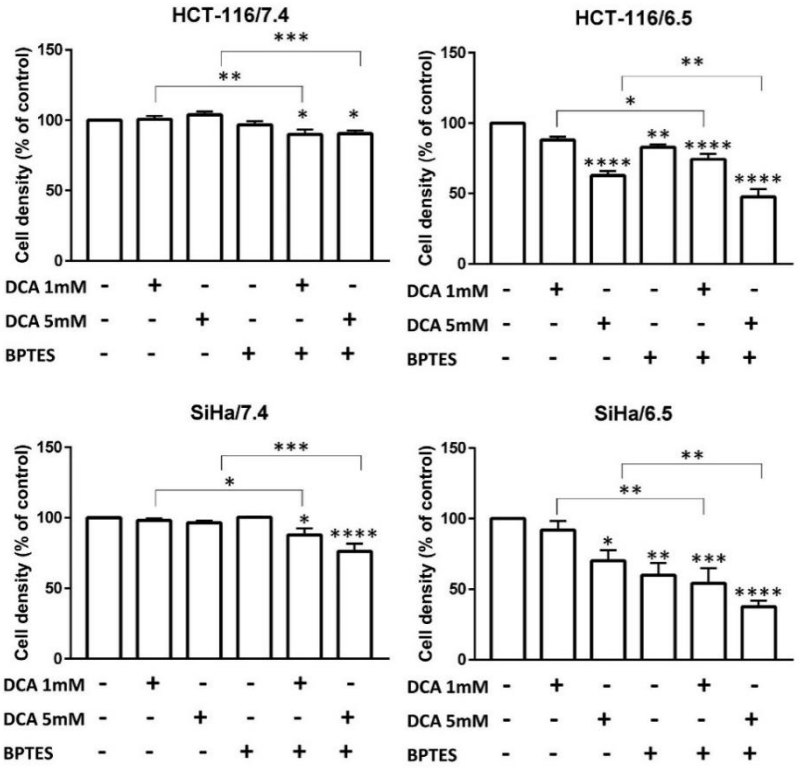

Fig. 6. Combined exposure to DCA and glutaminase inhibitor BPTES decreases tumor cell density more effectively in acid-adapted cells. SiHa and HCT-116 cells were exposed during 48h to increasing doses of DCA (0-1-5-mM) with or without 10 μM of BPTES (n = 3). Statistical analysis: One-way ANOVA Sidak's multiple comparisons test. *p < 0.05, **p < 0.01, ***p < 0.001, ****p < 0, 0001.

cytoplasm [12]. Here, we observed that DCA induced an increase in early and late apoptotic cells in acid-adapted cells (Fig. 4B–C), but not in parental cells. Altogether, these data suggest that DCA exacerbates the glycolytic to oxidative shift observed in acid-adapted cells, thereby decreasing the PPP flux, and reactivates mitochondrial-dependent apoptosis in these cancer cells that are intrinsically dependent on mitochondrial OXPHOS for growth and survival.

Because it has been reported that chronic exposure of tumor cells to acidosis is responsible for a higher dependency toward glutamine utilization [28], we also investigated the effect of DCA treatment on the glutamine pathway. As expected, the uptake of ^{13}C-glutamine was higher in acid-adapted cells (Fig. 5B). The increase in intracellular glutamine concentration in acid-adapted (Fig. 5C) cells as well as pyruvate production from glutamine (Fig. 5G) support the concept that chronic exposure to acidosis leads to an increase in glutamine metabolism via TCA cycling. In acid-adapted cells, we also found that DCA increased the intracellular concentration of glutamine, glutamate and malate in agreement with the DCA-based stimulation of the TCA cycle (Fig. 5C–E). We also found that DCA increased the aspartate production from glutamine in parental cells, in agreement with the DCA-based stimulation of the TCA cycle generating oxaloacetate, the aspartate precursor (Fig. 5F). The failure to detect aspartate in acid-adapted cancer cells suggests that its use to generate purine is by far higher than its production under acidosis. This may arise from a decreased TCA cycle turnover associated to the reduced glucose metabolism in acid-adapted cancer cells. The increased uptake of glutamine could thus reflect an attempt to compensate this alteration as supported by the anaplerotic formation of pyruvate from glutamine (Fig. 5G). This model also supports why the exacerbation of this process in DCA-treated acid-adapted cancer cells, as evidenced by the increased glutamine uptake, makes these cells particularly sensitive to glutaminase inhibitor BPTES (Fig. 6). The interaction between DCA and glutaminase inhibitor deserves to be studied more profoundly and the benefit of this combination should be investigated *in vivo* in order to open new perspectives for combined therapy.

In conclusion, the metabolic reprogramming induced by acidosis sensitizes cancer cells to DCA (Fig. 7) by stimulating apoptosis and thereby opens new perspectives of treatment as monotherapy but also in combination with glutaminase inhibitors since DCA exposure also exacerbates cancer cell addiction towards glutamine metabolism.

Author contribution

Conception and design: C. Schoonjans, B. Gallez.

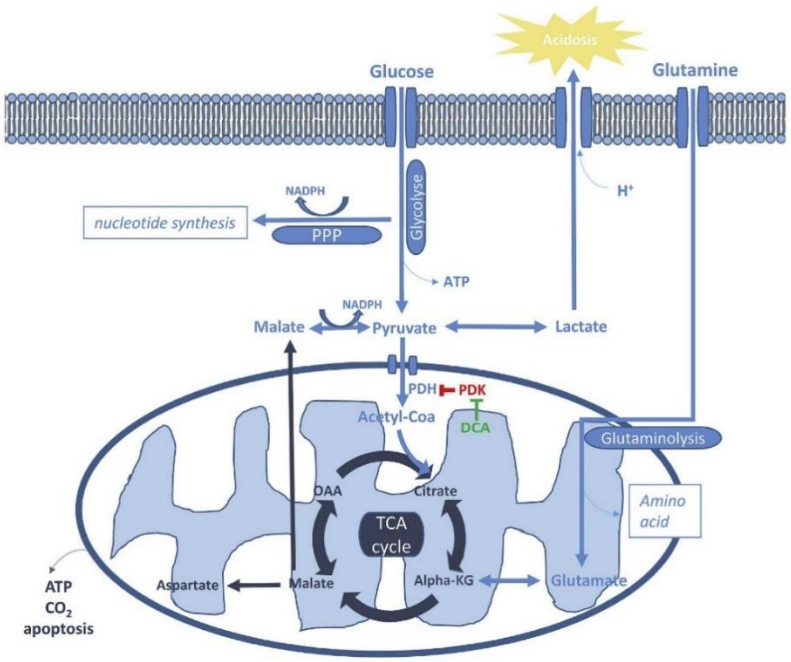

Fig. 7. Effect of DCA and acidosis on bioenergetics of cancer cells. Glucose metabolism through glycolysis produces ATP and carbon intermediates to sustain proliferation such as intermediates for the pentose phosphate pathway (PPP). PPP generates NADPH (defence against ROS) and is involved in nucleotide synthesis. The end-product of glycolysis, pyruvate, can be converted into lactate or acetyl-coA. Acetyl-coA fuels TCA cycle and lactate is exported outside of the cells with one proton and participate to the acidification of extracellular media. TCA cycle produces carbon intermediates for cellular proliferation such as aspartate, glutamate and precursors for lipid synthesis. Malate, through malic enzyme, is converted into pyruvate with generation of NADPH. In the presence of oxygen, TCA cycle via oxidative phosphorylation (OXPHOS) produces ATP. TCA cycle can also be replenished by glutamate. Glutamate is the result of glutaminolysis also involved in amino acid synthesis. In cells exposed to acidosis, DCA increases substrates fueling the TCA cycle by reactivating the PDH and increasing the glutamine utilization.

Development of methodology: C. Schoonjans, N. Joudiou, C. Corbet, D. Brusa.

Acquisition of data: C. Schoonjans.

Analysis and interpretation of data: C. Schoonjans, N. Joudiou, D. Brusa, C. Corbet, O. Feron, B. Gallez.

Writing, review, and/or revision of the manuscript: C. Schoonjans, N. Joudiou, D. Brusa, C. Corbet, O. Feron, B. Gallez.

Study supervision: B. Gallez, O. Feron.

Funding sources

Foundation against Cancer (2015-144 and 2016-087).

C. Schoonjans is a Televie PhD student.

The study used the facilities of the Nuclear and Electronic Spin Technologies (NEST) and Flow Cytometry platforms of UCLouvain.

Declaration of competing interest

The authors declare no potential conflicts of interest.

References

[1] R.J. DeBerardinis, N.S. Chandel, Fundamentals of cancer metabolism, Sci. Adv. 2 (2016) e1600200.

[2] I. Elia, G. Doglioni, S.M. Fendt, Metabolic hallmarks of metastasis formation, Trends Cell Biol. 28 (2018) 673–684.

[3] P.E. Porporato, S. Dhup, R.K. Dadhich, T. Copetti, P. Sonveaux, Anticancer targets in the glycolytic metabolism of tumors: a comprehensive review, Front. Pharmacol. 2 (2011) 49.

[4] R.A. Gatenby, R.J. Gillies, Why do cancers have high aerobic glycolysis? Nat. Rev. Cancer 4 (2004) 891–899.

[5] X.S. Chen, L.Y. Li, Y.D. Guan, J.M. Yang, Y. Cheng, Anticancer strategies based on the metabolic profile of tumor cells: therapeutic targeting of the Warburg effect, Acta Pharmacol. Sin. 37 (2016) 1013–1019.

[6] S. Fortunato, G. Bononi, C. Granchi, F. Minutolo, An update on patents covering agents that interfere with the cancer glycolytic cascade, ChemMedChem 13 (2018) 2251–2265.

[7] T. Golias, M. Kery, S. Radenkovic, I. Papandreou, Microenvironmental control of glucose metabolism in tumors by regulation of pyruvate dehydrogenase, Int. J. Cancer 144 (2019) 674–686.

[8] E. Saunier, C. Benelli, S. Bortoli, The pyruvate dehydrogenase complex in cancer: an old metabolic gatekeeper regulated by new pathways and pharmacological agents, Int. J. Cancer 138 (2016) 809–817.

[9] G. Kroemer, J. Pouyssegur, Tumor cell metabolism: cancer's Achilles' heel, Cancer Cell 13 (2008) 472–482.

[10] S. Bonnet, S.L. Archer, J. Allalunis-Turner, A. Haromy, C. Beaulieu, R. Thompson, C.T. Lee, G.D. Lopaschuk, L. Puttagunta, S. Bonnet, G. Harry, K. Hashimoto, C.J. Porter, M.A. Andrade, B. Thebaud, E.D. Michelakis, A mitochondria-K+ channel axis is suppressed in cancer and its normalization promotes apoptosis and inhibits cancer growth, Cancer Cell 11 (2007) 37–51.

[11] S. Kankotia, P.W. Stacpoole, Dichloroacetate and cancer: new home for an orphan drug? Biochim. Biophys. Acta 1846 (2014) 617–629.

[12] G. Sutendra, E.D. Michelakis, Pyruvate dehydrogenase kinase as a novel therapeutic

target in oncology, Front. Oncol. 3 (2013) 38.
[13] E.M. Dunbar, B.S. Coats, A.L. Shroads, T. Langaee, A. Lew, J.R. Forder, J.J. Shuster, D.A. Wagner, P.W. Stacpoole, Phase 1 trial of dichloroacetate (DCA) in adults with recurrent malignant brain tumors, Investig. New Drugs 32 (2014) 452–464.
[14] Q.S. Chu, R. Sangha, J. Spratlin, L.J. Vos, J.R. Mackey, A.J. McEwan, P. Venner, E.D. Michelakis, A phase I open-labeled, single-arm, dose-escalation, study of dichloroacetate (DCA) in patients with advanced solid tumors, Investig. New Drugs 33 (2015) 603–610.
[15] E.D. Michelakis, L. Webster, J.R. Mackey, Dichloroacetate (DCA) as a potential metabolic-targeting therapy for cancer, Br. J. Canc. 99 (2008) 989–994.
[16] G. De Preter, M.A. Neveu, P. Danhier, L. Brisson, V.L. Payen, P.E. Porporato, B.F. Jordan, P. Sonveaux, B. Gallez, Inhibition of the pentose phosphate pathway by dichloroacetate unravels a missing link between aerobic glycolysis and cancer cell proliferation, Oncotarget 7 (2016) 2910–2920.
[17] G. Sutendra, P. Dromparis, A. Kinnaird, T.H. Stenson, A. Haromy, J.M. Parker, M.S. McMurtry, E.D. Michelakis, Mitochondrial activation by inhibition of PDKII suppresses HIF1a signaling and angiogenesis in cancer, Oncogene 32 (2013) 1638–1650.
[18] M. Morfouace, L. Lalier, M. Bahut, V. Bonnamain, P. Naveilhan, C. Guette, L. Oliver, N. Gueguen, P. Reynier, F.M. Vallette, Comparison of spheroids formed by rat glioma stem cells and neural stem cells reveals differences in glucose metabolism and promising therapeutic applications, J. Biol. Chem. 287 (2012) 33664–33674.
[19] I. Papandreou, T. Goliasova, N.C. Denko, Anticancer drugs that target metabolism: is dichloroacetate the new paradigm? Int. J. Cancer 128 (2011) 1001–1008.
[20] J.W. Wojtkowiak, D. Verduzco, K.J. Schramm, R.J. Gillies, Drug resistance and cellular adaptation to tumor acidic pH microenvironment, Mol. Pharm. 8 (2011) 2032–2038.
[21] K.M. Bailey, J.W. Wojtkowiak, A.I. Hashim, R.J. Gillies, Targeting the metabolic microenvironment of tumors, Adv. Pharmacol. 65 (2012) 63–107.
[22] M. Damaghi, N.K. Tafreshi, M.C. Lloyd, R. Sprung, V. Estrella, J.W. Wojtkowiak, D.L. Morse, J.M. Koomen, M.M. Bui, R.A. Gatenby, R.J. Gillies, Chronic acidosis in the tumour microenvironment selects for overexpression of LAMP2 in the plasma membrane, Nat. Commun. 6 (2015) 8752.
[23] M. Damaghi, R. Gillies, Phenotypic changes of acid-adapted cancer cells push them toward aggressiveness in their evolution in the tumor microenvironment, Cell Cycle 16 (2017) 1739–1743.
[24] V. Estrella, T. Chen, M. Lloyd, J. Wojtkowiak, H.H. Cornnell, A. Ibrahim-Hashim, K. Bailey, Y. Balagurunathan, J.M. Rothberg, B.F. Sloane, J. Johnson, R.A. Gatenby, R.J. Gillies, Acidity generated by the tumor microenvironment drives local invasion, Cancer Res. 73 (2013) 1524–1535.
[25] S.R. Pillai, M. Damaghi, Y. Marunaka, E.P. Spugnini, S. Fais, R.J. Gillies, Causes, consequences, and therapy of tumors acidosis, Cancer Metastasis Rev. (2019).
[26] G. Lamonte, X. Tang, J.L. Chen, J. Wu, C.K. Ding, M.M. Keenan, C. Sangokoya, H.N. Kung, O. Ilkayeva, L.G. Boros, C.B. Newgard, J.T. Chi, Acidosis induces reprogramming of cellular metabolism to mitigate oxidative stress, Cancer Metabol. 1 (2013) 23.
[27] C. Corbet, O. Feron, Tumour acidosis: from the passenger to the driver's seat, Nat. Rev. Cancer 17 (2017) 577–593.
[28] C. Corbet, N. Draoui, F. Polet, A. Pinto, X. Drozak, O. Riant, O. Feron, The SIRT1/HIF2alpha axis drives reductive glutamine metabolism under chronic acidosis and alters tumor response to therapy, Cancer Res. 74 (2014) 5507–5519.
[29] C. Corbet, A. Pinto, R. Martherus, J.P. Santiago de Jesus, F. Polet, O. Feron, Acidosis drives the reprogramming of fatty acid metabolism in cancer cells through changes in mitochondrial and histone acetylation, Cell Metabol. 24 (2016) 311–323.
[30] O. Feron, L. Belhassen, L. Kobzik, T.W. Smith, R.A. Kelly, T. Michel, Endothelial nitric oxide synthase targeting to caveolae. Specific interactions with caveolin isoforms in cardiac myocytes and endothelial cells, J. Biol. Chem. 271 (1996) 22810–22814.
[31] Q. Teng, W. Huang, T.W. Collette, D.R. Ekman, C. Tan, A direct cell quenching method for cell-culture based metabolomics, Metabolomics 5 (2008) 199.
[32] B.F. Jordan, V. Gregoire, R.J. Demeure, P. Sonveaux, O. Feron, J. O'Hara, V.P. Vanhulle, N. Delzenne, B. Gallez, Insulin increases the sensitivity of tumors to irradiation: involvement of an increase in tumor oxygenation mediated by a nitric oxide-dependent decrease of the tumor cells oxygen consumption, Cancer Res. 62 (2002) 3555–3561.
[33] D.A. Scott, A.D. Richardson, F.V. Filipp, C.A. Knutzen, G.G. Chiang, Z.A. Ronai, A.L. Osterman, J.W. Smith, Comparative metabolic flux profiling of melanoma cell lines: beyond the Warburg effect, J. Biol. Chem. 286 (2011) 42626–42634.
[34] E. Tsouko, A.S. Khan, M.A. White, J.J. Han, Y. Shi, F.A. Merchant, M.A. Sharpe, L. Xin, D.E. Frigo, Regulation of the pentose phosphate pathway by an androgen receptor-mTOR-mediated mechanism and its role in prostate cancer cell growth, Oncogenesis 3 (2014) e103.
[35] M.J. Ovens, A.J. Davies, M.C. Wilson, C.M. Murray, A.P. Halestrap, AR-C155858 is a potent inhibitor of monocarboxylate transporters MCT1 and MCT2 that binds to an intracellular site involving transmembrane helices 7-10, Biochem. J. 425 (2010) 523–530.
[36] C.V. Linden, C. Corbet, Killing two birds with one stone: blocking the mitochondrial pyruvate carrier to inhibit lactate uptake by cancer cells and radiosensitize tumors, Mol. Cell. Oncol. 5 (2018) e1465016.
[37] C.W. Lu, S.C. Lin, K.F. Chen, Y.Y. Lai, S.J. Tsai, Induction of pyruvate dehydrogenase kinase-3 by hypoxia-inducible factor-1 promotes metabolic switch and drug resistance, J. Biol. Chem. 283 (2008) 28106–28114.
[38] H. Semba, N. Takeda, T. Isagawa, Y. Sugiura, K. Honda, M. Wake, H. Miyazawa, Y. Yamaguchi, M. Miura, D.M. Jenkins, H. Choi, J.W. Kim, M. Asagiri, A.S. Cowburn, H. Abe, K. Soma, K. Koyama, M. Katoh, K. Sayama, N. Goda, R.S. Johnson, I. Manabe, R. Nagai, I. Komuro, HIF-1alpha-PDK1 axis-induced active glycolysis plays an essential role in macrophage migratory capacity, Nat. Commun. 7 (2016) 11635.
[39] N. Ho, B.L. Coomber, Pyruvate dehydrogenase kinase expression and metabolic changes following dichloroacetate exposure in anoxic human colorectal cancer cells, Exp. Cell Res. 331 (2015) 73–81.

2. IMPACT OF DCA ON ENDOTHELIAL CELLS

Targeting endothelial cell metabolism by inhibition of pyruvate dehydrogenase kinase and glutaminase-1

Schoonjans, C. A., Mathieu, B., Joudiou, N., Zampieri, L. X., Brusa, D., Sonveaux, P., & Gallez, B. (2020). Journal of clinical medicine, 9(10), 3308.

For supplementary methodology information, see methodology section on ^{13}C fluxomic methodology (page 139).

Journal of Clinical Medicine

MDPI

Article

Targeting endothelial cell metabolism by inhibition of pyruvate dehydrogenase kinase and glutaminase-1

C.A. Schoonjans[1,2], B. Mathieu[1], N. Joudiou[3], L.X. Zampieri[2], D. Brusa[4], P. Sonveaux[2], O. Feron[2], and B. Gallez[1]*

[1] Université Catholique de Louvain (Uclouvain), Louvain Drug Research Institute, Biomedical Magnetic Resonance Research Group, Brussels, Belgium
[2] Université Catholique de Louvain (Uclouvain), Institut de Recherche Expérimentale et Clinique, Pole of Pharmacology and Therapeutics, Brussels, Belgium
[3] Université Catholique de Louvain (Uclouvain), Louvain Drug Research Institute, Nuclear and Electron Spin Technologies, Brussels, Belgium
[4] Université Catholique de Louvain (Uclouvain), Institut de Recherche Expérimentale et Clinique, CytoFlux - Flow Cytometry Platform, Belgium
* Correspondence: bernard.gallez@uclouvain.be

Abstract: Targeting endothelial cell (EC) metabolism should impair angiogenesis, regardless of how many angiogenic signals are present. The dependency of proliferating ECs on glucose and glutamine for energy and biomass production opens new opportunity for anti-angiogenic therapy in cancer. The aim of the present study was to investigate the role of pyruvate dehydrogenase kinase (PDK) inhibition with dichloroacetate (DCA), alone or in combination with the glutaminase-1 (GLS-1) inhibitor, BPTES, on Human umbilical vein endothelial cells (HUVECs) metabolism, proliferation, apoptosis, migration and vessel formation. We demonstrated that both drugs normalize HUVECs metabolism by decreasing glycolysis for DCA and by reducing glutamate production for BPTES. DCA and BPTES reduced HUVECs proliferation and migration but have no impact on tube formation. While DCA increased HUVECs respiration, BPTES decreased it. Using both drugs in combination further reduced HUVECs proliferation while normalizing respiration and apoptosis induction. Overall, we demonstrated that DCA, a metabolic drug under study to target cancer cell metabolism, also affect tumor angiogenesis. Combining DCA and BPTES may reduce adverse effect of each drug alone and favor tumor angiogenesis normalization.

Keywords: endothelial cell metabolism; tumor microenvironment; glycolysis inhibition**;** dichloroacetate; glutaminolysis inhibition; BPTES; ^{13}C-NMR

1. Introduction

Once activated by pro-angiogenic factors, endothelial cells (ECs) are sprouting to extend the vasculature and to supply the growing tumors with oxygen and nutrients (Li et al. 2019). While angiogenesis is an enticing target, therapies based on vascular endothelial growth factor (VEGF) blockade have shown limited results due to upregulation of alternative proangiogenic growth factors (Fitzgerald et al. 2018, Li et al. 2019). In contrast, targeting EC metabolism should impair angiogenesis, regardless of how many angiogenic signals are present (Li et al. 2019). The dependency of proliferating ECs on glucose but also glutamine and fatty acids for energy and biomass production opens new opportunity for anti-angiogenic therapy in cancer (De Bock et al. 2013, Schoors et al. 2015, Huang et al. 2017). High rate of glycolysis is a hallmark of proliferating ECs allowing a rapid ATP production and the generation of precursors for biomass synthesis (De Bock et al. 2013, Cantelmo et al. 2016). Even if glycolysis is crucial for ECs proliferation, mitochondria in ECs are still functional and can be fueled by several metabolites such as glutamine (Li et al. 2019). It has been shown that glutamine, the most abundant free amino acid, is essential for EC proliferation and migration (Huang et al. 2017, Kim et al. 2017). Glutamine is metabolized into glutamate through glutaminase-1 (GLS-1), which can fuel the mitochondrial tricarboxylic acid (TCA) cycle (Huang et al. 2017, Kim et al. 2017, Peyton et al. 2018). Together with TCA cycle intermediates, glutamine and glutamate are involved in anti-oxidant defense production, synthesis of nucleotides, proteins and fatty acids. Consequently, counteracting glycolysis and glutamine pathways are promising approaches to reduce angiogenesis. In this respect, it has been previously shown that blockade of the glycolytic activator PFKFB3 reduced cancer cell invasion, intravasation, and metastasis by normalizing tumor vessels (Cantelmo et al. 2016). It has also been shown that the inhibition of GLS-1 impaired ECs survival, proliferation and migration (Huang et al. 2017, Kim et al. 2017, Eelen et al. 2018, Peyton et al. 2018).

Based on the above considerations, we can hypothesize that inhibition of pyruvate dehydrogenase kinase (PDK) could decrease proliferative ECs metabolism and impact ECs migration and proliferation. The rationale behind this hypothesis is the following. PDK phosphorylates and inactivates the enzyme pyruvate dehydrogenase (PDH). The active unphosphorylated PDH metabolizes pyruvate to acetyl-CoA that fuels TCA cycle. Therefore, PDK inhibition reactivates PDH leading to a redirection of glucose metabolism from cytoplasmic glycolysis to mitochondrial oxidation. It is already known that PDK play a role in angiogenesis through the hypoxia-inducible factor-1α (HIF-1α). In 2017, a study on flow-induced metabolic reprogramming in ECs, reported that HIF-1α increased PDK-1 which reduced mitochondrial respiratory capacity (Wu et al. 2017). On cancer cells from various

origins, it has been shown that DCA, a PDK inhibitor currently studied in clinical trials, decreased HIF-1 activity resulting in a reduced expression of HIF-1α target genes including pro-angiogenic factors (Sonveaux et al. 2012, Sutendra et al. 2013) and a decreased tumor angiogenesis (Michelakis et al. 2010, Duan et al. 2013, Sutendra et al. 2013, Sutendra et al. 2013, Kinnaird et al. 2016). To our knowledge, besides this HIF-1α mediated effect by cancer cells, a direct effect of DCA through a metabolic reprogramming of ECs has not been previously considered. This is in sharp contrast with the established metabolic reprogramming induced by DCA on cancer cells (Kankotia et al. 2014). By reversing aerobic glycolysis in cancer cells, DCA reduces glycolytic intermediates available for proliferation, mainly through the pentose phosphate pathway (Sutendra et al. 2013). Consequently, this decrease of building blocks from glycolysis is responsible for the anti-proliferative effects of PDK inhibition observed in various cancer cells lines (Sutendra et al. 2013, Dunbar et al. 2014, Kankotia et al. 2014, Chu et al. 2015, De Preter et al. 2016, Schoonjans et al. 2020). In addition, by reactivating the mitochondrial activity, DCA reverses the abolition of mitochondria-dependent apoptosis (Michelakis et al. 2008, Sutendra et al. 2013). Of note, it was recently observed in cancer cells that DCA exposure may also exacerbate glutamine metabolism providing the rationale for the combination of DCA with the GLS-1 inhibitor, bis-2-(5-phenylacetamido-1,3,4-thiadiazol-2-yl) ethyl sulfide (BPTES)[12].

As glycolysis and glutamine pathways are essential for ECs fitness, the aim of the present study was to investigate the role of PDK inhibition with DCA, alone or in combination with the GLS-1 inhibitor, BPTES, on HUVECs metabolism, proliferation, apoptosis, migration and vessels formation.

2. Experimental Section

2.1. Cell culture and reagents

Primary Umbilical Vein Endothelial Cells (HUVECs) (ATCC® PCS-100-013™), SiHa cells and HCT-116 cells were acquired from the American Type Culture Collection (ATCC, Manassas, VA, USA). SiHa and HCT-116 cell lines were maintained in DMEM (D5030, Sigma-Aldrich, Saint-Louis, MO, USA) supplemented with 10 mM of glucose, 2 mM of glutamine, 10% heat-inactivated FBS (Thermo Fisher Scientific, Waltham, MA, USA) and with 25 mmol/L of both PIPES and HEPES. HUVECs were used until passage 5 and grown in Vascular Cell Basal Medium (ATCC® PCS-100-030™) supplements with Endothelial Cell Growth Kit-VEGF (ATCC® PCS-100-041™). Endothelial Cell Growth Kit-VEGF contains components that were added to Vascular Cell Basal Medium to create a complete, low serum culture environment.

For each component, the final concentration in complete endothelial growth medium is as follows:

- rh VEGF: 5 ng/mL
- rh EGF: 5 ng/mL
- rh FGF basic: 5 ng/mL
- rh IGF-1: 15 ng/mL
- L-glutamine: 10 mM
- Heparin sulfate: 0.75 Units/mL
- Hydrocortisone: 1 μg/mL
- Ascorbic acid: 50 μg/mL
- Fetal bovine serum: 2%

Dichloroacetate (DCA) was ordered from Sigma-Aldrich (Saint-Louis, MO, USA) and dissolved in culture media. Bis-2-(5-phenylacetamido-1,3,4-thiadiazol-2-yl)ethyl sulfide (BPTES) was ordered from Sigma-Aldrich and first dissolved in DMSO (Sigma-Aldrich) and then diluted in culture media (final DMSO concentration ≤ 0,1%).

2.2. Cell proliferation

Cell proliferation was assayed with a 5-bromo-2'-deoxyuridine (BrdU)-ELISA based kit (Roche, Bâle, Switzerland) following the provider's instructions. 2000 cells per well were seeded in a 96-well plate. After 24 hours, cells were treated with 5 or 10 mM DCA and/or 1μM BPTES. After 48 hours exposure, cells were incubated in the presence of BrdU for 2 hours. The amount of BrdU incorporated in the cells was quantified by measuring the absorbance at 370 nm using a SpectraMax M2e plate reader (Molecular Devices), which permitted the quantification of DNA synthesis in proliferative cells.

2.3. Cell Migration

8000 cells per well were seeded in a culture-insert 2 well (μ-Dish35mm, Ibidi, Munich, Germany). After 24h, 1μg/mL MitomycinC (MitoC, Sigma-Aldrich) was added in each well to stop cellular proliferation. 10h later, the insert was removed creating a cell-free gap of 500 μm. The dish was filled with 2 mL of media containing 1μg/mL MitoC and 5 or 10 mM of DCA and/or 1μM BPTES. Pictures of migration were taken at T0 and T0+14 hours with an inverted microscope **(**Life Cell Observer Z1 with AxioCam 504 mono). Cell migration was quantified with the wound healing tool ImageJ analysis software.

2.4. Tube formation

24-well plates were coated with 300 µl per well of Matrigel growth factor reduced (Corning, New York). Once the matrigel had solidified, 30 000 cells were seeded and treated with 5 or 10 mM of DCA and/or 1µM BPTES. After 4 hours incubation, pictures were taken with an inverted microscope (**Life Cell Observer Z1 with AxioCam 504 mono).** Tube formation was quantified using WimTube of Wimasis image analysis system (Wimasis GmbH, Munich, Germany)**.**

2.5. Western blotting analyses of PDH phosphorylation

Whole cellular lysates were collected after 24 hours of incubation with 5 or 10 mM DCA and immunoblot analysis were performed as previously described (Feron et al. 1996). The following primary antibodies were used: phospho-PDHE1-A (1/1000, #ABS204, Millipore, Burlington, MA, USA) and PDHE1a (1:1000,#3820, Cell Signaling, Danvers, MA, USA). HSP90 antibody (1/1000, 610419, BD Bioscience, San Jose, CA, USA) was used for gel loading normalization. Densitometry analysis was performed using Image J software. Band densities for PDHE1α and p-PDHE1α were normalized to the band density of HSP90 in the same sample. Results are expressed in percentage of the control condition.

2.6. ^{13}C NMR spectroscopy quantification of metabolites

Isotope-labeled glucose medium was prepared with DMEM media (D5030, Sigma-Aldrich) supplemented with Endothelial Cell Growth Kit-VEGF and with 5 mmol/L of D-Glucose-$^{13}C_6$ (Sigma-Aldrich). Isotope-labeled glutamine medium was prepared with vascular Cell Basal Medium supplemented with Endothelial Cell Growth Kit-VEGF except the glutamine component. Instead of the glutamine component, 10 mM of L-glutamine-5-^{13}C (Sigma-Aldrich) was supplemented in the isotope-labeled glutamine medium. 48 hours after seeding $4x10^5$ cells in a 100 mm dish (2 dishes per condition), cell culture medium was changed for isotope-labeled glucose or glutamine medium. Cells were incubated in the presence of 5 or 10 mM DCA and/or 1 µM BPTES from ^{13}C-glutamine experiments. 24h after treatments, intra and extracellular metabolites were extracted as previously described (Schoonjans et al. 2020). For each condition, extra dishes were seeded and protein quantification was performed using the BCA Protein Assay Kit (Pierce™ BCA Protein Assay Kit, Thermo Fisher). Results were quantified regarding the ratio of proteins levels between control and each treated condition.

2.7. Oxygen consumption rate

The effect of DCA and BPTES on the oxygen consumption rate was measured by Seahorse XF96 bioenergetic analyzer using the XF cell mito stress kit (Agilent Technologies) which allows to calculate basal OCR, maximal OCR after FCCP stimulation (carbonyl cyanide 4-(trifluoromethoxy)phenyl-hydrazone) and non-

mitochondrial respiration after rotenone rotenone/antimycin A injection. 2000 cells per well were seeded on XF96 culture plates. After 24 hours, cells were treated with 5 or 10 mM DCA and/or 1μM BPTES. After 24 hours exposure, culture media were replaced by DMEM containing 5 mM glucose, 10 mM glutamine. Cells were incubated for 1 hour in a CO_2-free incubator before analysis. To obtained basal and maximal mitochondrial OCR, non-mitochondrial OCR was subtracted to basal and maximal OCR. Data were normalized to cell numbers quantified right before OCR measurement using a SpectraMax miniMax 300 imaging cytometer.

2.8. Flow cytometry measurement of apoptosis

A total of $1x10^5$ cells were seeded in a 60 mm dish. 24 hours after, cells were incubated with in the presence of 5 or 10 mM DCA and/or 1 μM BPTES. 48 hours after treatment, cells were rinsed with PBS, trypsinized and resuspended in fresh media. Following provider's instructions, EBioscience™ Annexin V Apoptosis Detection Kit APC (Invitrogen™, Thermo Fisher Scientific) was used for the measurement of dead, apoptotic and livingcells. The cells were distinguished between dead: late apoptotic (AnnV+DAPI+), early/medium apoptotic (AnnV+DAPI−), and alive (double negative). Flow cytometry data were collected using a BD FACS Canto II flow cytometer and analyzed with FlowJo software. FACS analysis by FlowJo were processed for each cell line separately. At least 20,000 events were analyzed for each sample.

2.9. Statistical Analysis

Data are expressed as mean ± SEM (standard error of the mean). The number of replicates and the statistical test used are indicated in each figure caption. GraphPad Prism 8.0 software was used to analyzed all the data.

3. Results

3.1. DCA reduces HUVECs proliferation similarly to cancer cells and induces a metabolic shift from glycolysis to mitochondrial respiration through PDH activation

We first investigated if HUVECs where sensitive to DCA. We observed that the exposure to increasing concentration of DCA was correlated with a reduction in HUVECs proliferation (fig.1A). We determined that DCA at 5 mM was the lowest DCA concentration that induces a significant decrease in HUVECs proliferation. We compared our results with DCA effect on cancer proliferation (fig.1B). We used two cancer cell lines: HCT-116 (colorectal cancer cells) and SiHa (cervix cancer cells). We noticed that HUVECs were as sensitive to DCA exposure concentration than the SiHa cancer cell line and more sensitive than the HCT-116 cancer cell line. We then measured that these effects observed on HUVECs proliferation were associated to PDK inhibition, i.e. to a reduction in phosphorylated

PDH. In HUVECs exposed to 5 or 10 mM DCA, a reduction in phosphorylated PDH was observed (fig.1C-D). Next, we explored the consequences of PDK inhibition on HUVECs glycolytic metabolism. Using ^{13}C-NMR spectroscopy, we followed the metabolism of glucose. As previously observed by others (De Bock et al. 2013), we observed that proliferative HUVECs present a high glycolytic metabolism with a glycolytic index of 1.71 (ratio of lactate production on glucose consumed) (fig.1E). The HUVECs exposure to 5 or 10 mM DCA led to a reduction in the glycolytic index (fig.1E). To explore the impact of DCA on the mitochondrial activity of HUVECs, we measured the mitochondrial oxygen consumption rate (OCR). We observed an increase in mitochondrial basal OCR after DCA exposure (fig.1F). However, HUVECs exposure to high concentration of DCA (10 mM) gives the same increase in OCR than exposure to the lower DCA concentration (5 mM). Using FCCP, we measured the maximal mitochondrial respiration rate and observed no difference with or without DCA exposure (fig.1G). We then calculated the spare respiratory capacity (maximal OCR minus basal OCR) and noticed a reduction in spare respiratory capacity after DCA treatment (fig.1H). Finally, we noticed that only the higher DCA concentration significantly increased HUVECs apoptosis (fig.1I-J), while HUVECs exposure to 5 mM of DCA did not induce change in apoptosis.

1

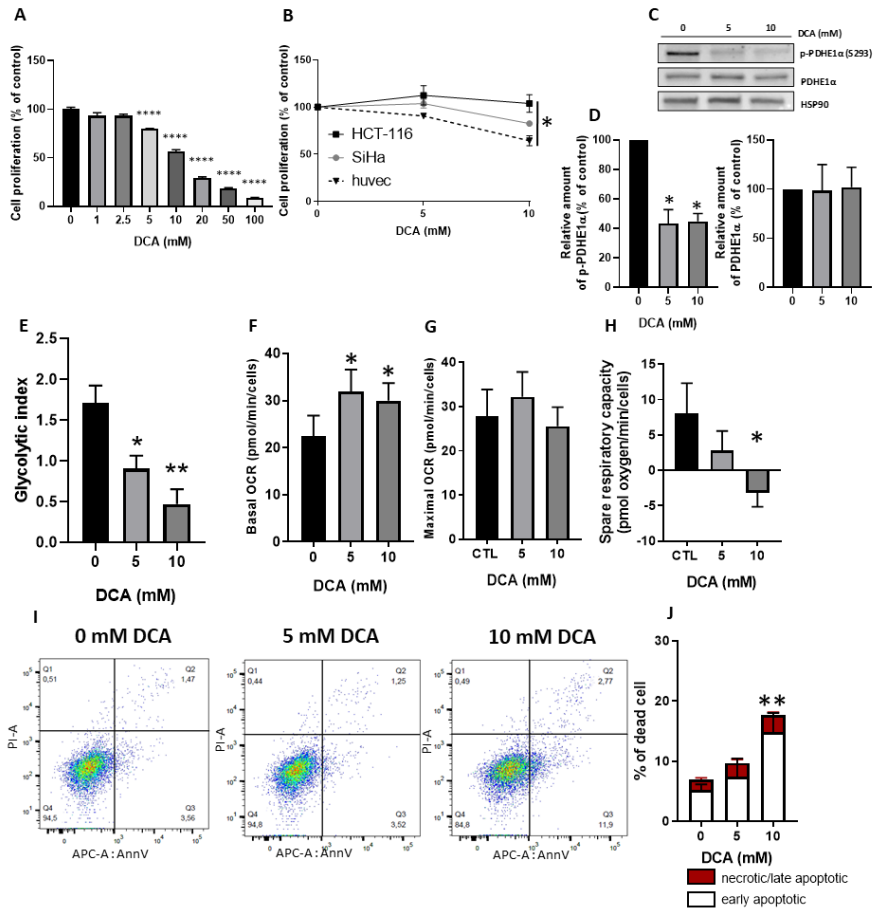

Figure 1: DCA reduces HUVECs proliferation and, through PDH activation, induces a metabolic shift towards decrease in glycolysis and in spare respiratory capacity. A, proliferation of HUVECs exposed to increasing doses of DCA (0-100 mM) (n=4). B, comparison of the effect of DCA exposure on cell proliferation between cancer cells (HCT-116 and SiHa) and HUVECs (n=3). C, representative immunoblotting of total (PDHE1α) and phosphorylated (p-PDHE1α) form of PDH in HUVECs after exposure to 0, 5 or 10 mM DCA (n = 3). D, densitometry analysis of p-PDHE1α and PDHE1α. E, lactate production from glucose in control and DCA treated HUVECs (5 and 10 mM DCA); results are presented as ratio of total lactate (sum of intra-and extracellular lactate) on glucose uptake (n=3). F - G, oxygen consumption rate (F, basal OCR and G, maximum OCR) measured in HUVECs treated with or without DCA (5 and 10 mM) (n=3). H, spare respiratory capacity (maximal OCR minus basal OCR). I, representative AnnexinV/PI flow cytometry plots of HUVECs treated with or without 5 or 10 mM of DCA. J, histograms of apoptotic and dead cells (n=4). Statistical analysis: One-way (A, D-H), or Two-way ANOVA (J) (Sidak's multiple comparison test), *p <0.05, **p <0.01, *** p <0.001, **** p <0.0001.

3.2. *DCA reduces HUVECs migration without impacting tube formation*

To explore the relevance of the DCA impact on HUVECs *in vitro* angiogenesis, we evaluated his effect on HUVECs migration and tube formation (figure 2). Using culture-inserts 2 well, we monitored the cell migration. To avoid the impact of cell proliferation, cells were incubated with mitomycin C, a cell division blocker. Fourteen hours after removal of the insert, we observed that HUVECs migration was significantly lower in DCA treated cells compared to control cells (fig.2A-B). We also measured HUVECs tube formation by seeding the cells on coated wells with matrigel. 4 hours after cells seeding, tubes were formed. We quantified the total tube length, the number of tubes, the number of branching points (where three or more tubes converge), and the number of loops (areas enclosed by tubes) (fig.2C-D). We measured no difference on tube formation between control and DCA treated HUVECs including all the quantified parameters.

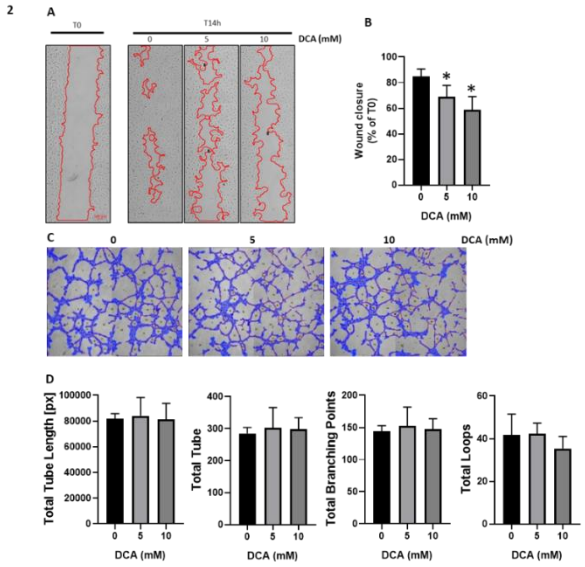

Figure 2: DCA reduces HUVECs migration without impact on tube formation. A-B, Wound healing assays: HUVECs were pre-treated with mitomycin C and DCA treatment started when inserts were removed (T0), percentage of wound closure is calculated after 14 hours (T14h) of cell migration (n=4). A, representative phase contrast microphotographs of wound healing assay. B, percentage of wound closure after 14 hours calculated from each T0 counterparts. C-D, Tube formation assays: HUVECs were seeded on matrigel for 4 hours with or without DCA treatment (n=3). C, representative phase contrast microphotographs of tube formation assays. D, quantitative analysis of specific parameters (total tube length, total number of tubes, total branching point and total loops) of tube formation assays. Statistical analysis: One-way ANOVA (B,D) (Sidak's multiple comparison test), *p <0.05.

3.3. *Inhibition of glutamine conversion to glutamate reduces HUVECs proliferation, migration and respiration without change in apoptosis induction and tube formation*

After glycolysis, glutaminolysis is the second most described metabolic pathway in ECs. We used the glutaminase-1 inhibitor, BPTES to evaluate the impact of the inhibition of glutamine conversion to glutamate on HUVECs fitness. By ^{13}C NMR, we first observed that BPTES reduces intracellular glutamate concentration by more than 80% (fig.3A). This reduction did not affect the glutamine uptake (fig.3B), but significantly increased intracellular glutamine concentration by more than 30% (fig3C). The glutamine index, which measures the production of glutamate from glutamine, was reduced by BPTES by more than 70% (fig.3D). We then measured the impact of this inhibition on HUVECs proliferation. We observed that the exposure to increasing concentration of BPTES was correlated with a reduction in HUVECs proliferation (fig.3E). We identified that 1µM BPTES was the lowest concentration that significantly reduced HUVECs proliferation. We then evaluated if BPTES also induced changes in mitochondrial activity since glutamate is fueling

the TCA cycle. We observed that BPTES significantly reduced the oxygen consumption rate (fig.3F). We noticed that BPTES had no cytotoxic effect on HUVECs since we observed no significant change in apoptosis induction (fig.3G). Finally, BPTES significantly reduced HUVECs migration, but, as observed for DCA, BPTES had no impact on tube formation (fig.3H-I).

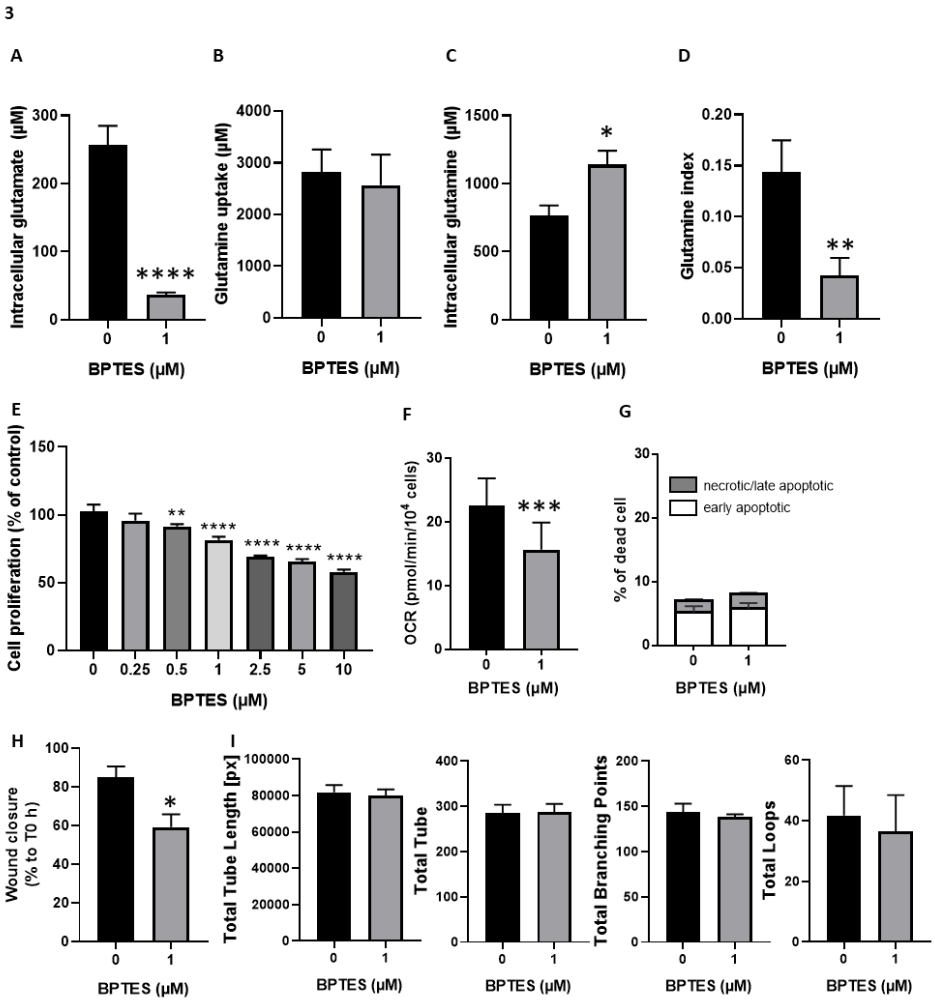

Figure 3: Inhibition of glutamine conversion to glutamate reduced HUVECs proliferation, migration and respiration without change in apoptosis induction and tube formation. A-D, HUVECs were exposed during 24h to 10 mM of L-glutamine-5-^{13}C and co-incubated with (or without) BPTES. Intra- and extracellular metabolites were quantified by ^{13}C NMR spectroscopy (n=5). A, glutamate production from glutamine (intracellular concentration of glutamate) B, glutamine uptake (extracellular concentration of glutamine at T0 minus extracellular concentration of glutamine after 24 hours). C, intracellular glutamine

concentration. . D, glutamine index, (ratio of glutamate production on glutamine uptake). E, proliferation of HUVECs (% of control) treated with increasing doses of BPTES (0-10 μM) (n=4). F, oxygen consumption rate (OCR), measured in HUVECs treated with or without 1 μM of BPTES (n=3). G, percentage of apoptotic and dead HUVECs treated with or without 1 μM of BPTES (n=4). H, percentage of wound closure after 14 hours calculated from each T0 counterparts. I, quantitative analysis of specific parameters (total tube length, total number of tubes, total branching point and total loops) of HUVECs tube formation after 4 hours incubation on matrigel in the presence (or not) of 1 μM of BPTES. Statistical analysis: Paired t-test (A-D, F, H-I), One-way (E), or Two-way ANOVA (G) (Sidak's multiple comparison test), comparison from control, *p <0.05, **p <0.01, *** p <0.001, **** p <0.0001.

3.4. *Combined exposure to BPTES and DCA increases the impact on HUVECs proliferation and migration, but normalize OCR and apoptosis*

Since DCA and BPTES are targeting two different pathways that both regulate HUVECs metabolism, we investigated the impact of their combination. We first observed that the combined exposure to DCA (5 mM or 10 mM) and BPTES (1 μM) significantly decreased HUVECs proliferation, with a larger effect compared to the effect observed for each drug used alone (fig.4A). Interestingly, the combination did not increase the cytotoxic effect when the DCA concentration was 5 mM. On the contrary, while DCA 10 mM significantly increased apoptosis when used alone, the combination of DCA 10mM with BPTES had no significant impact on apoptosis (fig.4B). We then measured the effect of the combination on OCR. We observed that the combination of both drugs abrogated the effects of either drug (fig.4C). While DCA alone increased OCR and BPTES alone decreased OCR, the combination of both drugs did not significantly change OCR compared to controls. Regarding HUVECs migration, we observed that the combined exposure to DCA and BPTES increased the reduction in migration induced by either drug used alone (fig.4D). Finally, we measured the impact of the combination on tube formation. We observed that only the combination with the highest concentration of DCA (10 mM) impacted tube formation with a significant reduction in the number of branching points and the number of loops (fig.4E).

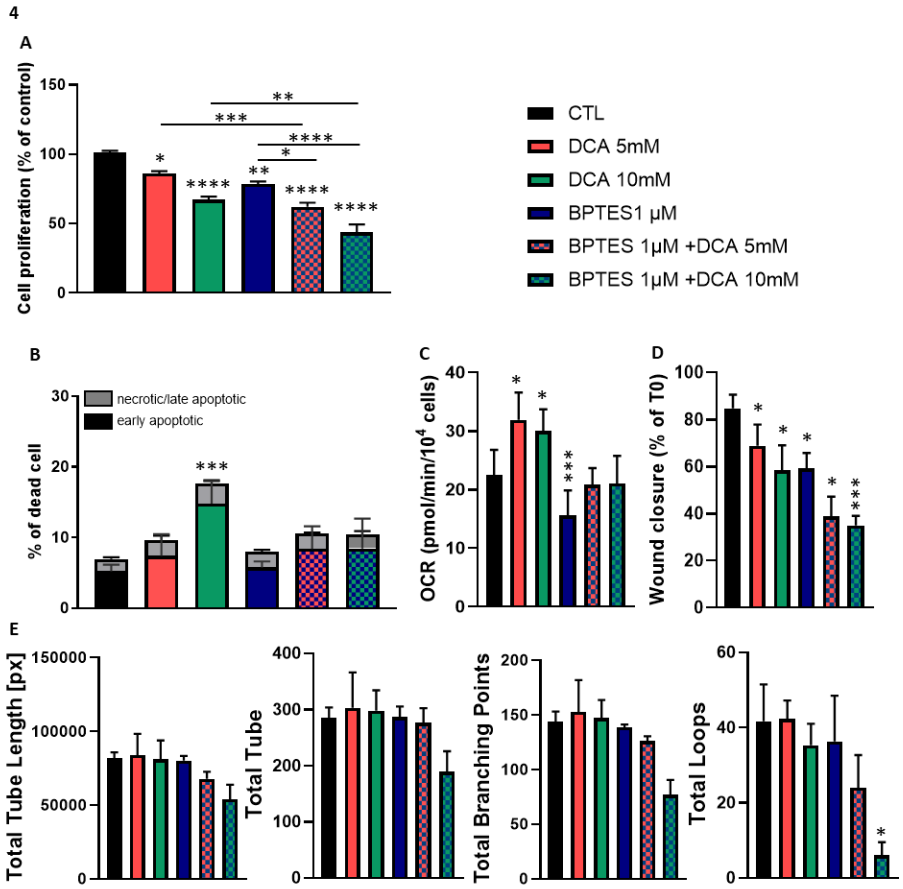

Figure 4: Combined exposure to DCA and BPTES enhances the reduction in HUVECs proliferation and migration, but normalizes OCR and apoptosis. A-E, HUVECs were treated with DCA (5 or 10 mM) and BPTES (1µM), alone and in combination. The following parameters were evaluated: A, cell proliferation (n=4), B, apoptotic and dead cells (n=4), C, oxygen consumption rate (n=3), D, wound closure (n=3) and E, tube formation (n=3). Statistical analysis: One-way (A, C-E), or Two-way ANOVA (B) (Sidak's multiple comparison test), comparison with control except for A where specific pairs are noted with a black line, *p <0.05, **p <0.01, *** p <0.001, **** p <0.0001.

3.5. BPTES and DCA modulate glutamine metabolism and reveal the importance of citrate on HUVECs homeostasis.

To go further on the characterization of BPTES and DCA impact on endothelial cell metabolism, we monitored their impact on ^{13}C-glutamine metabolism. We already observed that BPTES reduced the glutamate production and increased the intracellular glutamine concentration. We also observed that DCA alone had no impact on glutamine and glutamate concentration (fig.5 A-D). However, we noticed that DCA alone increased aspartate production from

glutamine. We observed that DCA alone had no impact on glutathione, citrate and proline production (fig.5 E-H). When HUVECs were exposed to BPTES, we observed no signal of aspartate, proline and glutathione in the ^{13}C-NMR spectra (fig.5 E-H). Interestingly, the signal of citrate was increased by BPTES, when used alone or in combination (fig 5E).

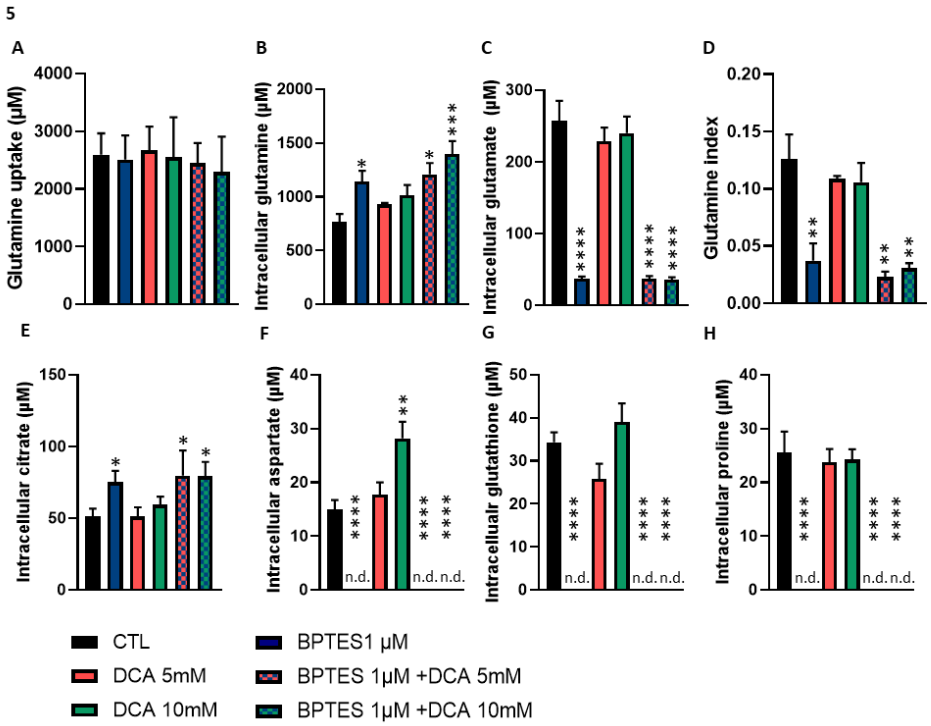

Figure 5: Downstream metabolites of glutamine are differentially impacted by BPTES and DCA. A-H, HUVECs were exposed during 24h to 10 mM of L-glutamine-5-13C and co-incubated with or without DCA (5 or 10 mM) and BPTES (1µM), alone and in combination. Intra- and extracellular metabolites were quantified by ^{13}C NMR spectroscopy (n=5). A, glutamine uptake. B, intracellular glutamine concentration. C, glutamate production from glutamine. D, glutamine index, ratio of glutamate production on glutamine uptake. E, citrate production from glutamine. F, aspartate production from glutamine. G, glutathione production from glutamine. H, proline production from glutamine. Statistical analysis: One-way ANOVA (A-H) (Sidak's multiple comparison test), comparison from control, *p <0.05, **p <0.01, *** p <0.001, **** p <0.0001.

4. Discussion

By demonstrating that HUVECs are sensitive to DCA (fig.1A), we highlight two important facts. First, the use of DCA as anti-cancer treatment may affect other cells in the tumor microenvironment than cancer cells. Indeed, we observed that

HUVECs are sensitive in the same range of DCA concentration than two different cancer cell lines (fig.1B). The second important fact is that DCA may be considered as an alternative (or complementary) anti-angiogenic agent. Actually, we showed that DCA reduces HUVECs proliferation (fig.1A) but only increases apoptosis at high DCA concentration (fig.1I). This means that, depending on the dose, DCA may exhibit a cytostatic effect without inducing cytotoxicity suggesting that there is room for a DCA dosage exhibiting antiangiogenic effects but sparing quiescent healthy ECs. This could be useful to normalize tumor angiogenesis since tumor vasculature is functionally and structurally abnormal due to aberrant proangiogenic factors signaling leading to a hyper activation of ECs metabolism (Li et al. 2019). In order to reduce cancer cell invasion and to improve chemotherapy, there is a growing interest to normalize vessel formation in tumors through a remodeling of tumor endothelial cell metabolism (Cantelmo et al. 2016). As previously reported by others (Cantelmo et al. 2016), we showed that HUVECs have a high glycolytic metabolism (fig.1E), the majority of glucose entering the cell being metabolized into lactate. We also showed that, as in cancer cells (Bonnet et al. 2007), DCA reduces PDH phosphorylation in HUVECs, an observation consistent with the inhibition of PDK by DCA that allows pyruvate to fuel the TCA cycle (fig.1C). Accordingly, we demonstrated that DCA was able to reduce this hyperglycolytic metabolism (reduction of the glycolytic index, fig.1E) and to increase mitochondrial respiration (fig.1F). By studying mitochondrial oxygen consumption, we showed that DCA stimulates OXPHOS activity in HUVECs. Moreover, we showed that DCA did not alter maximal respiratory capacity but decreased spare respiratory capacity. These data suggest that DCA did not increase the density of mitochondria. We observed that increase in OCR was the same at 5 and 10 mM DCA. We also observed that spare respiratory capacity was close to zero at a 5 mM DCA concentration, and all the respiratory capacity was used (negative value) at 10 mM DCA (fig.1H). This may explain why we observed no difference between 5 and 10 mM DCA, respiration being at the maximum of capacity. Moreover, using the low DCA concentration (5 mM), we noticed that this increase of mitochondrial activity was not accompanied by an increase in apoptosis, apoptosis being induced only at the highest DCA concentration (fig.1IJ). Finally, we observed that DCA reduced HUVECs migration (fig.2B) without however impacting tube formation (fig.2D). This discrepancy may arise from the nature of the assay matrices, Matrigel for tube formation assays and

ibiTreat surface for migration assays, that may engage distinct integrins on HUVEC surface.

Altogether, our observations highlight that appropriate dosing of DCA is able to alter *in vitro* key steps in the angiogenic process, prompting for further investigations to evaluate to which extent this strategy could support vessel normalization.

As tumor angiogenesis is not only dependent on glycolysis but also on glutaminolysis (Huang et al. 2017, Kim et al. 2017), we investigated the impact of glutamine metabolism disruption on HUVECs. Using the glutaminase inhibitor, BPTES, we observed that inhibition of glutamate production from glutamine (fig.3A) was associated with a reduction in HUVECs proliferation, respiration and migration (fig.3E, F, H) but had no impact on apoptosis induction and tube formation (fig.3G, I). Interestingly, although BPTES reduced glutamate production, citrate was still produced from glutamate (fig.5A-E), even to a higher level than in control ECs. This observation suggests that the residual production of glutamate (less than 20%) in the presence of BPTES is used for citrate production possibly upon reductive carboxylation as previously described (Kim et al. 2017). This underlines the crucial role of citrate for proliferating HUVECs metabolism in need of phospholipids to build up new lipid bilayers (fig.6) (Schoors et al. 2015). Disruption of fatty acid synthesis was actually shown to reduce ECs proliferation and impair angiogenesis (Schoors et al. 2015, Bruning et al. 2018). Of note, the deficit in glutamate availability is also very likely to influence non-mitochondrial pathways such as the glutathione and proline synthesis that we found to be completely inhibited in the presence of BPTES. More importantly, in BPTES-treated cells, we did not observe any NMR signal of aspartate (fig.5F). This finding was at odd with the effect of DCA (in particular at 10 mM, Fig. 5E) that increased aspartate production in HUVECs. These results can be related to the previously reported role of mitochondrial FA oxidation in aspartate production to support nucleotide synthesis in ECs (Schoors et al. 2015). We can therefore propose a model where DCA promotes the activity of the TCA cycle and thereby supports aspartate production from oxaloacetate while glutamine acts as an essential anaplerotic substrate (so that blocking glutaminase has dramatic consequences on TCA cycling). PDK and glutaminase inhibition deserve to be studied in vivo in order to have reliable data about their impact on tumor angiogenesis. To measure the potential effects on tumor

growth and metastasis, such approach would first require to conduct mouse experiments to select the optimal drug concentrations to normalize endothelial cell metabolism.

This study raises new opportunities for combining drugs acting on the metabolism, not only to target cancer cells directly, but also to target HUVECs. We showed that the metabolic reprogramming induced by both PDK and glutaminase inhibitors could affect tumor angiogenesis. However, it should be noted that in this study the impact of these drugs was evaluated on HUVECs and it would be interesting to use other ECs models, such as human microvascular endothelial cells, to further validate our observations. Our findings warrant further research regarding a potential normalization of tumor angiogenesis with these metabolic inhibitors.

6

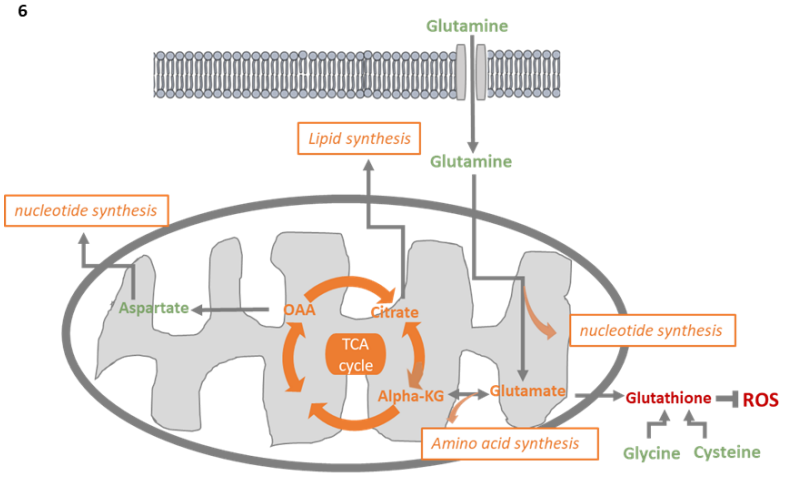

Figure 6: Glutamine metabolism: glutamine enters into the cell and can contribute to nucleotide synthesis or be converted into glutamate; glutamate participates in glutathione synthesis and can be converted to α-ketoglutarate (alpha-KG) which fuels the TCA cycle which produces oxaloacetate (OAA) and citrate. OAA can be converted to aspartate and participate in nucleotide synthesis, citrate supports lipid synthesis (FAS).

Author Contributions: Conception and design: C.A.S., B.G.; Development of methodology: C.A.S., N.J., L.X.Z., D.B.; Acquisition of data: C.A.S., B.M.; Analysis and interpretation of data: C.A.S., N.J., D.B., O.F., B.G.; Writing, review, and/or revision of the manuscript: C.A.S., N.J., L.X.Z., D.B., P.S., O.F., B.G.; Study supervision: B.G., O.F. All authors have read and agreed to the published version of the manuscript.

Funding: Foundation against Cancer (2015-144 and 2016-087). Fonds National de la Recherche Scientifique (FNRS J008220F and 7454416F). C. Schoonjans is a Televie Ph.D.

student. The study used the facilities of the Flow Cytometry platforms of UCLouvain and the Nuclear and Electronic Spin Technologies (NEST).

Conflicts of Interest: The authors declare no conflict of interest

References

1. Li, X.; Sun, X.; Carmeliet, P. Hallmarks of Endothelial Cell Metabolism in Health and Disease. *Cell Metab* **2019**, *30*, 414-433, doi:10.1016/j.cmet.2019.08.011.

2. Fitzgerald, G.; Soro-Arnaiz, I.; De Bock, K. The Warburg Effect in Endothelial Cells and its Potential as an Anti-angiogenic Target in Cancer. *Front Cell Dev Biol* **2018**, *6*, 100, doi:10.3389/fcell.2018.00100.

3. Schoors, S.; Bruning, U.; Missiaen, R.; Queiroz, K.C.; Borgers, G.; Elia, I.; Zecchin, A.; Cantelmo, A.R.; Christen, S.; Goveia, J., et al. Fatty acid carbon is essential for dNTP synthesis in endothelial cells. *Nature* **2015**, *520*, 192-197, doi:10.1038/nature14362.

4. De Bock, K.; Georgiadou, M.; Schoors, S.; Kuchnio, A.; Wong, B.W.; Cantelmo, A.R.; Quaegebeur, A.; Ghesquiere, B.; Cauwenberghs, S.; Eelen, G., et al. Role of PFKFB3-driven glycolysis in vessel sprouting. *Cell* **2013**, *154*, 651-663, doi:10.1016/j.cell.2013.06.037.

5. Huang, H.; Vandekeere, S.; Kalucka, J.; Bierhansl, L.; Zecchin, A.; Bruning, U.; Visnagri, A.; Yuldasheva, N.; Goveia, J.; Cruys, B., et al. Role of glutamine and interlinked asparagine metabolism in vessel formation. *EMBO J* **2017**, *36*, 2334-2352, doi:10.15252/embj.201695518.

6. Cantelmo, A.R.; Conradi, L.C.; Brajic, A.; Goveia, J.; Kalucka, J.; Pircher, A.; Chaturvedi, P.; Hol, J.; Thienpont, B.; Teuwen, L.A., et al. Inhibition of the Glycolytic Activator PFKFB3 in Endothelium Induces Tumor Vessel Normalization, Impairs Metastasis, and Improves Chemotherapy. *Cancer Cell* **2016**, *30*, 968-985, doi:10.1016/j.ccell.2016.10.006.

7. Kim, B.; Li, J.; Jang, C.; Arany, Z. Glutamine fuels proliferation but not migration of endothelial cells. *EMBO J* **2017**, *36*, 2321-2333, doi:10.15252/embj.201796436.

8. Peyton, K.J.; Liu, X.M.; Yu, Y.; Yates, B.; Behnammanesh, G.; Durante, W. Glutaminase-1 stimulates the proliferation, migration, and survival of human endothelial cells. *Biochem Pharmacol* **2018**, *156*, 204-214, doi:10.1016/j.bcp.2018.08.032.

9. Eelen, G.; Dubois, C.; Cantelmo, A.R.; Goveia, J.; Bruning, U.; DeRan, M.; Jarugumilli, G.; van Rijssel, J.; Saladino, G.; Comitani, F., et al. Role of glutamine synthetase in angiogenesis beyond glutamine synthesis. *Nature* **2018**, *561*, 63-69, doi:10.1038/s41586-018-0466-7.

10. Wu, D.; Huang, R.T.; Hamanaka, R.B.; Krause, M.; Oh, M.J.; Kuo, C.H.; Nigdelioglu, R.; Meliton, A.Y.; Witt, L.; Dai, G., et al. HIF-1alpha is required for disturbed flow-induced metabolic reprogramming in human and porcine vascular endothelium. *Elife* **2017**, *6*, doi:10.7554/eLife.25217.

11. Sonveaux, P.; Copetti, T.; De Saedeleer, C.J.; Vegran, F.; Verrax, J.; Kennedy, K.M.; Moon, E.J.; Dhup, S.; Danhier, P.; Frerart, F., et al. Targeting the lactate transporter MCT1 in endothelial cells inhibits lactate-induced HIF-1 activation and tumor angiogenesis. *PLoS One* **2012**, *7*, e33418, doi:10.1371/journal.pone.0033418.

12. Sutendra, G.; Michelakis, E.D. Pyruvate dehydrogenase kinase as a novel therapeutic target in oncology. *Front Oncol* **2013**, *3*, 38, doi:10.3389/fonc.2013.00038.

13. Sutendra, G.; Dromparis, P.; Kinnaird, A.; Stenson, T.H.; Haromy, A.; Parker, J.M.; McMurtry, M.S.; Michelakis, E.D. Mitochondrial activation by inhibition of PDKII suppresses HIF1a signaling and angiogenesis in cancer. *Oncogene* **2013**, *32*, 1638-1650, doi:10.1038/onc.2012.198.

14. Duan, Y.; Zhao, X.; Ren, W.; Wang, X.; Yu, K.F.; Li, D.; Zhang, X.; Zhang, Q. Antitumor activity of dichloroacetate on C6 glioma cell: in vitro and in vivo evaluation. *Onco Targets Ther* **2013**, *6*, 189-198, doi:10.2147/OTT.S40992.

15. Michelakis, E.D.; Sutendra, G.; Dromparis, P.; Webster, L.; Haromy, A.; Niven, E.; Maguire, C.; Gammer, T.L.; Mackey, J.R.; Fulton, D., et al. Metabolic modulation of glioblastoma with dichloroacetate. *Sci Transl Med* **2010**, *2*, 31ra34, doi:10.1126/scitranslmed.3000677.

16. Kinnaird, A.; Dromparis, P.; Saleme, B.; Gurtu, V.; Watson, K.; Paulin, R.; Zervopoulos, S.; Stenson, T.; Sutendra, G.; Pink, D.B., et al. Metabolic Modulation of Clear-cell Renal Cell Carcinoma with Dichloroacetate, an Inhibitor of Pyruvate Dehydrogenase Kinase. *Eur Urol* **2016**, *69*, 734-744, doi:10.1016/j.eururo.2015.09.014.

17. Kankotia, S.; Stacpoole, P.W. Dichloroacetate and cancer: new home for an orphan drug? *Biochim Biophys Acta* **2014**, *1846*, 617-629, doi:10.1016/j.bbcan.2014.08.005.

18. Dunbar, E.M.; Coats, B.S.; Shroads, A.L.; Langaee, T.; Lew, A.; Forder, J.R.; Shuster, J.J.; Wagner, D.A.; Stacpoole, P.W. Phase 1 trial of dichloroacetate (DCA) in adults with recurrent malignant brain tumors. *Invest New Drugs* **2014**, *32*, 452-464, doi:10.1007/s10637-013-0047-4.

19. Chu, Q.S.; Sangha, R.; Spratlin, J.; Vos, L.J.; Mackey, J.R.; McEwan, A.J.; Venner, P.; Michelakis, E.D. A phase I open-labeled, single-arm, dose-escalation, study of dichloroacetate (DCA) in patients with advanced solid tumors. *Invest New Drugs* **2015**, *33*, 603-610, doi:10.1007/s10637-015-0221-y.

20. Schoonjans, C.A.; Joudiou, N.; Brusa, D.; Corbet, C.; Feron, O.; Gallez, B. Acidosis-induced metabolic reprogramming in tumor cells enhances the anti-proliferative activity of the PDK inhibitor dichloroacetate. *Cancer Lett* **2020**, *470*, 18-28, doi:10.1016/j.canlet.2019.12.003.

21. De Preter, G.; Neveu, M.A.; Danhier, P.; Brisson, L.; Payen, V.L.; Porporato, P.E.; Jordan, B.F.; Sonveaux, P.; Gallez, B. Inhibition of the pentose phosphate pathway by dichloroacetate unravels a missing link between aerobic glycolysis and cancer cell proliferation. *Oncotarget* **2016**, *7*, 2910-2920, doi:10.18632/oncotarget.6272.

22. Michelakis, E.D.; Webster, L.; Mackey, J.R. Dichloroacetate (DCA) as a potential metabolic-targeting therapy for cancer. *Br J Cancer* **2008**, *99*, 989-994, doi:10.1038/sj.bjc.6604554.

23. Feron, O.; Belhassen, L.; Kobzik, L.; Smith, T.W.; Kelly, R.A.; Michel, T. Endothelial nitric oxide synthase targeting to caveolae. Specific interactions with caveolin isoforms in cardiac myocytes and endothelial cells. *J Biol Chem* **1996**, *271*, 22810-22814.

24. Bonnet, S.; Archer, S.L.; Allalunis-Turner, J.; Haromy, A.; Beaulieu, C.; Thompson, R.; Lee, C.T.; Lopaschuk, G.D.; Puttagunta, L.; Bonnet, S., et al. A mitochondria-K+ channel axis is suppressed in cancer and its normalization promotes apoptosis and inhibits cancer growth. *Cancer Cell* **2007**, *11*, 37-51, doi:10.1016/j.ccr.2006.10.020.

25. Bruning, U.; Morales-Rodriguez, F.; Kalucka, J.; Goveia, J.; Taverna, F.; Queiroz, K.C.S.; Dubois, C.; Cantelmo, A.R.; Chen, R.; Loroch, S., et al. Impairment of Angiogenesis by Fatty Acid Synthase Inhibition Involves mTOR Malonylation. *Cell Metab* **2018**, *28*, 866-880 e815, doi:10.1016/j.cmet.2018.07.019.

DISCUSSION AND PERSPECTIVES

1. Discussion of the principal findings about DCA

The results obtained during this thesis highlight that the tumor microenvironment plays an important role in DCA response. In particular we found that extracellular acidosis increases the sensitivity of cancer cells to DCA and that DCA induces a metabolic reprogramming toward glutamine pathway in cancer cells. Here below, we will discuss these results as well as the limitations of our analysis.

1.1. Tumor microenvironment modulates the sensitivity of cancer cells to DCA

Our first aim was to investigate if extracellular acidosis could modulate the sensitivity of cancer cells to DCA. For this purpose, we used a model of cancer cells chronically adapted to acidosis. Accordingly, these cells are able to proliferate when maintained at an acidic pH of 6.5 at the same rate as the counterpart parental cells cultured at pH 7.4. We used two parental cell lines, namely HCT-116 (colorectal cancer) and SiHa cells (cervical cancer). The team of Olivier Feron and Cyril Corbet has previously demonstrated that acid-adapted SiHa and HCT-116 cancer cells redirect their metabolism away from glycolysis and increase glutamine and fatty acid metabolism (Corbet et al. 2014, Corbet et al. 2016).

- Why less glycolytic acid-adapted cancer cells are more sensitive to the glycolytic modulator DCA?

At first glance, it is surprising that acid-adapted cancer cells are more sensitive than parental cells to DCA in terms of proliferation and tumor growth. Indeed, our first hypothesis was that DCA should affect acid-adapted cancer cells to a lesser extent since they rely more on glutamine and fatty acids to sustain biosynthetic pathways. However, we observed that acid-adapted SiHa cells produce more pyruvate from glutamine than parental SiHa cells. This suggests that glutamine-derived pyruvate could be the substrate for PDH in acid-adapted cells (fig. 33), meaning that even if acid-adapted cells are less dependent on glucose, the conversion of pyruvate (regardless of its origin) to acetyl-CoA is still important for these cells.

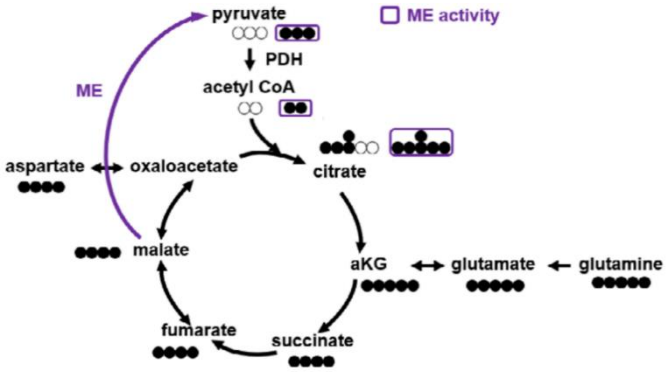

Figure 33. Glutamine metabolism routes highlighting the conversion of malate into pyruvate by the malic enzyme (ME) *(Kim et al. 2017).*

- How does extracellular acidosis modulate DCA uptake?

DCA uptake is a first indicator of cancer cells sensitivity to DCA. Thanks to ^{13}C NMR, we were able to measure DCA concentration in extracellular media. On NMR spectra of media from DCA treated cells, we observed the signal of both carbon 13 of DCA. Since there is no ^{13}C enriched-labeled DCA, signals correspond to the natural abundance of each ^{13}C (1.1%). Unfortunately, because of the very low signal of ^{13}C natural abundance, we were not able to measure intracellular concentration of DCA. Nevertheless, since we measured DCA concentration in the media at the beginning of the experiment (~5mM) and after 24 hours, we calculated the extent of DCA uptake for each cell line. We found that DCA uptake was significantly higher in acid-adapted cells than in parental cells. DCA uptake was of 351±60 and 263±54 µmoles/mg protein for acid-adapted HCT-116 and SiHa cells respectively. In parental cells, DCA uptake was of 59±12 and 53±22 µmoles/mg protein for HCT-116 and SiHa cells respectively. In agreement with the DCA uptake, we found a reduction in PDH phosphorylation confirming that PDK was inhibited in almost all cell lines. The reduction was less effective in parental cell lines than in acid-adapted cell lines, which is consistent with the observation that DCA uptake was lower in parental cells. This is also coherent with the lower (if any) reduction in the growth of parental cells than in that of acid-adapted cells. To investigate this differential uptake of DCA, we further focused on the DCA transport process (data not published). The team of Oliver Feron and Cyril Corbet has previously demonstrated that MCT1 is upregulated in acid-adapted cancer cells (Corbet et al. 2014). We used the MCT1 blocker AR-155858 to compare the DCA toxicity in acid-adapted and parental cell lines.

We compared cell growth after co-administration of the blocker and DCA (fig.34, not published).

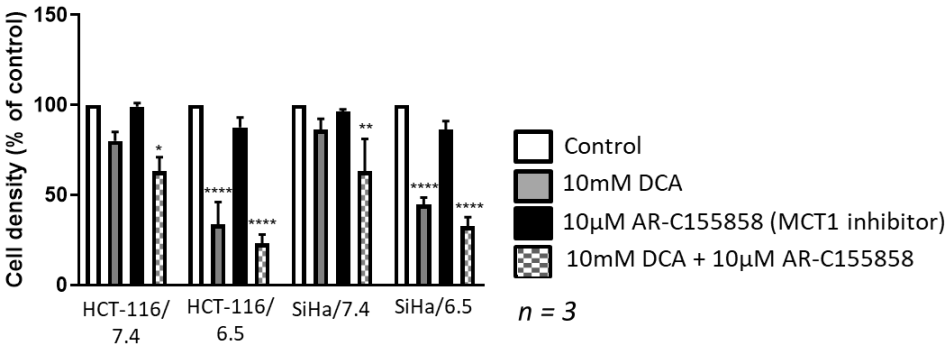

Figure 34: MCT1 inhibition did not prevent the reduction in cell density induced by DCA. *Cancer cells were treated with DCA (10 mM) alone or in combination with 10µM of AR-C155858 (MCT1 inhibitor) (n=3). 48 hours after treatments, cell density was measured using the Presto Blue reagent. Two-way ANOVA (Sidak's multiple comparison test, comparison from control). **p <0.01, *** p <0.001, **** p <0, 0001.*

In all cell lines, we observed that MCT1 inhibition was not able to prevent the reduction of cell density induced by DCA (fig. 34). Cell density was significantly reduced after co-administration of the blocker and DCA. These results indicate that MCT1 is not the major entry path of DCA (and associated toxicity) in cancer cells. A study of Babu *et al.,* demonstrated that SMCT1 transports DCA with a high affinity and that DCA, at low concentration (1mM), was able to induce apoptosis only in cancer cells transfected with SMCT1 cDNA. In different colon and breast cancer cell lines, the protein level of SMCT1 was lower than in normal colon and mammary cell lines (Babu et al. 2011). Researchers associated this result with the previous observation that

SMCT1 gene expression was silenced by DNA methylation in different cancer cells lines (Li et al. 2003, Ueno et al. 2004, Thangaraju et al. 2006, Park et al. 2007). Since metabolic adaptations induced by acidosis are in part due to epigenetic modification (deacetylation) (Corbet et al., 2016), we wondered if methylation-based silencing could also occur in acid-adapted cancer cells. We measured the protein levels of SMCT1 in our cell lines andfailed to observe differences between parental and acid-adapted cells (fig.35, data not published).

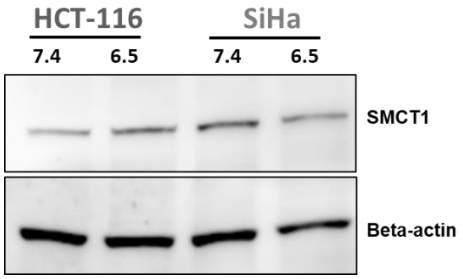

Figure 35: SMCT1 abundance. *Representative immunoblotting of SMCT1 abundance in SiHa, HCT-116 parental cell lines and acid–adapted (n=3). Beta-actin antibody was used as internal loading control.*

Another factor that could influence DCA influx is the proportion of the protonated (neutral) versus deprotonated (ionized) form of DCA. While DCA is mostly present under the ionized deprotonated form at pH 6.5 and 7.4 (due to its low pKa, 1.35), the proportion of neutral protonated form is about ten times higher at pH 6.5 compared to pH 7.4. This could contribute to a higher diffusion of DCA through the cell membrane. However, we did not observe a significant difference in cell growth between parental cells exposed to DCA under physiological pH or under acute exposure to an acidic pH. Further

investigation is needed to directly measure DCA uptake (rather than induced toxicity) to determine whether DCA protonation could somehow account for the increased uptake in acid-adapted cancer cells.

- How adaptation to extracellular acidosis increases DCA sensitivity?

In addition to the higher DCA uptake, the observed lower PDK abundance in acid-adapted cells could also participate in the higher sensitivity to DCA of acid-adapted cells. We did not investigate the reason for this PDK downregulation in acid-adapted cells. However, Corbet et al., observed a decrease in HIF-1 α expression in these cells (Corbet et al. 2014). As explained in the introduction of this thesis, it has been previously observed that PDK1 and PDK3 expression are increased by HIF-1 α while to the best of our knowledge, the regulation of PDK2 and PDK4 by HIF-1 α has not been studied yet. The decrease in HIF-1 α in acid-adapted cells could thus lead to a decrease in PDK expression. The larger decrease in PDH phosphorylation in acid-adapted cancer cells could thus result not only from a higher uptake of the inhibitor under acidic conditions but also a reduction in the abundance of the target enzyme.

The larger decrease in PDH phosphorylation induced by DCA under acidosis can also be related to the underlying metabolic shift. Indeed, we measured a larger decrease in lactate production from glucose as well as a higher oxygen consumption in acid-adapted cells compared to parental cells. We further detected only in acid-adapted cells an increase in mitochondria-dependent apoptosis and a decrease in PPP activity, supporting a major role in the metabolic shift in the decrease in the growth of acid-adapted cancer cells (vs.

parental cancer cells). Other information and potential limitations provided by the analysis of cellular metabolism by ^{13}C NMR and EPR

Monitoring the fate of $^{13}C_6$-glucose allows us to compare metabolic profiles of the different cell lines used in our study. We observed that the glycolytic phenotype did not correlate well with the intensity of the metabolic shifts observed after DCA exposure. HCT-116 parental cell line exhibits the highest basal lactate production from glucose (glycolytic phenotype) but presents the same reduction in lactate production when exposed to DCA than the most oxidative SiHa parental cells (i.e. cancer cells with a low basal lactate production from glucose). Also, the two acid-adapted cell lines showed the lowest basal lactate production from glucose (vs. corresponding parental cells) but led to the largest reduction in lactate in response to DCA.

Due to the low sensitivity of ^{13}C NMR, we were not able to detect all the downstream metabolites of glucose. In addition to lactate, we detected the signal of alanine in HCT-116 parental cells. Alanine is produced from pyruvate via transamination reaction with glutamate and concomitant production of alpha-Ketoglutarate. In HCT-116 parental cells, alanine showed the same trend of reduction as lactate after DCA treatment. This means that DCA, by controlling pyruvate fate, reduces transamination of pyruvate into alanine and may lower glutamate utilization for this reaction as well as alpha-KG production. In addition, alanine represses PKM2 activity. The decrease in alanine induced by DCA could exert a positive feedback by enhancing PKM2 activity and therefore increasing pyruvate formation. It would be interesting to detect other downstream glucose metabolites to have more information

about the respective contributions of glucose in the different biosynthetic pathways such as PPP, serine pathway and TCA cycle. Measuring oxygen consumption gave us part of the answer and showed that lactate reduction induced by DCA was correlated with an increase in oxygen consumption. However, we could not identify whether oxygen consumption (ie, TCA cycling) was fueled by glucose or by other bioenergetics such as glutamine (the metabolism of either source being stimulated by DCA exposure).

1.2. DCA can directly act on non-cancerous cells in the tumor microenvironment

In the second study, we revealed that ECs were sensitive to DCA. We noticed that, in terms of proliferation, cancer cells and ECs were sensitive to the same range of DCA concentration. In terms of glycolytic shift, DCA had the same effects in ECs that we previously measured in cancer cells: reduction in PDH phosphorylation and reduction in lactate production. In HCT-116 and SiHa cancer cells, only acid-adapted cells presented an increase in respiration and apoptosis after DCA exposure (5 mM). In the case of ECs, we observed an increase in respiration at 5 and 10 mM DCA while apoptosis was only detectable at 10 mM DCA. To further examine the effects of DCA on angiogenesis, we measured the impact of DCA on ECs migration and tube formation. Migration required actin remodelling in lamellipodia and filopodia (membrane protrusions) which is a high energy demanding process. Most of the ATP needed for actin remodelling is produced by glycolysis. (De Bock et al. 2013, Cantelmo et al. 2016). Although we observed no effect of DCA on tube formation, DCA significantly decreased ECs migration. The use of two

DCA concentrations (5 and 10 mM) also revealed some interesting differences: while the reduction in lactate production was larger at 10 mM (than at 5mM), the extents of the increase in respiration and of the decrease in migration were similar at 5 and 10 mM. Some clues to account for this observation can be derived from the measurements of the respiratory capacity of ECs. It is known that ECs have a low respiratory capacity with a reduced number of mitochondria (Li et al. 2019). Our Seahorse data allowed us to calculate the spare respiratory capacity (maximal respiration minus basal respiration). At DCA 5 mM, spare respiratory capacity was close to zero and the full respiratory capacity was reached (negative value) at 10 mM DCA. This may explain why we observed no difference between 5 and 10 mM DCA, i.e. cellular respiration was already at the maximum of its capacity. Since we observed apoptosis only at 10 mM DCA and no difference between 5 and 10 mM DCA in terms of migration, this study highlights that DCA may have cytostatic or cytotoxic effect in ECs, depending on the concentration of DCA.

In ECs, targeting both glycolytic and glutamine pathways, may be beneficial. Glutamine is essential for ECs proliferation and migration as it contributes to numerous metabolic and biosynthetic pathways. In proliferative ECs, glutamine by fueling TCA cycle, supports lipid, proteins and nucleotide synthesis but also sustains redox homeostasis via glutathione production (Huang et al. 2017, Kim et al. 2017, Peyton et al. 2018). In addition, glutamine metabolism in activated ECs has been associated with non-metabolic control of migration through post-translational protein modification of RhoJ, a membrane GTPase which regulates actin level and motility (Eelen et al. 2018). Eelen *et al.* have observed that glutamine synthase, the enzyme that converts

glutamate in glutamine, showed negligible glutamine-synthesizing activity in activated ECs, but sustained RhoJ palmitoylation, membrane localization, and activation. In our study, we observed that alone, BPTES, a glutaminase inhibitor reduced ECs proliferation, respiration and migration but had no impact on apoptosis and tube formation. Using BPTES and DCA in combination significantly reduced proliferation and migration induced by each drug alone. However, this combination waived the effects of either drug on respiration and apoptosis. Overall, the combination DCA and BPTES may allow to use lower concentration of each drug and thereby to reduce toxicity.

1.3. DCA and BPTES induces metabolic adaptations in glutamine pathway

Metabolic plasticity is a hallmark of cancer cell adaptation. In our study, we observed that DCA treatment was able to induce some modulations in glutamine metabolism. In cancer cells, we noticed that DCA increased the glutamine flux and stimulated TCA cycle. Also, we did not detect any signal of aspartate in acid-adapted cells while in parental cells, DCA increased aspartate concentration. Aspartate is generated by TCA cycle and is used to produce purines. In acid-adapted cells, aspartate request may be superior to aspartate production due to a lower TCA fueling by glucose metabolism.

In ECs DCA did not influence glutamine flux but increased aspartate levels. The distinct metabolic plasticity between cancer cells and ECs may explain the difference of adaptation to DCA. In cancer cells, intrinsic genetic mutations and response to external signals from the tumor

microenvironment are the driving force while the ECs phenotype is only determined by external stimuli. Still, cancer cells and angiogenic ECs are proliferating and the similar DCA-induced increase in aspartate production from glutamine in both cell types may underline the importance of this pathway in dividing cells. Indeed, aspartate generates purines which are essential for DNA replication.

We also measured the impact of BPTES on glutamine metabolism in ECs. We observed the expected reduction in glutamate production from glutamine which was accompanied by a decrease in some downstream metabolites of glutamate (aspartate, glutathione and proline) but not citrate. On the contrary, citrate production from glutamate was increased by BPTES. Citrate has a crucial role in metabolism since it supports fatty acid synthesis (FAS). FAS inhibition in ECs is known to reduce cell proliferation and impairs angiogenesis (Bruning et al. 2018). To preserve this lipid route under BPTES exposure, it may be proposed that the production of other downstream metabolites of glutamate are slowed down. A study on human breast cancer cell lines has also documented an increase in citrate production after BPTES exposure (Nagana Gowda et al. 2018) although these authors were not able to distinguish the upstream metabolite from which citrate was produced.

2. Limitations and Perspectives

2.1. Biological tools to study extracellular acidosis

Using the acid-adapted cell model is a good start to study metabolic adaptation to chronic exposure to extracellular acidosis. Since the two

populations come from the same cell line, it allows a comparison between either cell populations excluding inherent genotype differences that exist between cell lines. A clonal selection of cells that have acquired specific mutations can also be excluded since the same phenotype (in particular a metabolic shift toward glutamine and fatty acid metabolism) is observed in acid-adapted cancer cells from various tissue origins. However, this model is still artificial and does not recapitulate the full pH gradient within tumor areas. Moreover, since acidic pH is known to induce genetic mutations, we cannot totally exclude the apparition of mutations in the acid-adapted cells.
The use of spheroids could be the next step in our investigation since it tends to recapitulate 3D tumor organization. The team of Olivier Feron actually showed that an acidic pH develops spontaneously with the growth of spheroids (Corbet et al. 2020). Such 3D tumor spheroid models could thus be exploited to determine whether acidic areas overlap with a higher sensitivity to DCA. Finally, spatial resolution of MRI (magnetic resonance imaging) could be useful to identify, *in vivo,* acidic areas within tumors. CEST (chemical exchange saturation transfer) is a MRI technique that allows a mapping of extracellular pH within a tumor by measuring a pH-dependent signal from Iopamidol. Iopamidol is a contrast agent used in clinical diagnostic applications (X-Rays) for 30 years. Iopamidol has mobile protons that have a pH-dependent exchange rate with protons of water. The measurement of water signal modulation allows a mapping quantification of extracellular pH heterogeneity (Anemone et al. 2019). In our study, CEST could be useful to evaluate if more acidic tumors overlap with a higher sensitivity to DCA.

2.2. Interplay between acidic and hypoxic environments in DCA response

Since hypoxia increases extracellular acidosis, DCA could be more effective in hypoxic cells. On the other hand, because PDK expression is increased by HIF-1α, hypoxia could render cells more resistant to DCA via the increase in PDK expression. We have examined cell growth after DCA treatment under normoxia and hypoxia (21% O_2 vs 1% O_2) (fig.36, data not published). Our results showed that there was no difference in cell density under hypoxia vs. normoxia after 72h of DCA treatment (5 and 10mM DCA).

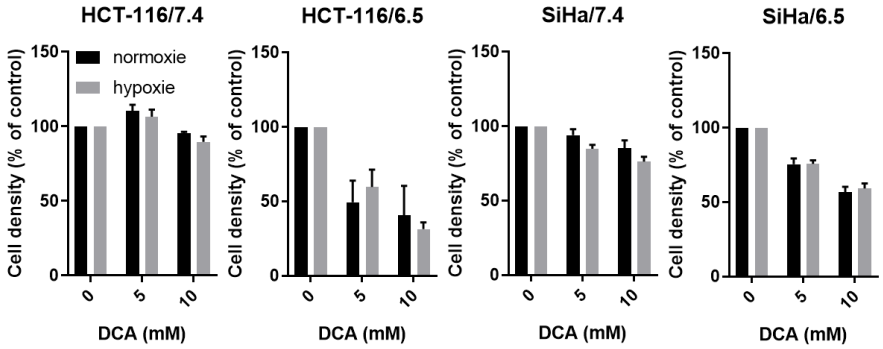

Figure 36: cell density after DCA treatment under normoxia and hypoxia. *Cancer cells were treated with 0, 5 or 10 mM of DCA and placed under normoxia or hypoxia (21% O_2 vs 1% O_2) (n=3). After 72 hours, cell density was measured using the Presto Blue reagent.*

However, long-term exposure to hypoxia could still have an effect on DCA sensitivity. Some studies have indeed demonstrated that DCA reverses hypoxic adaptation to chemotherapeutic agents or anti-angiogenic drugs

(Kumar et al. 2013, Xuan et al. 2014). Other studies have compared DCA-induced apoptosis between cells placed in normoxia or in hypoxia. Results showed that DCA increased apoptosis in normoxic human colorectal, cervical and pancreatic cancer cells but when these cells were placed under hypoxia, the DCA effect was lower (Anderson et al. 2009, Shahrzad et al. 2010). At first glance, these results do not fit our data, but they certainly highlight the importance to better characterize all the mechanisms that govern DCA response in order to find biomarkers that may select the best tumor type candidates for DCA treatment. This is yet more relevant that DCA could even favor tumor growth in some models (Shahrzad et al. 2010, Feuerecker et al. 2015).

2.3. Potential biomarkers of sensitivity to DCA

The differential sensitivity of cancer cells to DCA could be dependent on DCA ability to inhibit PDK, which is influenced by DCA uptake, by DCA inactivation by GSTZ1 and by PDK isoforms expression.

DCA transport into the cell/mitochondria is the first limiting factor to PDK inhibition by DCA. The inhibitory constant of DCA for PDK is between 0.2 and 1mM (depending on PDK isoforms) (Bowker-Kinley et al. 1998) and consequently lower than the concentration that is needed to observe in vitro the effect of DCA on cancer cells (Kankotia et al. 2014). To our knowledge, only one report has investigated properly DCA transport through the plasma membrane (Babu et al. 2011). Babu *et al.,* demonstrated that DCA is transported into the cells by the sodium-coupled monocarboxylate

transporter 1 (SMCT1) and that this transporter is epigenetically silenced in different tumor cell lines. Even if we did not observe any difference in SMCT1 protein level between parental and acid-adapted cell lines, we observed the presence of SMCT1 in our cell lines which is not the case for all cancer cell lines (Babu et al. 2011). Mitochondrial pyruvate transporter (MPC) is responsible for the transport of DCA into the mitochondria (Halestrap 1975) and its expression is also known to be downregulated is some cancers (Schell et al. 2014). Consequently, SMCT1 and MPC expression could be used as potential biomarkers for DCA response (Ho et al. 2015).

DCA metabolism was first described in the liver via DCA dechlorination into glycoxylate by GSTZ1. However, many cancer cell lines express GSTZ1 (www.proteinatlas.org) and a recent report has shown that cancer cell lines express GSTZ1 at different levels (Jahn et al. 2016). It has been described that high levels of GSTZ1 expression confer DCA resistance (Jahn et al. 2016). Moreover, it is known that DCA inhibits its own metabolism by GSTZ1 inhibition and that DCA accumulation can lead to peripheral neuropathy. The rate of DCA inactivation by GSTZ1 is influenced by *GSTZ1* haplotypes and by age (James et al. 2017). Different clinical studies have shown a correlation between *GSTZ1* haplotype and DCA metabolism (Dunbar et al. 2014, Langaee et al. 2018, Tian et al. 2019). Patients with a low enzyme activity variant display a stronger therapeutic response to DCA but also a stronger neuropathy than patients with high enzyme activity variants (Tian et al. 2019). In our experiments on cancer cells, on the one hand, we may probably exclude a differential *GSTZ1* haplotypes between acid-adapted and parental cells as they come from the same cell lines. But on the other hand, extracellular

acidosis is known to induce genetic mutations (Morita 1995). Consequently, it could be interesting to investigate GSTZ1 haplotypes in the cells used in the present thesis since it could potentially explain a difference in DCA response.

Since each PDK isoform has a different sensitivity to inhibition by DCA, a differential PDK expression profile could influence the response to DCA. PDK2 is the most sensitive to inhibition by DCA, PDK3 the most resistant and PDK1 and PDK 4 are relatively sensitive (Papandreou et al. 2011). In our study, we investigated the PDK protein levels. Since the level of all PDK isoforms was higher in parental than in acid-adapted cells, it was not possible to isolate the influence of one PDK specific isoform. However, this highlights that adaptation to extracellular acidosis modifies the expression profile of PDK isoforms. Other reports observed that PDK isoforms profile modulates the response to DCA. These reports suggest that higher PDK levels could be used as biomarkers of DCA sensitivity (Ho et al. 2015, Golias et al. 2019). These observations are not consistent with our results since we observed the opposite, i.e. acid-adapted cell lines exhibiting a lower PDK level and being more sensitive to DCA. This suggests that DCA response is not limited to the PDK isoforms profile and that DCA uptake and metabolism should be investigated in parallel.

PDP activity could also modulate DCA response between parental and acid-adapted cancer cells. A higher activity of PDP, the enzyme that dephosphorylates and activates PDH, could also be responsible for a larger decrease in PDH phosphorylation. In the literature, there is no report of direct

oncogenic signaling that increases PDP activity. Two reports have shown a decrease in PDP activity through PDP phosphorylation mediated by tyrosine kinase signaling (Fan et al. 2014, Shan et al. 2014). However, PDP activity is increased by Ca^{++}. Since HIF-1 α signaling modulates calcium influx in cancer (Azimi 2018) and since DCA may reduce calcium entry (Bonnet et al. 2007), it could be worth to investigate calcium influx to assess PDP activity.

2.4. Is DCA the better way to inhibit PDK in cancer?

Since we and others observed that the uptake of DCA by cancer cells is low, and since clinical studies have shown some adverse side effects (Babu et al. 2011, Garon et al. 2014), there is a growing interest to develop more effective ways to inhibit PDK. New biological tools such has nanoparticles and antibody–drug conjugates offer novel possibilities of drug delivery systems in order to increase selectivity and reduce toxicity of drugs. Nanoparticles take advantage of the high permeability of tumor vasculature. Passive diffusion of nanoparticles from leaky blood vessels to the tumor allows their accumulation selectively inside the tumor (Wang et al. 2010). Several research groups explored different protocols to develop nanoparticles containing DCA in order to promote endocytosis and cytosolic drug delivery (Abanades Lazaro et al. 2018, Štarha et al. 2018, Yang et al. 2018, Jin et al. 2019). One group has shown that functionalization of the zirconium terephthalate (UiO-66) nanoparticles with DCA enhances *in vitro* cytotoxicity in several cancer cells lines, did not induce cytotoxicity in healthy cells, and did not provoke immune system response (Abánades Lázaro et al. 2018). Antibody-drug conjugates (ADC) are composed of a cytotoxic drug attached to an antibody

that selectively binds to tumour-associated antigens (Kozak et al. 2013). ADCs offer the advantage to selectively deliver toxic drugs inside the cancer cells. To date, ADCs are limited to chemotherapeutic drugs, but using this technology to specifically deliver DCA inside the cancer cells could overcome the low uptake of DCA by cancer cells as well as increase the selectivity.

New PDK inhibitors with a different site of action than DCA have also been developed (DCA acts on the pyruvate binding site). To date, other PDK inhibitors have been designed to target the lipoyl binding pocket (that allows anchoring to PDC) and the ATP-binding pocket (that allows PDC phosphorylation). For some of them, early *in vitro* analyses showed promising results by reducing cancer cell proliferation with a lower IC_{50} than DCA (Moore et al. 2014, Tso et al. 2014, Zhang et al. 2015, Stacpoole 2017).

More recently, DCA has been studied in combination with Talaporfin sodium (TS), a photosensitizer used in photodynamic therapy (PDT) (Shinoda et al. 2020). The photosensitizer induces reactive oxygen species (ROS) production in response to laser irradiation to kill the ROS-exposed cancer cells. Despite the efficacy of TS in PDT for some cancers, the drug is expensive and leads to several side effects. In order to reduce the dose of TS, a combination of TS with DCA has been investigated since DCA has the potential to enhance the effects on PDT by increasing ROS production. U251 human astrocytoma were incubated with TS and DCA and after laser irradiation, cell viability was determined. Researchers observed that the combination synergistically enhanced the anti-cancer effect of TS.

However, none of these new strategies has already reached clinical trial and it will be interesting to see if the lower effective concentration of these new drugs/combination *in vitro* is still observed *in vivo* and in patients while assessing potential side effects.

Regarding our results, using the pH low insertion peptide (pHLIP) conjugate with DCA could offer promising benefits. Due to its structure, pHLIPs selectively target cells surrounded by an acidic microenvironment. Acidic pH induces a spontaneous folding and membrane insertion of pHLIPs that remain anchored across the membrane and the conjugate drug is directly translocated in the cytoplasm (Wyatt et al. 2018). This tool has already been studied in cancer with the chemotherapeutic agent doxorubicin. Doxorubicin was linked to pHLIP through a disulfur bond (pHLIP-SS-DOX), which is reduced in the cytoplasm allowing the release of the drug. *In vitro* results on cancer cells shown that pHLIP-SS-DOX induces no toxicity a pH 7.4 but significantly decreases cell density at pH 6 (Song et al. 2016). In the case of DCA, using pHLIPs could resolve the problem of the low DCA uptake while being more specific to cancer cells.

2.5. DCA and angiogenesis

Several mechanisms could be attributed to the anti-angiogenic effect of DCA. In the introduction, it has been detailed how some studies have demonstrated that DCA induces a HIF1- α signaling in cancer cells that could be responsible for an indirect anti-angiogenic effect on endothelial cells (Michelakis et al. 2010, Sutendra et al. 2013, Kinnaird et al. 2016). In addition,

an indirect effect could be mediated by the decrease in lactate induced by DCA. In the introduction, it was explained that, in ECs, imported lactate produced by cancer cells is involved in HIF1-α stabilization and triggers NF-kB/IL-8 autocrine signaling further enhancing angiogenesis (fig.25) (Vegran et al. 2011, Sonveaux et al. 2012). Since DCA reduces lactate production in cancer, this could lead to a decrease in lactate signaling in ECs. Independently from cancer, it has been shown that DCA was able to attenuate a lactate signaling that promotes the angiogenic response involved in age-related macular degradation (Lambert et al. 2020).

In our study, we have shown, *in vitro,* a direct effect of DCA on ECs viability, proliferation and migration. It would be interesting to use *in vivo* models that allow to measure a direct effect of DCA on angiogenesis independently from indirect effect on cancer cells. Several techniques allow to measure the impact of a drug on vasculature development (Nowak-Sliwinska et al. 2018). For instance, the *in vivo* angiogenesis plug assay is the most widely used technique for evaluation of pro- or antiangiogenic factors (Malinda 2009). In this assay, Matrigel, which is liquid at 4° C, is injected in the subcutaneous space of mice. At body temperature, the liquid solidifies to form a plug. The plug supports an intense vascular response when supplemented with angiogenic factors. The drug can be either mixed with Matrigel before injection or be given to mice during the experiment. Over time, blood vessels will extend into the plug. After plug resection, vessels density can be measured by immunohistochemical staining as well as vessels permeability after injection of tetramethylrhodamine (TRITC) labeled dextran. To measure the global impact DCA on tumor angiogenesis (indirect and direct effect), it

would be interesting to use imaging. Dynamic Contrast Enhanced Magnetic Resonance Imaging (DCE-MRI) is a powerful method to follow, over time, the impact of a drug on tumor vessels normalization (Cuenod et al. 2013). After injection of a gadolinium-based contrast agent, tumor vessel density, perfusion and permeability as well as blood flow are measured by acquisition of a dynamic series of images in a region of interest. These measurements can be repeated during the course of the *in vivo* experimentation. Therefore, this tool could be useful to monitor a potential tumor vessel normalization window during DCA treatment.

2.6. What consequences of DCA action on other non-cancerous cells in the microenvironment

In 2007, the first report on the anti-cancer action of DCA by the team of E. Michelakis claimed that DCA reduces tumor growth without affecting normal cells (Bonnet et al. 2007). However, this report was based on the study of a restricted panel of normal cells: small airway epithelial cells (SAEC), fibroblasts and pulmonary artery smooth. Moreover, they observed that these cells have a higher mitochondrial activity than the cancer cells used in the study. Nowadays it is known that other cells than cancerous cells harbor a Warburg phenotype. Our results on proliferative ECs, which also exhibit an elevated glycolytic index, show that they are also affected by DCA exposure. This raises the question of potential off-target effects of DCA on other non-cancerous cells that rely on glycolysis for energy and/or biomass production. Of note, since we observed a higher DCA efficacy on acid-adapted cells, which are less glycolytic than parental cells, DCA efficacy may not only be dependent on

the sole glycolytic index. Still, a high glycolytic index remains a good biomarker of DCA response (Stockwin et al. 2010, De Preter et al. 2016). In the tumor microenvironment, beside ECs, different types of cells have a high glycolytic turnover such as cancer-associated fibroblasts and certain types of immune cells (Ocana et al. 2019).

As explained above, reducing endothelial activity by DCA could be beneficial in order to lower the aberrant angiogenic activity, which favors functionally and structurally abnormal vasculature. Such approach may actually fit the paradigm of vessel normalization upon exposure to anti-angiogenic therapies. According to this theory, reduction in endothelial cell proliferation/migration (but not cell killing) may normalize the tumor vasculature and thereby offer more chance to chemotherapy to distribute homogeneously into the tumor (and radiotherapy to gain in efficacy in response to tumor re-oxygenation) (Zecchin et al. 2017).

Cancer-associated fibroblasts (CAFs) are fibroblasts that, upon activation by cancer cells, facilitate cancer cell invasion via matrix production and remodeling (Kuchnio et al. 2015). It has been demonstrated that CAFs have a higher glycolytic and glutamine-based metabolic activity than other fibroblasts (Ocana et al. 2019). In the introduction, we mentioned the lactate shuttle between CAFs and cancer cells, and described how cancer cells can induce a metabolic reprogramming through glycolysis in CAFs (Fu et al. 2017, Radhakrishnan et al. 2019). Zhang *et al.,* have also reported HIF-1 α stabilization in CAFs, which is independent of an external signal from cancer cells. These researchers observed a reduction in isocitrate dehydrogenase 3

α level (a TCA cycle enzyme) in CAFs leading to a decrease in alpha-ketoglutarate (a cofactor of PHD) resulting in HIF-1 α stabilization and a switch from OXPHOS to glycolysis (Zhang et al. 2015). This high glycolytic activity in CAFs makes them a potential target of DCA. It would be worth to evaluate the action of DCA on CAFs alone or in co-culture since, depending on the tumor type, the interplay between cancer cells and CAFs could be different.

Tumor microenvironment is also composed by immune cells such as tumor-associated macrophages (TAMs) and tumor-infiltrating lymphocytes (T-cells, B-cells and NK-cells). While healthy macrophages M1 rely on glycolysis and exhibit an anti-tumoral activity, TAMs that also rely on glycolysis promote tumor progression by stimulating angiogenesis and inhibiting the immune response (Ocana et al. 2019). Several studies have shown that TAMs are highly plastic and are able to adapt their metabolism to environmental constraints through upregulation of glycolysis, use of alternate metabolites to fuel TCA cycle, fatty acid synthesis and altered nitrogen cycle metabolism. These changes shape their functional phenotypes resulting in heterogeneity of TAMs populations within the tumor (Netea-Maier et al. 2018). It has been shown that PDK was involved in glucose metabolic reprogramming in primary macrophages and that the use of DCA reduced glucose metabolism and macrophage migration (Semba et al. 2016). Ohashi *et al.,* have also documented that acidosis induces arginase I expression in macrophages, which is responsible for reduction in $CD8^{+}$T-cell activation and proliferation. In this model, the authors showed that DCA, by reducing extracellular

acidosis, suppresses arginase I expression and restores CD8 $^{+}$T-cell proliferation (Ohashi et al. 2013).

Among the tumor-infiltrating lymphocytes population, different subtypes are characterized by a metabolic reprogramming that triggers their activation. For instance, cytolytic CD8^{+} T-cells rely on fatty acid oxidation and OXPHOS for survival and differentiation. CD 4^{+} T lymphocytes are either called effector (Teff) or regulator (Treg). While Teff lymphocytes drive immunity, Tregs suppress Teff activity to limit excessive inflammatory responses. Their activation is characterized by a distinct metabolic preferences: Teffs highly rely on glycolysis whereas Tregs are oxidative and require mitochondrial electron transport chain to proliferate (Ocana et al. 2019). Gerriets *et al.,* have shown that PDK expression was an important regulator of CD4^{+} T-cells activity since PDK inhibition by DCA affects Teff function but not Treg function (Gerriets et al. 2015). There is also some evidence that upregulation of glycolytic metabolism is essential for development and function of natural killer cells and for antibody production by B-cells (Caro-Maldonado et al. 2014, Donnelly et al. 2015). The above information regarding the influence of glycolysis on the phenotype of different types of immune cells raises the question of the overall impact of DCA on cancer progression. It certainly supports the conclusion that the balance between pro- and antitumor effects of the various sets of immune cells warrants further investigation to determine the effects of DCA in immunocompetent animal models bearing tumors in their original environment (ie, syngeneic models).

3. General conclusion

By demonstrating that extracellular acidosis paradoxically increases the sensitivity of cancer cells to DCA, we highlighted the need to take into account the characteristics of the tumor microenvironment to dissect the anti-cancer activity of a metabolism-targeting drug. Moreover, by documenting that DCA enhances glutamine metabolism, we opened new therapeutic perspectives to integrate metabolic plasticity in the selection of the best combination of drugs. Last, but not least, by showing that ECs are sensitive to DCA, we highlighted that anti-cancer metabolic drugs could target other cells in the microenvironment. As for ECs, DCA effect is largely beneficial since it reduces tumor angiogenesis but more work is needed to evaluate DCA effects on other non-cancerous cancer cells before drawing any therapeutic conclusion. Overall, we demonstrated that the tumor microenvironment is a key player in anti-cancer metabolic drug response and worth to be investigated in parallel to the study of the oncogenic drivers of tumor progression.

Methodology section

1. ^{13}C RMN fluxomics methodology

The use of ^{13}C-labeled substrates such as glucose or glutamine allows to monitor the metabolic fate of glucose or glutamine (fig.37).

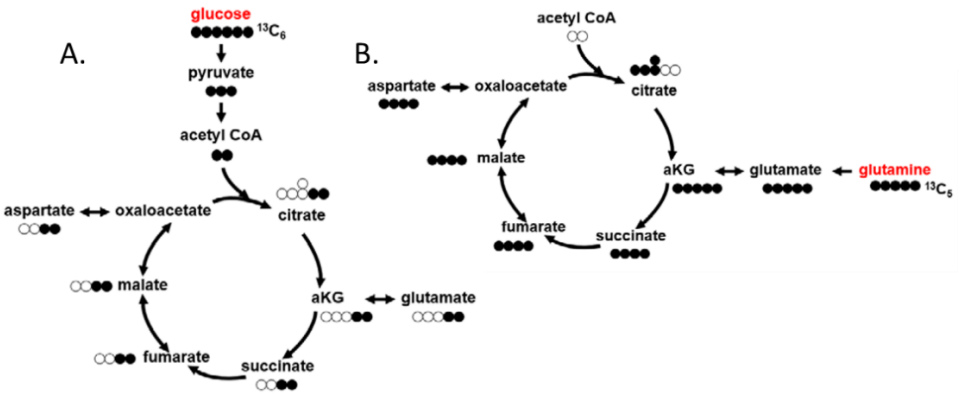

Figure 37: Schematic of labeling fate of glucose-$^{13}C_6$ (A.) and glutamine-5-^{13}C (B.) *(Kim et al. 2017).*

In order to follow the fate of glucose-$^{13}C_6$ in cancer cells, we used a DMEM culture media without glucose-$^{12}C_6$ and we added 10 mM of glucose-$^{13}C_6$ in the media. Per condition, two 100 mm dishes were seeded to reach 80% confluence at the day of the extraction. 24 hours after seeding, the culture media was removed and replaced by the culture media containing 10 mM of glucose-$^{13}C_6$. Cells were incubated for 24 hours in this labeled media. Then, extracellular media were collected and polar cellular metabolites were extracted using dual phase extraction procedure adopted from Teng *et al.*, (Teng et al. 2008). A mixture of methanol, chloroform and water in the volume

ratio 2:2:1 was used to generate two-phase extracts after centrifugation. The upper aqueous phase, containing polar metabolites, was collected. Then, the solvent was removed using a vacuum concentrator. The sample was reconstituted in 600 µl sodium phosphate buffer with 10% deuterium oxide containing 0.75 wt. % 3 – (trimethylsilyl) propionic-2,2,3,3-d_4 acid (TSP), corresponding to a final concentration of TSP in the NMR tube of 51.6 µM. For extracellular metabolites, 540 µl of media was used and 60 µl of deuterium oxide containing 0.75 wt. % TSP was added.

In our experiments, we performed 1024 scans. Each scan was composed by a RF pulse of 10 microseconds followed by an acquisition time of 0.8 seconds. A relaxation time of 10 seconds was applied between each RF pulse. The total duration time per sample was 3 hours and 6 minutes.

We used the software MestReNova to quantify the results. We have constructed a library with all the chemical shifts of the metabolites present in the spectra. We applied the library to each spectrum in order to identify each carbon of each metabolite present in the spectrum. Each identified signal was integrated and, as the concentration of TSP (used as internal standard) in the sample is known, the area under the curve of each signal was converted into a concentration (fig.38).

Compound	Integral	NH	Result (µM)
TSP			**51.60**
- Range 1 (-0.20-0.08)	1368.16	3	51.60
Lactate			**1387.48**
- Range 1 (184.74-185.67)	11559.80	1	1307.93
- Range 2 (21.84-23.84)	11518.48	1	1303.26
- Range 3 (70.78-71.58)	13710.28	1	1551.25
Alanine			**229.17**
- Range 1 (178.25-179.37)	2205.94	1	249.59
- Range 2 (17.82-19.81)	2036.59	1	230.43
- Range 3 (52.95-53.69)	1833.73	1	207.48
Glucose			**1240.48**
- Range 1 (93.64-99.74)	11360.03	1	1285.33
- Range 2 (71.88-72.98)	11204.93	1	1267.78
- Range 3 (62.05-64.83)	11105.04	1	1256.48
- Range 4 (77.93-79.36)	15601.48	1	1765.22
- Range 5 (76.39-77.55)	7449.48	1	842.87
- Range 6 (73.56-74.58)	9061.08	1	1025.21

Figure 38. Illustrative analysis: sample mixture analysis (SMA) report of intracellular metabolites of HCT-116 cancer cells incubated for 24 hours with media containing 10mM glucose-$^{13}C_6$. *Compound column reports the range of chemical shifts assigned to each ^{13}C of each metabolite. Integral gives the area under the curve of each identified ^{13}C signal. NH is the number of nuclei. Results column is the concentration of the metabolites expressed in µM. As the concentration of TSP is known, the other concentrations are calculated by comparison with the signal integral from the TSP: $(I_{compound}/NH_{compound})*((NH_{ref}/I_{ref}).51,6)$.*

2. Acid-adapted-cancer cells model

To study metabolic adaptations induced by long-term exposure to acidic pH, we used a model of cells chronically adapted to acid pH. This model was developed in the laboratory of Olivier Feron (fig.39) (Corbet et al. 2014). Starting from cancer cells usually maintained in DMEM medium adjusted to neutral pH (7.4), medium was changed for DMEM buffered at pH 6.5. 72 hours of incubation in the 6.5 medium led to a significant inhibition of tumor cell growth. Tumor cells were maintained in this medium (repeatedly renewed) for 8 to 10 weeks until they completely recovered and grew quite at the same rate as parental cells and consequently became chronically adapted to acidic pH.

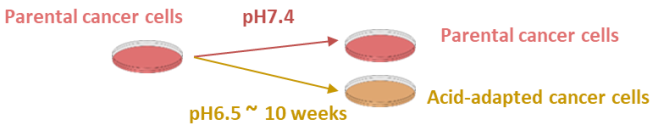

Figure 39: generation of acid-adapted cancer cells.

This methodology was used on three different cancer cell lines: FaDu (pharynx squamous cell), SiHa (cervix cancer cells) and HCT-116 (colon cancer cells). In our study we worked with SiHa and HCT-116 parental cells and their acid-adapted counterparts. All along our experiments, acid-adapted cancer cells were maintained in DMEM medium buffered a pH 6.5.

Pervious observations have been made on this model (Corbet et al. 2014, Corbet et al. 2016, Corbet et al. 2020). Corbet et al. described that chronic exposure to acidosis leads to metabolic reprograming towards glutamine and fatty acid metabolism (Corbet et al. 2014, Corbet et al. 2016). Glutamine

through reductive carboxylation was shown to contribute to fatty acid synthesis and changes in histone acetylation allowed concomitant fatty acid oxidation (FAO) (i.e. from fatty acids imported from the extracellular media). More recently, Corbet *et al*. demonstrated that acidosis favors the formation of lipid droplets used as sources of energy during metastases (Corbet et al. 2020).

BIBLIOGRAPHY

Abanades Lazaro, I., et al. (2018). "Enhancing anticancer cytotoxicity through bimodal drug delivery from ultrasmall Zr MOF nanoparticles." Chem Commun (Camb) 54(22): 2792-2795.
Abánades Lázaro, I., et al. (2018). "Mechanistic Investigation into the Selective Anticancer Cytotoxicity and Immune System Response of Surface-Functionalized, Dichloroacetate-Loaded, UiO-66 Nanoparticles." ACS Appl Mater Interfaces 10(6): 5255-5268.
Ahn, C. S. and C. M. Metallo (2015). "Mitochondria as biosynthetic factories for cancer proliferation." Cancer Metab 3(1): 1.
Akella, N. M., et al. (2019). "Fueling the fire: emerging role of the hexosamine biosynthetic pathway in cancer." BMC Biol 17(1): 52.
Akoka, S. "UNE INTRODUCTION A LA RESONANCE MAGNETIQUE NUCLEAIRE." Université de Nantes.
Altman, B. J., et al. (2016). "From Krebs to clinic: glutamine metabolism to cancer therapy." Nat Rev Cancer 16(11): 749.
Anderson, K. M., et al. (2009). "In vitro effects of dichloroacetate and CO2 on hypoxic HeLa cells." Anticancer Res 29(11): 4579-4588.
Anemone, A., et al. (2019). "Imaging tumor acidosis: a survey of the available techniques for mapping in vivo tumor pH." Cancer Metastasis Rev 38(1-2): 25-49.
Arneth, B. (2019). "Tumor Microenvironment." Medicina (Kaunas) 56(1).
Azimi, I. (2018). "The interplay between HIF-1 and calcium signalling in cancer." Int J Biochem Cell Biol 97: 73-77.
Babu, E., et al. (2011). "Role of SLC5A8, a plasma membrane transporter and a tumor suppressor, in the antitumor activity of dichloroacetate." Oncogene 30(38): 4026-4037.
Bayer, C. and P. Vaupel (2012). "Acute versus chronic hypoxia in tumors: Controversial data concerning time frames and biological consequences." Strahlenther Onkol 188(7): 616-627.
Bhutia, Y. D., et al. (2015). "Amino Acid transporters in cancer and their relevance to "glutamine addiction": novel targets for the design of a new class of anticancer drugs." Cancer Res 75(9): 1782-1788.
Boedtkjer, E. and S. F. Pedersen (2020). "The Acidic Tumor Microenvironment as a Driver of Cancer." Annu Rev Physiol 82: 103-126.

Bonnet, S., et al. (2007). "A mitochondria-K+ channel axis is suppressed in cancer and its normalization promotes apoptosis and inhibits cancer growth." Cancer Cell 11(1): 37-51.
Boroughs, L. K. and R. J. DeBerardinis (2015). "Metabolic pathways promoting cancer cell survival and growth." Nat Cell Biol 17(4): 351-359.
Bowker-Kinley, M. M., et al. (1998). "Evidence for existence of tissue-specific regulation of the mammalian pyruvate dehydrogenase complex." Biochem J 329 (Pt 1): 191-196.
Bruning, U., et al. (2018). "Impairment of Angiogenesis by Fatty Acid Synthase Inhibition Involves mTOR Malonylation." Cell Metab 28(6): 866-880 e815.
Cairns, R. A., et al. (2011). "Regulation of cancer cell metabolism." Nat Rev Cancer 11(2): 85-95.
Cantelmo, A. R., et al. (2016). "Inhibition of the Glycolytic Activator PFKFB3 in Endothelium Induces Tumor Vessel Normalization, Impairs Metastasis, and Improves Chemotherapy." Cancer Cell 30(6): 968-985.
Carmeliet, P. (2005). "VEGF as a key mediator of angiogenesis in cancer." Oncology 69 Suppl 3: 4-10.
Caro-Maldonado, A., et al. (2014). "Metabolic reprogramming is required for antibody production that is suppressed in anergic but exaggerated in chronically BAFF-exposed B cells." J Immunol 192(8): 3626-3636.
Charni, S., et al. (2010). "Oxidative phosphorylation induces de novo expression of the MHC class I in tumor cells through the ERK5 pathway." J Immunol 185(6): 3498-3503.
Chavhan, G. B. (2007). "MRI made easy."
Chen, J. L., et al. (2008). "The genomic analysis of lactic acidosis and acidosis response in human cancers." PLoS Genet 4(12): e1000293.
Choi, Y. W. and I. K. J. C. l. Lim (2014). "Sensitization of metformin-cytotoxicity by dichloroacetate via reprogramming glucose metabolism in cancer cells." 346(2): 300-308.
Chokchaitaweesuk, C., et al. (2019). "Enhanced hexosamine metabolism drives metabolic and signaling networks involving hyaluronan production and O-GlcNAcylation to exacerbate breast cancer." Cell Death Dis 10(11): 803.
Chou, T. Y., et al. (1995). "c-Myc is glycosylated at threonine 58, a known phosphorylation site and a mutational hot spot in lymphomas." J Biol Chem 270(32): 18961-18965.

Chu, Q. S., et al. (2015). "A phase I open-labeled, single-arm, dose-escalation, study of dichloroacetate (DCA) in patients with advanced solid tumors." Invest New Drugs 33(3): 603-610.
Cluntun, A. A., et al. (2017). "Glutamine Metabolism in Cancer: Understanding the Heterogeneity." Trends Cancer 3(3): 169-180.
Corbet, C., et al. (2020). "TGFbeta2-induced formation of lipid droplets supports acidosis-driven EMT and the metastatic spreading of cancer cells." Nat Commun 11(1): 454.
Corbet, C., et al. (2014). "The SIRT1/HIF2alpha axis drives reductive glutamine metabolism under chronic acidosis and alters tumor response to therapy." Cancer Res 74(19): 5507-5519.
Corbet, C. and O. Feron (2017). "Tumour acidosis: from the passenger to the driver's seat." Nat Rev Cancer 17(10): 577-593.
Corbet, C., et al. (2016). "Acidosis Drives the Reprogramming of Fatty Acid Metabolism in Cancer Cells through Changes in Mitochondrial and Histone Acetylation." Cell Metab 24(2): 311-323.
Cuenod, C. A. and D. Balvay (2013). "Perfusion and vascular permeability: basic concepts and measurement in DCE-CT and DCE-MRI." Diagn Interv Imaging 94(12): 1187-1204.
De Bock, K., et al. (2013). "Role of PFKFB3-driven glycolysis in vessel sprouting." Cell 154(3): 651-663.
De Preter, G., et al. (2016). "Inhibition of the pentose phosphate pathway by dichloroacetate unravels a missing link between aerobic glycolysis and cancer cell proliferation." Oncotarget 7(3): 2910-2920.
DeBerardinis, R. J. and N. S. Chandel (2016). "Fundamentals of cancer metabolism." Sci Adv 2(5): e1600200.
DeBerardinis, R. J., et al. (2007). "Beyond aerobic glycolysis: transformed cells can engage in glutamine metabolism that exceeds the requirement for protein and nucleotide synthesis." Proc Natl Acad Sci U S A 104(49): 19345-19350.
Delaney, L. M., et al. (2015). "Dichloroacetate affects proliferation but not survival of human colorectal cancer cells." Apoptosis 20(1): 63-74.
Dhar, S. and S. J. Lippard (2009). "Mitaplatin, a potent fusion of cisplatin and the orphan drug dichloroacetate." Proc Natl Acad Sci U S A 106(52): 22199-22204.
Dhup, S., et al. (2012). "Multiple biological activities of lactic acid in cancer: influences on tumor growth, angiogenesis and metastasis." Curr Pharm Des 18(10): 1319-1330.

Donnelly, R. P. and D. K. Finlay (2015). "Glucose, glycolysis and lymphocyte responses." Mol Immunol 68(2 Pt C): 513-519.
Duan, Y., et al. (2013). "Antitumor activity of dichloroacetate on C6 glioma cell: in vitro and in vivo evaluation." Onco Targets Ther 6: 189-198.
Dunbar, E. M., et al. (2014). "Phase 1 trial of dichloroacetate (DCA) in adults with recurrent malignant brain tumors." Invest New Drugs 32(3): 452-464.
Eales, K. L., et al. (2016). "Hypoxia and metabolic adaptation of cancer cells." Oncogenesis 5: e190.
Eelen, G., et al. (2018). "Role of glutamine synthetase in angiogenesis beyond glutamine synthesis." Nature 561(7721): 63-69.
Emwas, A. H. (2015). "The strengths and weaknesses of NMR spectroscopy and mass spectrometry with particular focus on metabolomics research." Methods Mol Biol 1277: 161-193.
Fan, J., et al. (2013). "Glutamine-driven oxidative phosphorylation is a major ATP source in transformed mammalian cells in both normoxia and hypoxia." Mol Syst Biol 9: 712.
Fan, J., et al. (2014). "Tyr phosphorylation of PDP1 toggles recruitment between ACAT1 and SIRT3 to regulate the pyruvate dehydrogenase complex." Mol Cell 53(4): 534-548.
Feron, O., et al. (1996). "Endothelial nitric oxide synthase targeting to caveolae. Specific interactions with caveolin isoforms in cardiac myocytes and endothelial cells." J Biol Chem 271(37): 22810-22814.
Feuerecker, B., et al. (2015). "DCA promotes progression of neuroblastoma tumors in nude mice." Am J Cancer Res 5(2): 812-820.
Fitzgerald, G., et al. (2018). "The Warburg Effect in Endothelial Cells and its Potential as an Anti-angiogenic Target in Cancer." Front Cell Dev Biol 6: 100.
Flavin, D. F. (2010). "Non-Hodgkin's Lymphoma Reversal with Dichloroacetate." Journal of oncology 2010: 414726.
Frezza, C. (2016). "Cancer metabolism: Addicted to serine." Nat Chem Biol 12(6): 389-390.
Fu, Y., et al. (2017). "The reverse Warburg effect is likely to be an Achilles' heel of cancer that can be exploited for cancer therapy." Oncotarget 8(34): 57813-57825.
Fuchs, B. C. and B. P. Bode (2005). "Amino acid transporters ASCT2 and LAT1 in cancer: partners in crime?" Semin Cancer Biol 15(4): 254-266.

Garon, E. B., et al. (2014). "Dichloroacetate should be considered with platinum-based chemotherapy in hypoxic tumors rather than as a single agent in advanced non-small cell lung cancer." J Cancer Res Clin Oncol 140(3): 443-452.
Gatenby, R. A. and R. J. Gillies (2004). "Why do cancers have high aerobic glycolysis?" Nat Rev Cancer 4(11): 891-899.
Geck, R. C. and A. Toker (2016). "Nonessential amino acid metabolism in breast cancer." Adv Biol Regul 62: 11-17.
Gerriets, V. A., et al. (2015). "Metabolic programming and PDHK1 control CD4+ T cell subsets and inflammation." J Clin Invest 125(1): 194-207.
Golias, T., et al. (2019). "Microenvironmental control of glucose metabolism in tumors by regulation of pyruvate dehydrogenase." Int J Cancer 144(4): 674-686.
Halestrap, A. P. (1975). "The mitochondrial pyruvate carrier. Kinetics and specificity for substrates and inhibitors." Biochem J 148(1): 85-96.
Harting, T. P., et al. (2017). "Dichloroacetate affects proliferation but not apoptosis in canine mammary cell lines." PLoS One 12(6): e0178744.
Haugrud, A. B., et al. (2014). "Dichloroacetate enhances apoptotic cell death via oxidative damage and attenuates lactate production in metformin-treated breast cancer cells." Breast Cancer Res Treat 147(3): 539-550.
Hitosugi, T., et al. (2011). "Tyrosine phosphorylation of mitochondrial pyruvate dehydrogenase kinase 1 is important for cancer metabolism." Mol Cell 44(6): 864-877.
Hjelmeland, A. B., et al. (2011). "Acidic stress promotes a glioma stem cell phenotype." Cell Death Differ 18(5): 829-840.
Ho, N. and B. L. Coomber (2015). "Pyruvate dehydrogenase kinase expression and metabolic changes following dichloroacetate exposure in anoxic human colorectal cancer cells." Exp Cell Res 331(1): 73-81.
Hosios, A. M., et al. (2016). "Amino Acids Rather than Glucose Account for the Majority of Cell Mass in Proliferating Mammalian Cells." Dev Cell 36(5): 540-549.
Huang, H., et al. (2017). "Role of glutamine and interlinked asparagine metabolism in vessel formation." EMBO J 36(16): 2334-2352.
Iommarini, L., et al. (2017). "Non-Canonical Mechanisms Regulating Hypoxia-Inducible Factor 1 Alpha in Cancer." Front Oncol 7: 286.

Isaacs, J. S., et al. (2005). "HIF overexpression correlates with biallelic loss of fumarate hydratase in renal cancer: novel role of fumarate in regulation of HIF stability." Cancer Cell 8(2): 143-153.
Jahn, S. C., et al. (2016). "GSTZ1 expression and chloride concentrations modulate sensitivity of cancer cells to dichloroacetate." Biochim Biophys Acta 1860(6): 1202-1210.
James, M. O., et al. (2017). "Therapeutic applications of dichloroacetate and the role of glutathione transferase zeta-1." Pharmacol Ther 170: 166-180.
Jiang, P., et al. (2014). "Regulation of the pentose phosphate pathway in cancer." Protein Cell 5(8): 592-602.
Jin, S., et al. (2019). "Targeting Energy Metabolism by a Platinum(IV) Prodrug as an Alternative Pathway for Cancer Suppression." Inorg Chem 58(9): 6507-6516.
Jones, W. and K. Bianchi (2015). "Aerobic glycolysis: beyond proliferation." Front Immunol 6: 227.
Junttila, M. R. and F. J. de Sauvage (2013). "Influence of tumour micro-environment heterogeneity on therapeutic response." Nature 501(7467): 346-354.
Kamphorst, J. J., et al. (2014). "Quantitative analysis of acetyl-CoA production in hypoxic cancer cells reveals substantial contribution from acetate." Cancer Metab 2: 23.
Kamphorst, J. J., et al. (2013). "Hypoxic and Ras-transformed cells support growth by scavenging unsaturated fatty acids from lysophospholipids." Proc Natl Acad Sci U S A 110(22): 8882-8887.
Kamphorst, J. J., et al. (2015). "Human pancreatic cancer tumors are nutrient poor and tumor cells actively scavenge extracellular protein." Cancer Res 75(3): 544-553.
Kankotia, S. and P. W. Stacpoole (2014). "Dichloroacetate and cancer: new home for an orphan drug?" Biochim Biophys Acta 1846(2): 617-629.
Khan, A., et al. (2016). "Long-term stabilization of stage 4 colon cancer using sodium dichloroacetate therapy." World J Clin Cases 4(10): 336-343.
Khan, A., et al. (2017). "Long-term stabilization of metastatic melanoma with sodium dichloroacetate." World J Clin Oncol 8(4): 371-377.
Khan, A. U. H., et al. (2017). "The PDK1 Inhibitor Dichloroacetate Controls Cholesterol Homeostasis Through the ERK5/MEF2 Pathway." Sci Rep 7(1): 10654.

Kim, B., et al. (2017). "Glutamine fuels proliferation but not migration of endothelial cells." EMBO J 36(16): 2321-2333.
Kim, H. and Y. J. Park (2018). "Links between Serine Biosynthesis Pathway and Epigenetics in Cancer Metabolism." Clinical nutrition research 7(3): 153-160.
Kim, J. and K. L. Guan (2019). "mTOR as a central hub of nutrient signalling and cell growth." Nat Cell Biol 21(1): 63-71.
Kim, J. W., et al. (2006). "HIF-1-mediated expression of pyruvate dehydrogenase kinase: a metabolic switch required for cellular adaptation to hypoxia." Cell Metab 3(3): 177-185.
Kinnaird, A., et al. (2016). "Metabolic Modulation of Clear-cell Renal Cell Carcinoma with Dichloroacetate, an Inhibitor of Pyruvate Dehydrogenase Kinase." Eur Urol 69(4): 734-744.
Kinnaird, A. and E. D. Michelakis (2015). "Metabolic modulation of cancer: a new frontier with great translational potential." J Mol Med (Berl) 93(2): 127-142.
Kolesnik, D. L., et al. (2015). "Effect of dichloroacetate on Lewis lung carcinoma growth and metastasis." Exp Oncol 37(2): 126-129.
Kolesnik, D. L., et al. (2020). "Metformin enhances cytotoxic action of dichloroacetate against Lewis lung carcinoma cells in vitro." Exp Oncol 42(1): 35-39.
Kondo, A., et al. (2017). "Extracellular Acidic pH Activates the Sterol Regulatory Element-Binding Protein 2 to Promote Tumor Progression." Cell Rep 18(9): 2228-2242.
Koukourakis, M. I., et al. (2005). "Lactate dehydrogenase 5 (LDH5) relates to up-regulated hypoxia inducible factor pathway and metastasis in colorectal cancer." Clin Exp Metastasis 22(1): 25-30.
Kozak, K. R., et al. (2013). "Total antibody quantification for MMAE-conjugated antibody-drug conjugates: impact of assay format and reagents." Bioconjug Chem 24(5): 772-779.
Krall, A. S., et al. (2016). "Asparagine promotes cancer cell proliferation through use as an amino acid exchange factor." Nat Commun 7: 11457.
Kroemer, G. and J. Pouyssegur (2008). "Tumor cell metabolism: cancer's Achilles' heel." Cancer Cell 13(6): 472-482.
Kruiswijk, F., et al. (2015). "p53 in survival, death and metabolic health: a lifeguard with a licence to kill." Nat Rev Mol Cell Biol 16(7): 393-405.

Kuchnio, A., et al. (2015). "The Cancer Cell Oxygen Sensor PHD2 Promotes Metastasis via Activation of Cancer-Associated Fibroblasts." Cell Rep 12(6): 992-1005.
Kumar, K., et al. (2013). "Dichloroacetate reverses the hypoxic adaptation to bevacizumab and enhances its antitumor effects in mouse xenografts." J Mol Med (Berl) 91(6): 749-758.
Lakhter, A. J., et al. (2016). "Glucose-independent Acetate Metabolism Promotes Melanoma Cell Survival and Tumor Growth." J Biol Chem 291(42): 21869-21879.
Lambert, V., et al. (2020). "Pyruvate dehydrogenase kinase/lactate axis: a therapeutic target for neovascular age-related macular degeneration identified by metabolomics." J Mol Med (Berl) 98(12): 1737-1751.
Lamonte, G., et al. (2013). "Acidosis induces reprogramming of cellular metabolism to mitigate oxidative stress." Cancer Metab 1(1): 23.
Langaee, T., et al. (2018). "Personalized Dosing of Dichloroacetate Using GSTZ1 Clinical Genotyping Assay." Genet Test Mol Biomarkers 22(4): 266-269.
Laurenti, G. and D. A. Tennant (2016). "Isocitrate dehydrogenase (IDH), succinate dehydrogenase (SDH), fumarate hydratase (FH): three players for one phenotype in cancer?" Biochem Soc Trans 44(4): 1111-1116.
Le, A., et al. (2012). "Glucose-independent glutamine metabolism via TCA cycling for proliferation and survival in B cells." Cell Metab 15(1): 110-121.
Li, B., et al. (2016). "Dichloroacetate and metformin synergistically suppress the growth of ovarian cancer cells." Oncotarget 7(37): 59458-59470.
Li, F., et al. (2007). "Regulation of HIF-1alpha stability through S-nitrosylation." Mol Cell 26(1): 63-74.
Li, H., et al. (2003). "SLC5A8, a sodium transporter, is a tumor suppressor gene silenced by methylation in human colon aberrant crypt foci and cancers." Proc Natl Acad Sci U S A 100(14): 8412-8417.
Li, X., et al. (2019). "Hallmarks of Endothelial Cell Metabolism in Health and Disease." Cell Metab 30(3): 414-433.
Li, Y., et al. (2020). "Acetate supplementation restores chromatin accessibility and promotes tumor cell differentiation under hypoxia." Cell Death Dis 11(2): 102.
Li, Z., et al. (2003). "A global transcriptional regulatory role for c-Myc in Burkitt's lymphoma cells." Proc Natl Acad Sci U S A 100(14): 8164-8169.

Lieu, E. L., et al. (2020). "Amino acids in cancer." Exp Mol Med 52(1): 15-30.
Lu, C. W., et al. (2008). "Induction of pyruvate dehydrogenase kinase-3 by hypoxia-inducible factor-1 promotes metabolic switch and drug resistance." J Biol Chem 283(42): 28106-28114.
Lukey, M. J., et al. (2017). "Targeting amino acid metabolism for cancer therapy." Drug Discov Today 22(5): 796-804.
Luo, W. and G. L. Semenza (2011). "Pyruvate kinase M2 regulates glucose metabolism by functioning as a coactivator for hypoxia-inducible factor 1 in cancer cells." Oncotarget 2(7): 551-556.
Lyssiotis, C. A. and A. C. Kimmelman (2017). "Metabolic Interactions in the Tumor Microenvironment." Trends Cell Biol 27(11): 863-875.
Malinda, K. M. (2009). "In vivo matrigel migration and angiogenesis assay." Methods Mol Biol 467: 287-294.
Mathupala, S. P., et al. (2001). "Glucose catabolism in cancer cells: identification and characterization of a marked activation response of the type II hexokinase gene to hypoxic conditions." J Biol Chem 276(46): 43407-43412.
Mazurek, S., et al. (2005). "Pyruvate kinase type M2 and its role in tumor growth and spreading." Semin Cancer Biol 15(4): 300-308.
McGuirk, S., et al. (2013). "PGC-1alpha supports glutamine metabolism in breast cancer." Cancer Metab 1(1): 22.
Mendes, C. and J. Serpa (2020). "Revisiting lactate dynamics in cancer-a metabolic expertise or an alternative attempt to survive?" J Mol Med (Berl) 98(10): 1397-1414.
Metallo, C. M., et al. (2011). "Reductive glutamine metabolism by IDH1 mediates lipogenesis under hypoxia." Nature 481(7381): 380-384.
Meyer, K. A., et al. (2016). "Adipocytes promote pancreatic cancer cell proliferation via glutamine transfer." Biochem Biophys Rep 7: 144-149.
Michelakis, E. D., et al. (2010). "Metabolic modulation of glioblastoma with dichloroacetate." Sci Transl Med 2(31): 31ra34.
Michelakis, E. D., et al. (2008). "Dichloroacetate (DCA) as a potential metabolic-targeting therapy for cancer." Br J Cancer 99(7): 989-994.
Minchenko, A., et al. (2002). "Hypoxia-inducible factor-1-mediated expression of the 6-phosphofructo-2-kinase/fructose-2,6-bisphosphatase-3 (PFKFB3) gene. Its possible role in the Warburg effect." J Biol Chem 277(8): 6183-6187.

Moore, J. D., et al. (2014). "VER-246608, a novel pan-isoform ATP competitive inhibitor of pyruvate dehydrogenase kinase, disrupts Warburg metabolism and induces context-dependent cytostasis in cancer cells." Oncotarget 5(24): 12862-12876.
Morfouace, M., et al. (2012). "Comparison of spheroids formed by rat glioma stem cells and neural stem cells reveals differences in glucose metabolism and promising therapeutic applications." J Biol Chem 287(40): 33664-33674.
Morita, T. (1995). "Low pH leads to sister-chromatid exchanges and chromosomal aberrations, and its clastogenicity is S-dependent." Mutat Res 334(3): 301-308.
Movafagh, S., et al. (2015). "Regulation of hypoxia-inducible factor-1a by reactive oxygen species: new developments in an old debate." J Cell Biochem 116(5): 696-703.
Mullen, A. R., et al. (2011). "Reductive carboxylation supports growth in tumour cells with defective mitochondria." Nature 481(7381): 385-388.
Nagana Gowda, G. A., et al. (2018). "A Metabolomics Study of BPTES Altered Metabolism in Human Breast Cancer Cell Lines." Front Mol Biosci 5: 49.
Nakazawa, M. S., et al. (2016). "Oxygen availability and metabolic adaptations." Nat Rev Cancer 16(10): 663-673.
Netea-Maier, R. T., et al. (2018). "Metabolic changes in tumor cells and tumor-associated macrophages: A mutual relationship." Cancer Lett 413: 102-109.
Nowak-Sliwinska, P., et al. (2018). "Consensus guidelines for the use and interpretation of angiogenesis assays." 21(3): 425-532.
Ocana, M. C., et al. (2019). "Metabolism within the tumor microenvironment and its implication on cancer progression: An ongoing therapeutic target." Med Res Rev 39(1): 70-113.
Ohashi, T., et al. (2013). "Dichloroacetate improves immune dysfunction caused by tumor-secreted lactic acid and increases antitumor immunoreactivity." Int J Cancer 133(5): 1107-1118.
Palm, W., et al. (2015). "The Utilization of Extracellular Proteins as Nutrients Is Suppressed by mTORC1." Cell 162(2): 259-270.
Papandreou, I., et al. (2006). "HIF-1 mediates adaptation to hypoxia by actively downregulating mitochondrial oxygen consumption." Cell Metab 3(3): 187-197.

Papandreou, I., et al. (2011). "Anticancer drugs that target metabolism: Is dichloroacetate the new paradigm?" Int J Cancer 128(5): 1001-1008.
Park, J. Y., et al. (2007). "Candidate tumor suppressor gene SLC5A8 is frequently down-regulated by promoter hypermethylation in prostate tumor." Cancer Detect Prev 31(5): 359-365.
Patel, M. S., et al. (2014). "The pyruvate dehydrogenase complexes: structure-based function and regulation." J Biol Chem 289(24): 16615-16623.
Pathak, R. K., et al. (2014). "Mito-DCA: a mitochondria targeted molecular scaffold for efficacious delivery of metabolic modulator dichloroacetate." ACS Chem Biol 9(5): 1178-1187.
Pavlova, N. N. and C. B. Thompson (2016). "The Emerging Hallmarks of Cancer Metabolism." Cell Metab 23(1): 27-47.
Pereira-Nunes, A., et al. (2020). "Lactate and Lactate Transporters as Key Players in the Maintenance of the Warburg Effect." Adv Exp Med Biol 1219: 51-74.
Peyton, K. J., et al. (2018). "Glutaminase-1 stimulates the proliferation, migration, and survival of human endothelial cells." Biochem Pharmacol 156: 204-214.
Pietrocola, F., et al. (2015). "Acetyl coenzyme A: a central metabolite and second messenger." Cell Metab 21(6): 805-821.
Pillai, S. R., et al. (2019). "Causes, consequences, and therapy of tumors acidosis." Cancer Metastasis Rev.
Polet, F., et al. (2016). "Reducing the serine availability complements the inhibition of the glutamine metabolism to block leukemia cell growth." Oncotarget 7(2): 1765-1776.
Polet, F. and O. Feron (2013). "Endothelial cell metabolism and tumour angiogenesis: glucose and glutamine as essential fuels and lactate as the driving force." J Intern Med 273(2): 156-165.
Porporato, P. E., et al. (2011). "Anticancer targets in the glycolytic metabolism of tumors: a comprehensive review." Front Pharmacol 2: 49.
Rabanal-Ruiz, Y., et al. (2017). "mTORC1 as the main gateway to autophagy." Essays Biochem 61(6): 565-584.
Radhakrishnan, R., et al. (2019). "Ovarian cancer cell-derived lysophosphatidic acid induces glycolytic shift and cancer-associated fibroblast-phenotype in normal and peritumoral fibroblasts." Cancer Lett 442: 464-474.

Ratcliffe, P. J. (2007). "HIF-1 and HIF-2: working alone or together in hypoxia?" J Clin Invest 117(4): 862-865.
Rohrig, F. and A. Schulze (2016). "The multifaceted roles of fatty acid synthesis in cancer." Nat Rev Cancer 16(11): 732-749.
San-Millan, I. and G. A. Brooks (2017). "Reexamining cancer metabolism: lactate production for carcinogenesis could be the purpose and explanation of the Warburg Effect." Carcinogenesis 38(2): 119-133.
Saunier, E., et al. (2016). "The pyruvate dehydrogenase complex in cancer: An old metabolic gatekeeper regulated by new pathways and pharmacological agents." Int J Cancer 138(4): 809-817.
Schell, J. C., et al. (2014). "A role for the mitochondrial pyruvate carrier as a repressor of the Warburg effect and colon cancer cell growth." Mol Cell 56(3): 400-413.
Schoonjans, C. A., et al. (2020). "Acidosis-induced metabolic reprogramming in tumor cells enhances the anti-proliferative activity of the PDK inhibitor dichloroacetate." Cancer Lett 470: 18-28.
Schoors, S., et al. (2015). "Fatty acid carbon is essential for dNTP synthesis in endothelial cells." Nature 520(7546): 192-197.
Schroder, J. and A. Tauch (2010). "Transcriptional regulation of gene expression in Corynebacterium glutamicum: the role of global, master and local regulators in the modular and hierarchical gene regulatory network." FEMS Microbiol Rev 34(5): 685-737.
Schug, Z. T., et al. (2015). "Acetyl-CoA synthetase 2 promotes acetate utilization and maintains cancer cell growth under metabolic stress." Cancer Cell 27(1): 57-71.
Selak, M. A., et al. (2005). "Succinate links TCA cycle dysfunction to oncogenesis by inhibiting HIF-alpha prolyl hydroxylase." Cancer Cell 7(1): 77-85.
Semba, H., et al. (2016). "HIF-1α-PDK1 axis-induced active glycolysis plays an essential role in macrophage migratory capacity." Nature communications 7: 11635-11635.
Semenza, G. L. (2001). "HIF-1 and mechanisms of hypoxia sensing." Curr Opin Cell Biol 13(2): 167-171.
Shahrzad, S., et al. (2010). "Sodium dichloroacetate (DCA) reduces apoptosis in colorectal tumor hypoxia." Cancer Lett 297(1): 75-83.
Shan, C., et al. (2014). "Tyr-94 phosphorylation inhibits pyruvate dehydrogenase phosphatase 1 and promotes tumor growth." J Biol Chem 289(31): 21413-21422.

Shinoda, Y., et al. (2020). "Synergistic effect of dichloroacetate on talaporfin sodium-based photodynamic therapy on U251 human astrocytoma cells." Photodiagnosis Photodyn Ther: 101850.
Song, Q., et al. (2016). "A smart tumor targeting peptide-drug conjugate, pHLIP-SS-DOX: synthesis and cellular uptake on MCF-7 and MCF-7/Adr cells." Drug Deliv 23(5): 1734-1746.
Sonveaux, P. (2008). "Provascular strategy: targeting functional adaptations of mature blood vessels in tumors to selectively influence the tumor vascular reactivity and improve cancer treatment." Radiother Oncol 86(3): 300-313.
Sonveaux, P., et al. (2012). "Targeting the lactate transporter MCT1 in endothelial cells inhibits lactate-induced HIF-1 activation and tumor angiogenesis." PLoS One 7(3): e33418.
Sonveaux, P., et al. (2008). "Targeting lactate-fueled respiration selectively kills hypoxic tumor cells in mice." J Clin Invest 118(12): 3930-3942.
Sousa, C. M., et al. (2016). "Pancreatic stellate cells support tumour metabolism through autophagic alanine secretion." Nature 536(7617): 479-483.
Stacpoole, P. W. (1989). "The pharmacology of dichloroacetate." Metabolism 38(11): 1124-1144.
Stacpoole, P. W. (2011). "The dichloroacetate dilemma: environmental hazard versus therapeutic goldmine--both or neither?" Environ Health Perspect 119(2): 155-158.
Stacpoole, P. W. (2017). "Therapeutic Targeting of the Pyruvate Dehydrogenase Complex/Pyruvate Dehydrogenase Kinase (PDC/PDK) Axis in Cancer." J Natl Cancer Inst 109(11).
Stacpoole, P. W. and J. M. Felts (1970). "Diisopropylammonium dichloroacetate (DIPA) and sodium dichloracetate (DCA): effect on glucose and fat metabolism in normal and diabetic tissue." Metabolism 19(1): 71-78.
Stacpoole, P. W. and Y. J. Greene (1992). "Dichloroacetate." Diabetes Care 15(6): 785-791.
Stacpoole, P. W., et al. (1998). "Pharmacokinetics, metabolism and toxicology of dichloroacetate." Drug Metab Rev 30(3): 499-539.
Stacpoole, P. W., et al. (1978). "Metabolic effects of dichloroacetate in patients with diabetes mellitus and hyperlipoproteinemia." N Engl J Med 298(10): 526-530.
Stacpoole, P. W., et al. (1992). "A controlled clinical trial of dichloroacetate for treatment of lactic acidosis in adults. The

Dichloroacetate-Lactic Acidosis Study Group." N Engl J Med 327(22): 1564-1569.
Štarha, P., et al. (2018). "Half-Sandwich Ru(II) and Os(II) Bathophenanthroline Complexes Containing a Releasable Dichloroacetato Ligand." Molecules 23(2).
Stockwin, L. H., et al. (2010). "Sodium dichloroacetate selectively targets cells with defects in the mitochondrial ETC." Int J Cancer 127(11): 2510-2519.
Su, X., et al. (2016). "Metabolic control of methylation and acetylation." Curr Opin Chem Biol 30: 52-60.
Sullivan, L. B., et al. (2015). "Supporting Aspartate Biosynthesis Is an Essential Function of Respiration in Proliferating Cells." Cell 162(3): 552-563.
Sun, R. C., et al. (2011). "Targeting metabolism with arsenic trioxide and dichloroacetate in breast cancer cells." Mol Cancer 10: 142.
Sun, R. C., et al. (2010). "Reversal of the glycolytic phenotype by dichloroacetate inhibits metastatic breast cancer cell growth in vitro and in vivo." Breast Cancer Res Treat 120(1): 253-260.
Sutendra, G., et al. (2013). "Mitochondrial activation by inhibition of PDKII suppresses HIF1a signaling and angiogenesis in cancer." Oncogene 32(13): 1638-1650.
Sutendra, G. and E. D. Michelakis (2013). "Pyruvate dehydrogenase kinase as a novel therapeutic target in oncology." Front Oncol 3: 38.
Taddei, M. L., et al. (2013). "Microenvironment and tumor cell plasticity: an easy way out." Cancer Lett 341(1): 80-96.
Tajan, M. and K. H. Vousden (2016). "The Quid Pro Quo of the Tumor/Stromal Interaction." Cell Metab 24(5): 645-646.
Tang, X., et al. (2012). "Functional interaction between responses to lactic acidosis and hypoxia regulates genomic transcriptional outputs." Cancer Res 72(2): 491-502.
Tardito, S., et al. (2015). "Glutamine synthetase activity fuels nucleotide biosynthesis and supports growth of glutamine-restricted glioblastoma." Nat Cell Biol 17(12): 1556-1568.
Tataranni, T. and C. Piccoli (2019). "Dichloroacetate (DCA) and Cancer: An Overview towards Clinical Applications." Oxid Med Cell Longev 2019: 8201079.
Teng, Q., et al. (2008). "A direct cell quenching method for cell-culture based metabolomics." Metabolomics 5(2): 199.

Teuwen, L. A., et al. (2019). "How glucose, glutamine and fatty acid metabolism shape blood and lymph vessel development." Dev Biol 447(1): 90-102.
Thangaraju, M., et al. (2006). "SLC5A8 triggers tumor cell apoptosis through pyruvate-dependent inhibition of histone deacetylases." Cancer Res 66(24): 11560-11564.
Tian, D. D., et al. (2019). "GSTZ1 genotypes correlate with dichloroacetate pharmacokinetics and chronic side effects in multiple myeloma patients in a pilot phase 2 clinical trial." Pharmacol Res Perspect 7(6): e00526.
Tso, S. C., et al. (2014). "Structure-guided development of specific pyruvate dehydrogenase kinase inhibitors targeting the ATP-binding pocket." J Biol Chem 289(7): 4432-4443.
Ueno, M., et al. (2004). "Aberrant methylation and histone deacetylation associated with silencing of SLC5A8 in gastric cancer." Tumour Biol 25(3): 134-140.
Vegran, F., et al. (2011). "Lactate influx through the endothelial cell monocarboxylate transporter MCT1 supports an NF-kappaB/IL-8 pathway that drives tumor angiogenesis." Cancer Res 71(7): 2550-2560.
Verma, A., et al. (2019). "Combined use of arginase and dichloroacetate exhibits anti-proliferative effects in triple negative breast cancer cells." J Pharm Pharmacol 71(3): 306-315.
Wang, M. and M. Thanou (2010). "Targeting nanoparticles to cancer." Pharmacol Res 62(2): 90-99.
Warburg, O. (1956). "On respiratory impairment in cancer cells." Science 124(3215): 269-270.
Warburg, O. (1956). "On the origin of cancer cells." Science 123(3191): 309-314.
Ward, N. P., et al. (2017). "Complex I inhibition augments dichloroacetate cytotoxicity through enhancing oxidative stress in VM-M3 glioblastoma cells." PLoS One 12(6): e0180061.
Weinberg, F., et al. (2010). "Mitochondrial metabolism and ROS generation are essential for Kras-mediated tumorigenicity." Proc Natl Acad Sci U S A 107(19): 8788-8793.
Whitehouse, S. and P. J. Randle (1973). "Activation of pyruvate dehydrogenase in perfused rat heart by dichloroacetate (Short Communication)." Biochem J 134(2): 651-653.

Wise, D. R., et al. (2011). "Hypoxia promotes isocitrate dehydrogenase-dependent carboxylation of alpha-ketoglutarate to citrate to support cell growth and viability." Proc Natl Acad Sci U S A 108(49): 19611-19616.
Wong, B. W., et al. (2017). "Endothelial cell metabolism in health and disease: impact of hypoxia." EMBO J 36(15): 2187-2203.
Wu, D., et al. (2017). "HIF-1alpha is required for disturbed flow-induced metabolic reprogramming in human and porcine vascular endothelium." Elife 6.
Wu, Z., et al. (2019). "Crosstalk of intracellular post-translational modifications in cancer." Arch Biochem Biophys 676: 108138.
Wyatt, L. C., et al. (2018). "Applications of pHLIP Technology for Cancer Imaging and Therapy: (Trends in Biotechnology 35, 653-664, 2017)." Trends Biotechnol 36(12): 1300.
Xuan, Y., et al. (2014). "Dichloroacetate attenuates hypoxia-induced resistance to 5-fluorouracil in gastric cancer through the regulation of glucose metabolism." Exp Cell Res 321(2): 219-230.
Xue, X., et al. (2012). "Mitaplatin increases sensitivity of tumor cells to cisplatin by inducing mitochondrial dysfunction." Mol Pharm 9(3): 634-644.
Yang, C., et al. (2018). "A facile doxorubicin-dichloroacetate conjugate nanomedicine with high drug loading for safe drug delivery." Int J Nanomedicine 13: 1281-1293.
Yang, L., et al. (2016). "Targeting Stromal Glutamine Synthetase in Tumors Disrupts Tumor Microenvironment-Regulated Cancer Cell Growth." Cell Metab 24(5): 685-700.
Yang, M. and K. H. Vousden (2016). "Serine and one-carbon metabolism in cancer." Nat Rev Cancer 16(10): 650-662.
Ye, J., et al. (2014). "Serine catabolism regulates mitochondrial redox control during hypoxia." Cancer Discov 4(12): 1406-1417.
Yi, W., et al. (2012). "Phosphofructokinase 1 glycosylation regulates cell growth and metabolism." Science 337(6097): 975-980.
Yu, F., et al. (2001). "HIF-1alpha binding to VHL is regulated by stimulus-sensitive proline hydroxylation." Proc Natl Acad Sci U S A 98(17): 9630-9635.
Yuneva, M., et al. (2007). "Deficiency in glutamine but not glucose induces MYC-dependent apoptosis in human cells." J Cell Biol 178(1): 93-105.
Zecchin, A., et al. (2017). "How Endothelial Cells Adapt Their Metabolism to Form Vessels in Tumors." Front Immunol 8: 1750.
Zhang, D., et al. (2015). "Metabolic reprogramming of cancer-associated fibroblasts by IDH3alpha downregulation." Cell Rep 10(8): 1335-1348.

Zhang, J., et al. (2014). "13C isotope-assisted methods for quantifying glutamine metabolism in cancer cells." Methods Enzymol 542: 369-389.
Zhang, J., et al. (2020). "Acetyl-CoA synthetase 3 promotes bladder cancer cell growth under metabolic stress." Oncogenesis 9(5): 46.
Zhang, J., et al. (2017). "Cancer cell metabolism: the essential role of the nonessential amino acid, glutamine." EMBO J 36(10): 1302-1315.
Zhang, S. L., et al. (2015). "Development of pyruvate dehydrogenase kinase inhibitors in medicinal chemistry with particular emphasis as anticancer agents." Drug Discov Today 20(9): 1112-1119.
Zhang, W., et al. (2015). "Targeting Tumor Metabolism for Cancer Treatment: Is Pyruvate Dehydrogenase Kinases (PDKs) a Viable Anticancer Target?" Int J Biol Sci 11(12): 1390-1400.